SIAM J. Applied Dynamical Systems
Vol. 3, No. 3, pp. 261–351
© 2004 Society for Industrial and Applied Mathematics

Analysis of Rotation–Vibration Relative Equilibria on the Example of a Tetrahedral Four Atom Molecule*

K. Efstathiou†, D. A. Sadovskii†, and B. I. Zhilinskii†

Abstract. We study relative equilibria (RE) of a nonrigid molecule, which vibrates about a well-defined equilibrium configuration and rotates as a whole. Our analysis unifies the theory of rotational and vibrational RE. We rely on the detailed study of the symmetry group action on the initial and reduced phase space of our system and consider the consequences of this action for the dynamics of the system. We develop our approach on the concrete example of a four-atomic molecule A_4 with tetrahedral equilibrium configuration, a dynamical system with six vibrational degrees of freedom. Further applications and illustrations of our results can be found in [van Hecke et al., *Eur. Phys. J. D At. Mol. Opt. Phys.*, 17 (2001), pp. 13–35].

Key words. small vibrations, vibration-rotation of molecules, spherical top, relative equilibria, 1:1:1 resonant oscillator, normalization, reduction, bifurcations, orbit space, finite group action, reversing symmetry, Molien generating function, integrity basis

AMS subject classifications. 37J15, 37J35, 37J40, 81V55, 58D19

DOI. 10.1137/030600015

1. Introduction.

This paper unifies modern methods of classical theory of symmetric Hamiltonian dynamical systems and quantum theory of molecules (and other isolated finite-particle systems). Considerable progress was achieved in both directions in the last decades and deep relations between these seemingly distant theories became evident. Significant effort by mathematicians and molecular physicists to converge the two fields resulted in the qualitative theory of highly excited quantum molecular systems based on recent mathematical developments. We join the two approaches and demonstrate what kind of concrete results can be immediately obtained in molecular systems [1, 2, 3, 4] by applying powerful methods of symmetric Hamiltonian systems [5, 6, 7, 8, 9, 10, 11]. We choose a concrete problem of rotation–vibration of a four-atomic molecule with tetrahedral equilibrium configuration [12, 13] in order to explain the details of our approach.

1.1. Vibrational relative equilibria or nonlinear normal modes.

Montaldi, Roberts, and Stewart [14, 15, 16] gave a general description of periodic solutions near equilibria of symmetric Hamiltonian systems: the so-called nonlinear normal modes or relative equilibria (RE). They related the number of RE to the symmetry group of the system and showed, on several examples of bound systems of vibrating particles, that this number can be significantly larger than the number of vibrational degrees of freedom. This mathematical result was not fully

*Received by the editors January 30, 2003; accepted for publication (in revised form) by D. Holm October 30, 2003; published electronically July 6, 2004. This work was supported by the EU project Mechanics and Symmetry in Europe (MASIE), contract HPRN-CT-2000-00113.
http://www.siam.org/journals/siads/3-3/60001.html
†Université du Littoral, UMR 8101 du CNRS, 59 140 Dunkerque, France (konstantinos@efstathiou.gr, sadovski@univ-littoral.fr, zhilin@univ-littoral.fr).

appreciated by molecular physicists until it was reproduced by an alternate technique [17, 18, 19] based on the analysis of the reduced system in the so-called polyad approximation, a generalization of the approximation used for two-oscillator systems in [20, 21, 22, 23, 24, 25, 26, 27] and others. It was shown that fixed points of the symmetry group action on the reduced phase space correspond to vibrational RE. Later work [28, 29, 30][1] uncovered more fully the correspondence of both approaches and bridged the differences in their tools and terminology.

1.2. Rotational RE or stationary axes of rotation. Similar analysis of stationary points of the reduced rotational system [31, 32, 33, 34, 35, 36, 37, 38, 39, 40, 41, 42, 43] was initiated in molecular physics even before the analysis of vibrational RE. In terms of symmetric Hamiltonian systems [45, 46, 44], this analysis is equivalent to studying rotational RE [28, 29]. This was demonstrated in the recent study [12] of the rotational structure of the tetrahedral molecule P_4 [47],[2] where the energy of rotational RE is derived from the parameters of the internuclear potential. Our present analysis extends the method in [12] to rotation–vibration systems.

1.3. Applications in molecular physics and spectroscopy. Classical analysis of different kinds of RE is used for the description of molecular energy level spectra on the basis of the classical quantum correspondence principle, which links the topological description of the classical dynamical system to such qualitative aspects of quantum spectra as existence of bands, polyads, clusters, and their persistence under small modifications of parameters. Some of these qualitative characteristics are discussed in the present paper. Review articles [48, 49, 50, 51, 52, 53][3] give more examples of molecular applications and initiation to formal theory.

Much of the work in molecular spectroscopy is done using so-called effective model Hamiltonians H_{eff}, which describe explicitly only a fraction of degrees of freedom of the system and treat other degrees effectively. In other words, H_{eff} describe reduced systems, where reduction is based on a model assumption of approximate separability and/or approximate dynamical symmetries. Equilibria (stationary points) of H_{eff} are RE of the initial system.

In practice, reduction often remains only an abstract theoretical possibility because parameters in the full initial molecular Hamiltonian are unknown. So, parameters of H_{eff} are simply fitted to experimental data. Classical analogues of such phenomenological model Hamiltonians can be constructed if excitation is sufficiently high to validate the classical limit. When, as it is often the case, only some degrees of freedom described by H_{eff} (e.g., rotation) can be meaningfully treated as classical, the rest (e.g., vibration) is kept quantum. The energies of such hybrid "semiquantum" systems are eigenvalues that depend on the dynamical variables of the classical subsystem. The most well-known example of semiquantum energy is the rotational energy surfaces of vibration-rotation systems [36, 35, 41].

[1]The approach of Montaldi and Roberts is less oriented to the reduced problem and thus can be potentially extended to molecules in which separation of vibration and rotation and the introduction of the molecule-fixed frame is problematic. For the relatively rigid molecules, we consider their approach as being equivalent to ours.

[2]Among the few different molecules of type A_4, the phosphorus P_4 is studied experimentally; see [47].

[3]Our approach follows closely the ideas in [48, 49, 50], which review group actions and their applications in physics.

The semiquantum approach turned out to be very fruitful, and numerous vibration-rotation systems at low vibrational excitation were analyzed in great detail [37, 38, 18, 54, 55, 56, 42, 57, 43, 58]. In particular, typical (universal) modifications of the cluster structure of the energy level spectrum, or quantum bifurcations, were described in terms of modifications of the set of stationary points of the energy surfaces. Direct, explicit relation of these stationary points to classical RE was established recently in [58, 13]. Other important qualitative quantum phenomena include rearrangements (crossings) of energy level bands [59, 43, 60] and quantum monodromy [61, 62], which are interpreted as crossings of semiquantum energies and are also related to classical RE [60, 63, 64, 65].

1.4. Main idea. We combine recent theories of rotational RE and vibrational nonlinear normal modes in order to study the rotation–vibration problem. Using symmetry and topology, we find particular solutions (critical orbits) common to a whole class of model systems with given symmetry and with different potentials. Subsequently, we define a concrete potential, normalize the classical system, and construct explicitly the effective Hamiltonian H_{eff}. Using this Hamiltonian, we obtain quantitative predictions for concrete molecular models, which illustrate general qualitative results. We explain our approach in the example of rotation–vibration of the four-atomic homonuclear molecule A_4 with tetrahedral equilibrium configuration [47].

2. Basic aspects of the analysis. We review certain general definitions, which are used later in the paper, and give the plan of the analysis.

2.1. Symmetry group T_d and its extensions. Along with translation and rotational symmetry, which are present for any isolated finite-particle system in the absence of external fields, each molecule possesses its own internal symmetry related to the existence of identical particles. The symmetry group of our system originates from the spatial symmetry group T_d of the tetrahedral equilibrium configuration of A_4 and momentum reversal $\mathcal{T}$, which in the original system sends (q, p) to $(q, -p)$, and is discussed in more detail in section 3.1. Our initial Hamiltonian is invariant with respect to these symmetries. As an abstract group, T_d is the permutation group of four identical objects. We use the Schönflis point group notation [67, 66], which is standard in molecular physics. Irreducible representations of T_d are most frequently labeled in molecular physics as A_1, A_2 (one-dimensional), E (two-dimensional), and F_1, F_2 (three-dimensional).

2.2. Vibrational degrees of freedom of an A_4 molecule. The A_4 molecule has six vibrational degrees of freedom, which constitute the nondegenerate "breathing" mode A_1, and the doubly and triply degenerate modes E and F_2. The spectroscopic notation of these modes is $\nu_1^{A_1}$, ν_2^{E}, $\nu_3^{F_2}$. We use a simplified notation for the coordinates and conjugate momenta of the modes given in Table 1 and we also use classical complex oscillator variables

$$z = q + ip, \quad \bar{z} = q - ip. \tag{2.1}$$

The zero order vibrational Hamiltonian H_0 of A_4 represents a 1-oscillator, a 1:1 oscillator, and a 1:1:1 oscillator with frequencies ω_{A_1}, ω_E, and ω_{F_2}, respectively.

2.3. Rotation–vibration Hamiltonian. Assuming that the static equilibrium configuration of A_4 about which the atoms are vibrating is well defined and the amplitudes of vibrations

Table 1

Notation for vibrational and rotational dynamical variables of the A_4 molecule. Expression of angular momenta j_α in terms of dynamical variables of a two-dimensional oscillator (Schwinger representation) is used in this table and throughout the paper.

Subsystem	Traditional notation	This paper
F_2 mode	$q_\alpha^{F_2}$, $p_\alpha^{F_2}$, $\alpha = x, y, z$	q_i, p_i, $i = 1, 2, 3$
E mode	q_α^{E}, p_α^{E}, $\alpha = a, b$ or $1, 2$	q_i, p_i, $i = 4, 5$
A_1 mode	q^{A_1}, p^{A_1}	q_a, p_a
rotation	momenta j_α, $\alpha = x, y, z$	q_i, p_i, $i = 6, 7$

are small, we can separate molecular rotation and define the frame rotating with the molecule. The molecule is isolated, external fields are absent, and translation of the center of mass is therefore excluded.

To derive the rotation–vibration Hamiltonian H, we can follow the procedure described in Chapter 11 of [1] and, more rigorously, in Chapter 7.10 of [68]. The molecule-fixed frame is related to the equilibrium configuration by the Eckart conditions. The kinetic energy T is a complicated function

$$2T = \sum_i m_i \left[(\Omega \wedge (\mathbf{R}_i^0 + \mathbf{r}_i))^2 + \dot{\mathbf{r}}_i^2 + 2\Omega(\mathbf{r}_i \wedge \dot{\mathbf{r}}_i) \right] \tag{2.2}$$

of small vibrational displacement velocities and angular velocities defined with respect to this frame. The intramolecular potential U can be simply written in terms of vibrational coordinates. The Hamiltonian form requires rotational angular momenta j, defined in the molecule-fixed frame, and vibrational coordinates q and momenta p.

To put the initial Hamiltonian in the form suitable for normalization, we Taylor expand $H = T(q, p, j) + U(q)$ in q and rescale (p, q) to bring the harmonic part to the standard form. We then express the components of $\mathbf{j}$ in terms of coordinates and momenta of the auxiliary two-dimensional harmonic oscillator in order to treat vibrational and rotational variables in the same way and use complex variables z in (2.1). The resulting formal power series expression

$$H = \omega(H_0 + \epsilon H_1 + \epsilon^2 H_2 + \epsilon^3 H_3 + \cdots) \tag{2.3}$$

is the starting point of the normal form transformation.

We use the concrete example of the phosphorus molecule P_4 with the tetrahedral equilibrium configuration and harmonic atom–atom bond potential [13] to illustrate our results. The only two molecular parameters in this example are the energy scale ω and the dimensional smallness parameter $\epsilon = (kmr)^{-1}$ in the series expansion. Here r, m, and k stand for the interatomic distance, the mass of the atoms, and the force constant of the potential, respectively. The values of ϵ and ω can be used as phenomenological parameters to reproduce experimental data qualitatively: $\epsilon \approx 2 \times 10^{-2}$ and $\omega \approx 329$ cm^{-1} for P_4 [13].

2.4. Reduced system. The approximate dynamical symmetry of the system with Hamiltonian (2.3) is defined by the zero order term H_0. We suppose that the frequencies ν_{A_1}, ν_E, and ν_{F_2} are incommensurate; i.e., we assume the absence of any resonances between different

vibrational modes. In such a case, we can introduce reduced phase spaces for each of the subsystems simultaneously. The total reduced phase space is the product of these spaces. The normal form H_{eff} is an effective rotation–vibration Hamiltonian describing polyads of nonresonant modes A_1, E, and F_2. For simplicity, we neglect the A_1 mode (i.e., we set $q^{A_1} = p^{A_1} = 0$) and focus on modes E and F_2.

2.4.1. Rotational subsystem; rotational space $\mathbb{S}^2$. Conservation of the total angular momentum is the consequence of the isotropy of physical space (in the absence of external fields). The rotational dynamical variables j_α ($\alpha = 1, 2, 3$) are subjected to the constraint $j_1^2 + j_2^2 + j_3^2 = \text{const}$ and the rotational phase space is a two-dimensional sphere $\mathbb{S}^2$, which can be constructed in the space $\mathbb{R}^3$ with coordinates j_α. For the auxiliary two-dimensional oscillator, used to represent the momenta j_α (Table 1), the restriction $\mathbf{j}^2 = \text{const}$ is equivalent to fixing the sum of two actions.

2.4.2. E-mode subsystem, vibrational space $\mathbb{C}P^1 \sim \mathbb{S}^2$. Exploiting the well-known equivalence of the two-dimensional 1:1 harmonic oscillator and an angular momentum system, we introduce vibrational angular momenta v_1, v_2, v_3 [69, 20, 21]. The internal structure of vibrational polyads formed by the doubly degenerate vibrational mode E can be described in terms of these dynamical variables. The E-mode polyad sphere $\mathbb{S}^2$ is defined by the equation

$$v_1^2 + v_2^2 + v_3^2 = n_e^2 = \text{const}$$

in the ambient space $\mathbb{R}^3$ with coordinates (v_1, v_2, v_3). Any point on this sphere is uniquely represented by the values of (v_1, v_2, v_3) if we keep in mind that $v_1^2 + v_2^2 + v_3^2$ is a constant. The diffeomorphic space $\mathbb{C}P^1$ can be defined in $C_2 - \{0\}$ using the equivalence class of points $z_4{:}z_5$. Two complex numbers (z_4, z_5) can be used as coordinates on $\mathbb{C}P^1_{n_e}$ if their modules are restricted as

$$|z_4|^2 + |z_5|^2 = 2n_e$$

and all pairs (z_4, z_5), which differ in a common phase factor $e^{i\phi}$, correspond to the same point of $\mathbb{C}P^1$. For example, coordinates $(v_1, v_2, v_3) = (0, 1, 0)$ and $(z_4, z_5) = (1, -i) = (e^{i\phi}, e^{i\phi - \pi/2})$ define the same point.

2.4.3. F_2-mode subsystem; vibrational space $\mathbb{C}P^2$. Generalization of the above construction for the F_2-mode 1:1:1 oscillator [17, 18, 70] leads to the reduced phase space $\mathbb{C}P^2_{n_f}$. The approximate integral of motion equals

$$\tfrac{1}{2}(z_1\bar{z}_1 + z_2\bar{z}_2 + z_3\bar{z}_3) = n_f \approx \text{const},$$

and (z_1, z_2, z_3) can be used as coordinates on $\mathbb{C}P^2$. In fact, we can define a point on the $\mathbb{C}P^k$ space as an equivalence class of points on C_{k+1} given by their homogeneous coordinates $z_1 : z_2 : \cdots : z_{k+1}$ or, equivalently, as a class of points on $(z_1, z_2, \ldots, z_{k+1}) \in C_{k+1}$ defined up to a common phase $(z_1, z_2, \ldots, z_{k+1}) \sim e^{i\phi}(z_1, z_2, \ldots, z_{k+1})$ and such that $|z_1|^2 + |z_2|^2 + \cdots + |z_{k+1}|^2$ is a constant.

2.4.4. Full reduced phase space $\mathbb{C}P^2 \times \mathbb{C}P^1 \times \mathbb{S}^2$. Before reduction, our initial molecular system has five vibrational degrees of freedom (if the nondegenerate A_1 mode is neglected) and two auxiliary oscillatory degrees of freedom introduced to describe the rotational subsystem. Three independent reductions fix the strict integral of motion j (the amplitude of the total angular momentum) and polyad integrals n_e and n_f of the doubly degenerate mode E and the triply degenerate mode F_2. The reduced system is left with only four degrees of freedom. Reduction makes the topology of the reduced phase space more complicated. The total reduced space is a direct product of the rotational phase sphere, $\mathbb{S}^2_j$, E-mode vibrational polyad sphere $\mathbb{C}P^1_{n_e} \sim \mathbb{S}^2$, and F_2-mode vibrational polyad phase space $\mathbb{C}P^2_{n_f}$. Omitting extra indexes and shortening the notation, we represent the topology of the reduced phase space simply as $\mathbb{C}P^2 \times \mathbb{C}P^1 \times \mathbb{S}^2$, where $\mathbb{S}^2$ and $\mathbb{C}P^1$ stand for the rotational and vibrational E-mode phase spaces, respectively.

2.4.5. Normal form. Once the Hamiltonian function H is in the oscillator form (2.3), we can normalize it using the standard Lie transform method [71, 72, 73, 74]. All odd orders [odd degrees in $(z, \bar{z})$] vanish in the normal form

$$\mathcal{H}_{\text{nf}} = \omega(H_0 + \epsilon^2 \mathcal{H}_2 + \epsilon^4 \mathcal{H}_4 + \epsilon^6 \mathcal{H}_6 + \cdots), \tag{2.4}$$

which is a power series in ϵ^2. To obtain the reduced Hamiltonian H_{eff}, the terms $\mathcal{H}_{2k}$ in (2.4) should be expressed as functions of basic invariant polynomials (of all generators of the algebra of invariant polynomials) on the reduced phase space $\mathbb{C}P^2 \times \mathbb{C}P^1 \times \mathbb{S}^2$. Due to algebraic dependencies between generators (or "sygyzies") a special polynomial basis should be constructed. A general solution to this problem is provided by a Gröbner basis. Two more specialized polynomial bases—an integrity basis used in invariant theory, and a tensorial basis used by spectroscopists to represent effective Hamiltonians—can be used. We further discuss these bases in section 6.4.

2.5. Scheme of the analysis. Our analysis of a finite-particle quantum system includes several steps: (i) construction of the initial complete classical Hamiltonian H and of the corresponding quantum operator; (ii) reduction of H, taking into account strict and approximate integrals of motion, i.e., the "model"; (iii) analysis of classical RE, relative periodic orbits, and invariant submanifolds;

(iv) interpretation in terms of quantum energy spectrum. Each step has a general part and a concrete part. Many important general results follow from the topology of the reduced phase space and the symmetry group action on it, i.e., from the model.

In the first half of the paper, which includes sections 4 and 5, we find as much information about our system as possible before any concrete interaction potential bounding the particles is introduced explicitly and even before any dynamics is studied. After establishing the topology of the reduced phase space $\mathbb{C}P^2 \times \mathbb{C}P^1 \times \mathbb{S}^2$ and the invariance symmetry group $T_d \times \mathcal{T}$ of our system, we study the action of the group $T_d \times \mathcal{T}$ on $\mathbb{C}P^2 \times \mathbb{C}P^1 \times \mathbb{S}^2$. To this end, we first consider the action on the individual factor spaces $\mathbb{C}P^2$, $\mathbb{C}P^1$, and $\mathbb{S}^2$ and then extend it to the full reduced space. Time reversal $\mathcal{T}$ and other reversing symmetries, which include $\mathcal{T}$, are antisymplectic and should be treated differently from purely spatial symplectic symmetries.

We assume that the reduced Hamiltonian H_{eff} is a generic $T_d \times \mathcal{T}$ invariant Morse function on $\mathbb{C}P^2 \times \mathbb{C}P^1 \times \mathbb{S}^2$. The RE of our system are stationary points of H_{eff}, which exist anywhere

Table 2

Classes of conjugated and invariant subgroups of the $T_d \times \mathcal{T}$ group. Part I.

	Class[4]	Structure[5]	Description and comments
	Subgroups of order 1		
1	C_1	$\{1\}$	Trivial subgroup.
	Subgroups of order 2		
1	$\mathcal{T}$	$\{1, \mathcal{T}\}$	Momentum (or time) reversal, also denoted as Z_2.
6	C_s	$\{1, \sigma^\alpha\}$	Reflection in a plane, T_d has six conjugated operations σ^α.
6	$\mathcal{T}_s$	$\{1, \mathcal{T}_s\}$	Simultaneous reflection and time reversal,[8] also denoted as $(\sigma\mathcal{T})$ or (σZ_2).
3	C_2	$\{1, C_2\}$	Rotation by π around one of axes S_4^a, $a = (x, y, z)$.
3	$\mathcal{T}_2$	$\{1, \mathcal{T}_2\}$	Rotation by π and time reversal,[6] also denoted as $(C_2\mathcal{T})$ or $(C_2 Z_2)$.
	Subgroups of order 3		
3	C_3	$\{1, C_3, C_3^2\}$	Cyclic rotational subgroups corresponding to four different C_3 axes of the T_d group.
	Subgroups of order 4		
1	D_2	$\{1, C_2^x, C_2^y, C_2^z\}$	An invariant subgroup of the T_d group.
3	S_4	$\{1, S_4, C_2, S_4^3\}$	Cyclic groups generated by the S_4^a operations $a = (x, y, z)$.
3	$\mathcal{T}_4$	$\{1, \mathcal{T}_{+4}, C_2, \mathcal{T}_{-4}\}$	Cyclic groups generated by the $S_4^a \circ \mathcal{T} = \mathcal{T}_{+4}^a$ operations.[9]
3	$C_2 \times \mathcal{T}_2$	$\{1, C_2^a, \mathcal{T}_2^b, \mathcal{T}_2^c\}$	(a, b, c) is one of the three cyclic permutations of (x, y, z).[6]
6	$C_s \times \mathcal{T}_2$	$\{1, \sigma^{a_1}, \mathcal{T}_2^a, \mathcal{T}_s^{a_2}\}$	These correspond to six different choices of the σ^{a_1} symmetry plane.[6,7,8]
3	C_{2v}	$\{1, C_2^a, \sigma^{a_1}, \sigma^{a_2}\}$	Subgroup of T_d. Axis a is one of (x, y, z).[7]
3	$C_2 \times \mathcal{T}_s$	$\{1, C_2^a, \mathcal{T}_s^{a_1}, \mathcal{T}_s^{a_2}\}$	Obtained from C_{2v} by combining two reflections and time reversal[7,8]
3	$C_2 \times \mathcal{T}$	$\{1, C_2, \mathcal{T}, \mathcal{T}_2\}$	direct product of C_2^a and time reversal. Axis a is one of (x, y, z)[6]
6	$C_s \times \mathcal{T}$	$\{1, \sigma, \mathcal{T}, \mathcal{T}_s\}$	corresponding to one of the six conjugated symmetry planes σ of the T_d group.[8]
	Subgroups of order 6		
4	$C_3 \times \mathcal{T}$	$\{1, C_3, C_3^2, \mathcal{T}, C_3\mathcal{T}, C_3^2\mathcal{T}\}$	Direct product of C_3 and time reversal $\mathcal{T}$ corresponding to four different axes C_3.
4	C_{3v}	$\{1, 2C_3, 3\sigma\}$	Conjugated subgroups of the spatial symmetry group T_d.
4	$C_3 \wedge \mathcal{T}_s$	$\{1, 2C_3, 3\mathcal{T}_s\}$	This group has $\mathcal{T}_s$ instead of σ_d in C_{3v} and is isomorphic to C_{3v} as an abstract group.[8]

close to the limit of linearization (i.e., at any arbitrarily small perturbation ϵ). In the simplest case, RE are entirely defined by the finite symmetry $T_d \times \mathcal{T}$ of our system. They lie on the *critical orbits* of the $T_d \times \mathcal{T}$ action on $\mathbb{C}P^2 \times \mathbb{C}P^1 \times \mathbb{S}^2$ (they are isolated fixed points of this action). The position of these orbits is independent of the interaction potential (and thus of the particular Hamiltonian). We combine information about critical orbits on each of the factor spaces of $\mathbb{C}P^2 \times \mathbb{C}P^1 \times \mathbb{S}^2$ in order to find all critical orbits on the total space. Considering Morse theory requirements, local symmetry, and local symplectic coordinates, we suggest possible stabilities of RE.

Sections 6–9 focus on the dynamical analysis of the reduced system; concrete applications are presented in sections 10 and 11. As soon as the interaction potential and the Hamiltonian

[4–9] See the footnotes to Table 3 on the following page.

Table 3

Classes of conjugated and invariant subgroups of the $T_d \times \mathcal{T}$ group. Part II.

	Class[4]	Structure[5]	Description and comments
	Subgroups of order 8		
1	$D_2 \times \mathcal{T}$	$\{1, C_2^x, C_2^y, C_2^z, \mathcal{T}, \mathcal{T}_2^x, \mathcal{T}_2^y, \mathcal{T}_2^z\}$	Direct product of the D_2 subgroup of T_d and time reversal $\mathcal{T}$.
3	$C_{2v} \times \mathcal{T}$	$\{1, C_2^a, \sigma^{a_1}, \sigma^{a_2}, \mathcal{T}, \mathcal{T}_2^a, \mathcal{T}_s^{a_1}, \mathcal{T}_s^{a_2}\}$	Direct product of the C_{2v}^a subgroup of T_d and time reversal $a = (x, y, z)$.
3	D_{2d}	$\{1, C_2^a, \sigma^{a_{1,2}}, C_2^{b,c}, S_4^{\pm 1}\}$	Conjugated subgroups of the spatial symmetry group T_d.
3	$C_{2v} \wedge \mathcal{T}_2$	$\{1, C_2^a, \sigma^{a_{1,2}}, \mathcal{T}_2^{b,c}, \mathcal{T}_{\pm 4}^a\}$	Isomorphic to D_{2d} as an abstract group[6,7,9]; two conjugated C_2 rotations and two conjugated S_4 operations of D_{2d} are replaced for their products with $\mathcal{T}$.
3	$D_2 \wedge \mathcal{T}_s$	$\{1, C_2^a, \mathcal{T}_s^{a_{1,2}}, C_2^{b,c}, \mathcal{T}_{\pm 4}^a\}$	Isomorphic to D_{2d} as an abstract group; has two conjugated σ reflections and two conjugated S_4 operations[7,8,9] of D_{2d} replaced for their products with $\mathcal{T}$.
3	$S_4 \times \mathcal{T}$	$\{1, S_4, C_2, S_4^{-1}, \mathcal{T}, \mathcal{T}_4, \mathcal{T}_2, \mathcal{T}_{-4}\}$	Direct product of the cyclic subgroup S_4^a of T_d and time reversal.[9]
3	$S_4 \wedge \mathcal{T}_2$ ($S_4 \wedge \mathcal{T}_s$)	$\{1, C_2^a, \mathcal{T}_s^{a_{1,2}}, \mathcal{T}_2^{b,c}, S_4^{\pm 1}\}$	Isomorphic to D_{2d} as an abstract group; has two conjugated σ_d reflections and two conjugated C_2 rotations[6,7,8,9] of D_{2d} replaced for their products with time reversal $\mathcal{T}$.
	Subgroups of order 12		
1	T		Rotational subgroup of the T_d group.
4	$C_{3v} \times \mathcal{T}$		Direct product of a C_{3v} subgroup of T_d and time reversal.
	Subgroups of order 16		
3	$D_{2d} \times \mathcal{T}$		Direct product of one of the three D_{2d}^a subgroups of T_d and time reversal $\mathcal{T}$.
	Subgroups of index two (order 24)		
1	$T \times \mathcal{T}$		Direct product of T and time reversal, also denoted as $T \times Z_2$.
1	T_d		Tetrahedral group, isomorphic to the permutation group π_4 as an abstract group.
1	$T \wedge \mathcal{T}_s$		Another realization of π_4 obtained from T_d by replacing all improper rotations, namely six σ^α and six S_4 operations, for their products with time reversal $\mathcal{T}$.
	Complete group (order 48)		
1	$T_d \times \mathcal{T}$		Direct product of T_d and time reversal group $\mathcal{T}$.

[4]The leftmost column gives the number of conjugated subgroups in the class.

[5]When all operations in the group correspond to the same rotation axis a, we do not specify the choice of the axis and omit index a.

[6]The operation $\mathcal{T}_2^a = C_2^a \circ \mathcal{T}$ is rotation by π around axes a and time reversal; by convention $a = (x, y, z)$ is one of the axes S_4.

[7]In the T_d group, reflection planes σ^{a_1} and σ^{a_2} intersect on axis C_2^a, where by convention a is one of (x, y, z); in the O_h group these planes are called σ_d.

[8]The operation $\mathcal{T}_s = \sigma \circ \mathcal{T}$ is reflection in one of the six planes σ_d and time reversal; in particular, $\mathcal{T}_s^{a_{1,2}} = \mathcal{T} \circ \sigma^{a_{1,2}}$.

[9]The operations $\mathcal{T}_{\pm 4}^a = \mathcal{T}(S_4^a)^{\pm 1} = \mathcal{T} \circ (S_4^a)^{\pm 1}$, where $a = (x, y, z)$, are operations S_4 or S_4^{-1} combined with time reversal $\mathcal{T}$.

are introduced explicitly, the value of H_{eff} at critical orbits is found. This gives analytic expressions for the energy of RE as a function of actions N_e, N_f, and J. Using these energies, we characterize the multiplet of quantum states with quantum numbers N_e, N_f, and J. We can also use the quantum analogue of H_{eff} in order to compute energies of individual states. Using the concrete Hamiltonian, we can check the Morse indexes of all known RE and find, if necessary, additional RE which do not lie on critical orbits but are nevertheless required by Morse theory conditions.

3. Finite symmetry group of the system. We briefly review the structure of the tetrahedral group T_d and its extension $T_d \times \mathcal{T}$. This group and its subgroups can be considered as magnetic (or color) crystallographic symmetry groups; see Chapter 2 of [67]. Notation for such groups is not commonly established. Below we explain our conventions and describe the abstract group structure of $T_d \times \mathcal{T}$ given by its subgroup lattice (see Tables 2 and 3). We distinguish only the nonconjugate subgroups of $T_d \times \mathcal{T}$ and study certain sublattices corresponding to reduced or partial symmetry groups. This information is vital for understanding the stratification of different reduced phase spaces by the action of $T_d \times \mathcal{T}$ and, in particular, for finding fixed points and invariant subspaces of this action.

3.1. Time reversal symmetry $\mathcal{T}$. Momentum reversal symmetry $\mathcal{T}$ is a nonsymplectic symmetry operation defined for the original physical 3-space coordinates and conjugate momenta as

$$(q, p) \to (q, -p).$$

We denote this operation as $\mathcal{T}$, or simply as Z_2, and imply that its action in each particular context is either known or should be specified. We will distinguish the two types of behavior (two representations of Z_2) with regard to momentum reversal by "parity" indexes g (*gerade*) and u (*ungerade*), respectively.

The symmetry operation $\mathcal{T}$ is also sometimes called *time reversal*. We like to make clear that our operation $\mathcal{T}$ acts only on the phase space variables (q, p) and does not involve time t. This implies that the action of $\mathcal{T}$ on the extended phase space is

$$\mathcal{T} : (q, p, t) \to (q, -p, t).$$

It can be seen that, even when the Hamiltonian of the system is invariant with regard to such operation $\mathcal{T}$, the corresponding equations of motion are not. In fact, this is due to the fact that the action of $\mathcal{T}$ on (q, p) is antisymplectic. Operation $\mathcal{T}$ is an example of reversing symmetries. Another commonly used definition of time reversal extends nontrivially our operation $\mathcal{T}$ to time t:

$$\mathcal{T}_t : (q, p, t) \to (q, -p, -t).$$

This operation preserves the flow of the system with $\mathcal{T}$-invariant Hamiltonian function. In quantum mechanics, operation $\mathcal{T}$ changes the signs of all commutator relations while $\mathcal{T}_t$ preserves these signs.

Of course, one can use either $\mathcal{T}$ or $\mathcal{T}_t$ for the analysis, as long as one understands their action. For example, action of $\mathcal{T}$ and $\mathcal{T}_t$ on equilibria is the same, while their action on the

trajectories $\gamma : t \to (q, p)$ is different. Trajectories $\mathcal{T}(\gamma)$ and $\mathcal{T}_t(\gamma)$ coincide in the phase space but have different direction. Reversing direction is the result of $t \to -t$, which cannot be represented as a geometric transformation of the phase space. Since in most cases we do not work with extended phase spaces, we prefer to define $\mathcal{T}$ as just another transformation of the phase space with coordinates (q, p).

The action of $\mathcal{T} \sim Z_2$ on vibrational normal mode coordinates and conjugate momenta is, of course, the same as on the 3-space q's and p's, and as we go to the complex variables

$$z = q - ip, \quad \bar{z} = q + ip,$$

this action becomes

$$(z_1, z_2, z_3, z_4, z_5) \to (\bar{z}_1, \bar{z}_2, \bar{z}_3, \bar{z}_4, \bar{z}_5). \tag{3.1a}$$

Note that this operation differs from plain "complex conjugation" as shown by

$$z_1 + iz_2 \to \bar{z}_1 + i\bar{z}_2. \tag{3.1b}$$

Molecular angular momentum components (j_1, j_2, j_3) are not invariant with respect to Z_2:

$$(j_1, j_2, j_3) \to (-j_1, -j_2, -j_3). \tag{3.1c}$$

This property of (j_1, j_2, j_3) follows, of course, from the explicit Wilson–Howard definition of rotational angular momenta in terms of particle coordinates and momenta. At the same time, we can simply note that time reversal changes the direction of classical rotation and therefore changes signs of (j_1, j_2, j_3).

3.2. Spatial finite symmetry T_d. The spatial symmetry group of the A_4 molecule is the point group of its tetrahedral equilibrium configuration T_d. This group, and cubic groups O and O_h (and to a lesser extent, T and T_h) are well known to molecular physicists and crystallographers. It is generated by the three-fold rotation C_3 and the four-fold inversion rotation S_4. The latter can be realized as $C_4 \circ C_i$, a rotation C_4 by angle $\pi/2$ followed by a 3-space inversion C_i, or alternately as rotation by angle $-\pi/2$ followed by reflection in the plane orthogonal to the rotation axis. A particular realization of T_d is given in Table 4 and is illustrated in Figure 1. We will use the three symmetry operations in Table 4 for explicit demonstrations later in the paper. Conventionally, axes x, y, and z are chosen as S_4 axes. Three operations S_4 and three inverse operations S_4^{-1} form a class of six conjugate elements. Three operations $C_2 = S_4^2$, which rotate by π about the same axes, form a separate class. Operations C_3, which rotate by $\pm 2\pi/3$ about four diagonal axes, such as axis $[1, 1, 1]$ in Table 4, form one class of eight elements. Finally, there is a class of six reflection planes denoted σ or C_s; each element C_s can be considered as a combination $C_2 \circ C_i$, where axis C_2 is orthogonal to the reflection plane.

3.3. Full finite symmetry group $T_d \times \mathcal{T}$. The total symmetry group of our system is the tetrahedral group T_d extended to include the time reversal operation $\mathcal{T}$. We exploit the isomorphism $T_d \times \mathcal{T} \sim O_h \sim O \times \mathcal{T}$ to explain the notation for symmetry operations and different subgroups of $T_d \times \mathcal{T}$. Table 5 summarizes correspondence of notation for the symmetry operations of the three groups.

Table 4

Matrix representations of basic operations of the T_d group illustrated in Figure 1.

	A_1	A_2	F_2	E	F_1
	z_a		(z_1, z_2, z_3)	(z_4, z_5)	(j_1, j_2, j_3)
$C_3^{[111]}$	1	1	$\begin{pmatrix} 0 & 0 & 1 \\ 1 & 0 & 0 \\ 0 & 1 & 0 \end{pmatrix}$	$\frac{1}{2}\begin{pmatrix} -1 & -\sqrt{3} \\ \sqrt{3} & -1 \end{pmatrix}$	$\begin{pmatrix} 0 & 0 & 1 \\ 1 & 0 & 0 \\ 0 & 1 & 0 \end{pmatrix}$
S_4^z	1	-1	$\begin{pmatrix} 0 & 1 & 0 \\ -1 & 0 & 0 \\ 0 & 0 & -1 \end{pmatrix}$	$\begin{pmatrix} 1 & 0 \\ 0 & -1 \end{pmatrix}$	$\begin{pmatrix} 0 & -1 & 0 \\ 1 & 0 & 0 \\ 0 & 0 & 1 \end{pmatrix}$
C_s^{xy}	1	-1	$\begin{pmatrix} 0 & 1 & 0 \\ 1 & 0 & 0 \\ 0 & 0 & 1 \end{pmatrix}$	$\begin{pmatrix} 1 & 0 \\ 0 & -1 \end{pmatrix}$	$-\begin{pmatrix} 0 & 1 & 0 \\ 1 & 0 & 0 \\ 0 & 0 & 1 \end{pmatrix}$

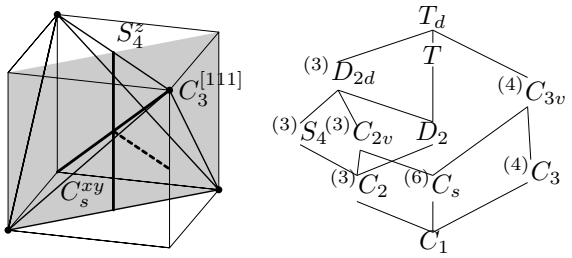

Figure 1. *Basic operations of the T_d point group (left). The symmetry axis C_2 (dashed line) of the O_h and O groups is orthogonal to the C_s reflection plane (shadowed) of T_d. This C_2 should not be confused with axis $C_2 = S_4^2$, which has the same orientation as axis S_4. Right: lattice of conjugate subgroups of the T_d group. Left: superscripts give the number of conjugate subgroups in each class.*

The lattices of conjugate subgroups of the O_h and $T_d \times \mathcal{T}$ groups are shown in Figures 2 and 3, respectively, in order to compare the Schönflis notation for the classes of O_h [67] to our notation of the $T_d \times \mathcal{T}$ classes. The 33 classes of conjugate subgroups of $T_d \times \mathcal{T}$ are arranged according to their order and are further described in Tables 2 and 3. Left superscripts in Figures 2 and 3 indicate, where necessary, the number of conjugate subgroups in the class. Invariant subgroups are unique in their class which needs, therefore, no such superscripts. Subgroups of O_h, which are distinguished by primes, C_{2v}, C'_{2v}, and C''_{2v}, D_{2d} and D'_{2d}, D_{2h} and D'_{2h}, D_2 and D'_2, C_{2h} and C'_{2h}, C_2 and C'_2, C_s and C'_s, are nonconjugate in O_h but become conjugate in the larger group SO(3). Such notation is less informative in comparison with the $T_d \times \mathcal{T}$ notation for the corresponding nonconjugate subgroups, which highlights the differences between the subgroups explicitly.

3.4. Sublattices corresponding to different images of $T_d \times \mathcal{T}$ and broken symmetries.

The action of the symmetry group $T_d \times \mathcal{T}$ on the vibrational E-mode polyad space $\mathbb{C}P^1$ is not effective; the invariant subgroup D_2 forms the kernel, and the image $(T_d \times \mathcal{T})/D_2$ is the group isomorphic (as an abstract group) to $C_{3v} \times \mathcal{T}$ or D_{3h}, see Table 6. We compare the subgroup lattice of $(T_d \times \mathcal{T})/D_2$ in Figure 4, right, to the equivalent lattice of D_{3h} (Figure 4, left) in order to better explain the action of $T_d \times \mathcal{T}$ on $\mathbb{C}P^1$. When characterizing the subgroups of $(T_d \times \mathcal{T})/D_2$ we take into account their extension by the kernel D_2 in order to preserve the

Table 5

Correspondence between classes of conjugate elements of the groups O_h, $T_d \times \mathcal{T}$, and $O \times \mathcal{T}$.

O_h	$T_d \times \mathcal{T}$	$O \times \mathcal{T}$	O_h	$T_d \times \mathcal{T}$	$O \times \mathcal{T}$
1	1	1	C_i	$\mathcal{T}$	$\mathcal{T}$
$8C_3$	$8C_3$	$8C_3$	$8S_6$	$8(\mathcal{T}C_3)$	$8(\mathcal{T}C_3)$
$3C_2$	$3C_2$	$3C_2$	$3\sigma_h$	$3(\mathcal{T}C_2)$	$3(\mathcal{T}C_2)$
$6C_2'$	$6\sigma_d$	$6C_2'$	$6\sigma_d$	$6(\mathcal{T}\sigma_d)$	$6(\mathcal{T}C_2')$
$6C_4$	$6S_4$	$6C_4$	$6S_4$	$6(\mathcal{T}S_4)$	$6(\mathcal{T}C_4)$

Table 6

Homomorphism $T_d \times \mathcal{T} \to D_{3h}$, which defines the group of symmetry transformations of the vibrational reduced polyad phase space $\mathbb{C}P^1$ of the doubly degenerate mode E. Each element in D_{3h} is an image of four elements of $T_d \times \mathcal{T}$. In particular, the identity in D_{3h} is the image of the invariant subgroup D_2 of $T_d \times \mathcal{T}$.

$\{T_d \times \mathcal{T}\}$	$\to$	D_{3h}	$\{T_d \times \mathcal{T}\}$	$\to$	D_{3h}
$\{1, 3C_2\}$	$\to$	1	$\{\mathcal{T}, 3(\mathcal{T}C_2)\}$	$\to$	σ_h
$\{8C_3\}$	$\to$	$2C_3$	$\{8(\mathcal{T}C_3)\}$	$\to$	$2S_3$
$\{6S_4, 6\sigma_d\}$	$\to$	$3C_2$	$\{6(\mathcal{T}S_4), 6(\mathcal{T}\sigma_d)\}$	$\to$	$3\sigma_v$

relation to the $T_d \times \mathcal{T}$ action on the subspaces $\mathbb{C}P^2$ and $\mathbb{S}^2$ (where $T_d \times \mathcal{T}$ acts effectively).

The $T_d \times \mathcal{T}$ group has a number of subgroups whose action on classical phase spaces $\mathbb{C}P^2$ and $\mathbb{S}^2$ was described earlier in [17, 70, 18]; action of the $D_2 \times \mathcal{T}$ group on $\mathbb{C}P^2$ was studied in detail in [70]. The Schönflis notation for spatial finite groups used in these studies can be misleading if the actual spatial-temporal symmetry operations are not defined explicitly. In order to compare our present work to [70] we give in Figure 5 the correspondence of the subgroup lattice of $D_2 \times \mathcal{T}$ to that of the group D_{2h}. These two groups realize the same abstract Abelian group of order 8, and all their subgroups are invariant. As shown in Figure 5, certain invariant subgroups of $D_2 \times \mathcal{T}$ (or D_{2h}) can be assembled in sets of three according to the axes C_2^a, $a = \{x, y, z\}$, of the D_2 group. These subgroups become conjugate when lifted to the higher symmetry group $T_d \times \mathcal{T}$ (or O_h).

4. Group action. When a group element acts on the point x on the space $\mathcal{P}$, it can map x either to a different point x' on $\mathcal{P}$ or to itself. In the latter case the group element belongs to the local symmetry group or *stabilizer* of x. The set of points obtained from x by applying all group elements is called an *orbit*. Orbits of a finite group G are, obviously, finite sets, and the maximum number of points in an orbit of the G action equals the number of group elements or the order $[G]$ of the group. If the stabilizer G_x of the point x is nontrivial, then the number of points in the orbit equals $[G]/[G_x]$. In particular, if x is a fixed point of the group action, it forms a one-point orbit.

Out of all the orbits of the action of the group G on the space $\mathcal{P}$, we distinguish *critical orbits* [75, 76]. The stabilizer of a point x on the critical orbit differs from that of any point in a sufficiently small open neighborhood of x; i.e., points on critical orbits are isolated. As a consequence, these points must be stationary or critical points of any G-invariant function $f(x)$ on $\mathcal{P}$. When $\mathcal{P}$ is a reduced phase space and $f(x)$ is a reduced Hamiltonian H_{eff}, these points correspond to RE of the initial system. This makes finding critical orbits the primary purpose of our group action study [48, 49, 50]. In general, we also look for invariant subspaces

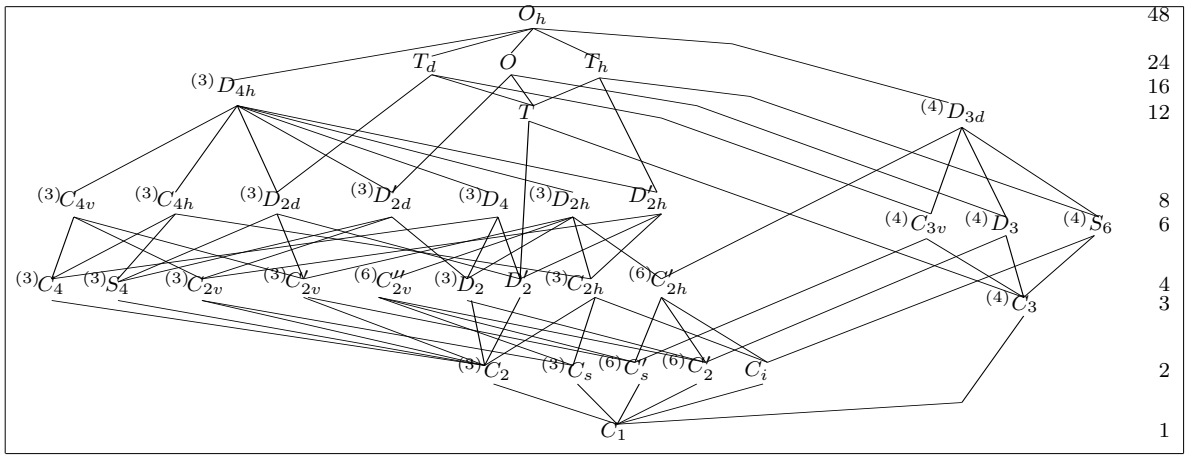

Figure 2. *Lattice of conjugate subgroups of the O_h group. The order of all subgroups on the same row is indicated on the right of the graph.*

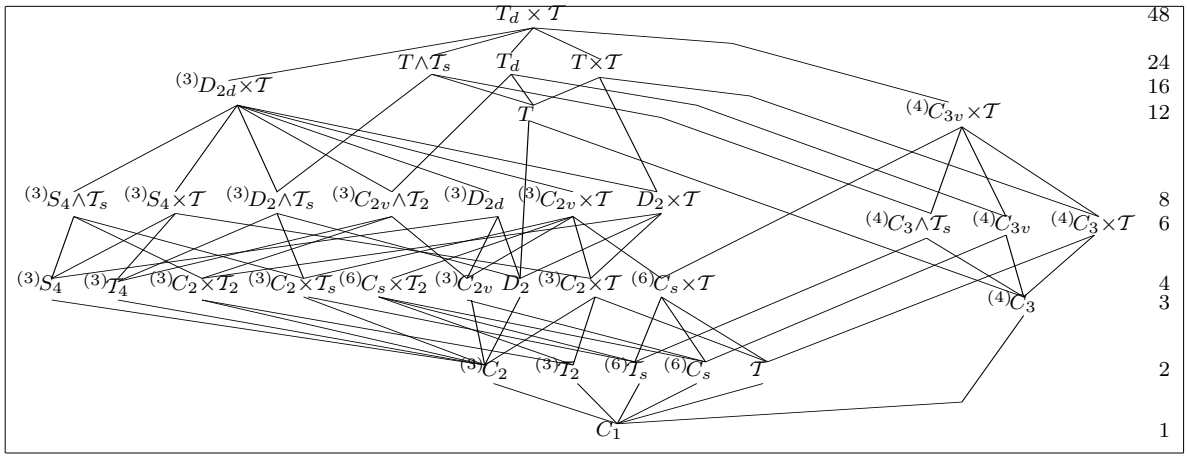

Figure 3. *Lattice of conjugate subgroups of the $T_d \times \mathcal{T}$ group; cf. Figure 2. Shorthand notation $\mathcal{T}_2$, $\mathcal{T}_s$, and $\mathcal{T}_4$ is used for stabilizers $\mathcal{T}C_2$, $\mathcal{T}\sigma_d$, and $\mathcal{T}S_4$; the order of all subgroups on the same row is indicated on the right of the graph.*

of the reduced phase space $\mathcal{P}$—and especially for the invariant subspaces whose stabilizer is a purely spatial symmetry subgroup of G.

The symmetry group T_d was originally defined as a point group of transformations in the Euclidean 3-space $\mathbb{R}^3$ with coordinates (x, y, z), which transform in the same way as components of the F_2 mode (q_1, q_2, q_3). The action of T_d is subsequently extended symplectically on (p_1, p_2, p_3), which transform in the same way as (q_1, q_2, q_3). This defines the action on (z_1, z_2, z_3). At the same time, momentum reversal $\mathcal{T}$ or Z_2 is introduced as an antisymplectic symmetry.

The E-mode variables and rotational variables (j_1, j_2, j_3) transform according to the E and F_1 irreducible representations of the T_d group. The action of the symmetry group in these

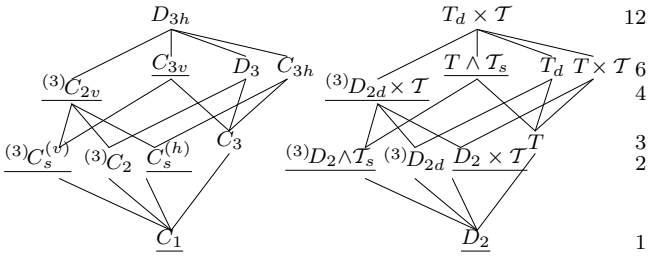

Figure 4. *Left: lattice of conjugate subgroups of the D_{3h} group. Underlined subgroups appear as stabilizers of the strata of the D_{3h} action on the $\mathbb{S}^2$ sphere. Right: part of the lattice of conjugate subgroups common to $T_d \times \mathcal{T}$ and $(T_d \times \mathcal{T})/D_2$. Underlined subgroups appear as stabilizers of the $T_d \times \mathcal{T}$ action on the E-mode polyad reduced phase space $\mathbb{C}P^1 \sim \mathbb{S}^2$.*

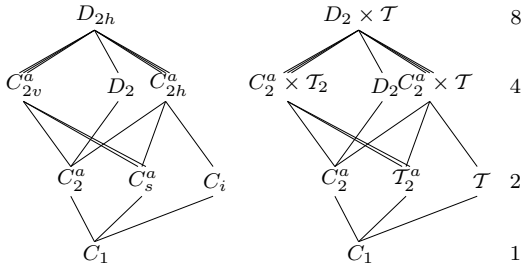

Figure 5. *Subgroup lattices of the D_{2h} group (left) and the $D_2 \times \mathcal{T}$ subgroup of $T_d \times \mathcal{T}$ (right); subgroups distinguished by superscript $a = \{x, y, z\}$ are conjugate in the higher groups O_h and $T_d \times \mathcal{T}$, respectively.*

representations is defined by the *image* of the initial symmetry group. To find the action of the symmetry group T_d and its extension $T_d \times \mathcal{T}$ on different components of the reduced phase space (the F_2-mode space $\mathbb{C}P^2$, the E-mode space $\mathbb{C}P^1$, and the rotational sphere $\mathbb{S}^2$), we first need to know the image of our symmetry group in the corresponding representations. We find the image of the group in the particular representation Γ by acting explicitly on the variables which realize Γ.

Group images and their actions can be very nontrivial even for finite symmetry groups and should be studied with care. Thus the action of spatial inversion on the reduced phase space of our system is equivalent to identity, and as a consequence, it suffices to consider pure rotations C_4 and C_2 of the O group instead of operations S_4 and C_s of the T_d group. We will also see that the image of T_d in the E representation is a smaller group C_{3v} and that its action on the E-mode reduced phase space $\mathbb{C}P^1$ is equivalent to that of a dihedral group D_3. We begin by explaining actions of $T_d \times \mathcal{T}$ on the reduced phase spaces $\mathbb{C}P^2$, $\mathbb{C}P^1$, and $\mathbb{S}^2$ and on the total reduced space $\mathbb{C}P^2 \times \mathbb{C}P^1 \times \mathbb{S}^2$ with the action of the rotation group SO(2) (or C_∞) and its finite subgroups C_k, $k = 2, 3, 4, \ldots$, of which C_2 is a special case, and by explaining the action of time reversal $\mathcal{T}$ (or Z_2). We use operations from Table 4 to illustrate group actions.

4.1. Rotational subsystem: Action of $T_d \times \mathcal{T}$ on $\mathbb{S}^2$. Unlike components of polar vectors (x, y, z) and (q_1, q_2, q_3), the angular momenta (j_1, j_2, j_3) are invariant with regard to the 3-space inversion C_i (i.e., they do not change sign). The image of T_d in the F_1 representation realized by (j_1, j_2, j_3) is an isomorphic group O generated by pure rotations. (This group can

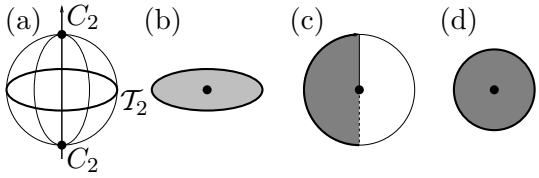

Figure 6. *Action of the $C_2 \times \mathcal{T}$ group on the rotational sphere $\mathbb{S}^2$ and construction of the corresponding orbit space.* (a) *Two points with stabilizer C_2 are shown as filled black circles; points with stabilizer $\mathcal{T}_2$ lie on the circle shown in bold.* (b) *The $\mathcal{T}_2$ symmetry is reduced; all points inside the disc represent two-point orbits.* (c)–(d) *The C_2 and $\mathcal{T}$ symmetries are reduced; the disc is cut and glued conewise. All points in the shaded interior in* (d) *represent generic four-point orbits with stabilizer C_1; the black circle corresponds to the two-point orbit with stabilizer C_2; two-point orbits with stabilizer $\mathcal{T}_2$ form the boundary, which is a one-dimensional stratum $\mathbb{S}^1$.*

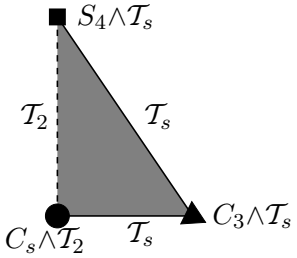

Figure 7. *Space of orbits of the $T_d \times \mathcal{T}$ symmetry group action on the rotational phase space $\mathbb{S}^2$. Critical orbits with stabilizers $S_4 \wedge \mathcal{T}_s$, $C_3 \wedge \mathcal{T}_s$, and $C_s \wedge \mathcal{T}_2$ (C_{4v}, C_{3v}, and C_{2v} in the O_h notation) are shown by the black square, triangle, and disc, respectively. One-dimensional strata with stabilizers $\mathcal{T}_s$ (C_s') and $\mathcal{T}_2$ (C_s) are shown by solid and dashed border lines. Generic C_1 orbits correspond to points in the shaded interior.*

be obtained from T_d if S_4 is replaced with $C_4 = S_4 \circ C_i$ and C_s with $C_2 = C_s \circ C_i$; see Table 5.) On the other hand, time reversal $\mathcal{T}$ changes the signs of all three components of the angular momentum, and therefore (j_1, j_2, j_3) realize the F_{1u} representation of $T_d \times \mathcal{T}$. The image of $T_d \times \mathcal{T}$ in this representation is the group $O \times \mathcal{T}$. The three isomorphic groups $T_d \times \mathcal{T}$, $O \times \mathcal{T}$, and O_h are realizations of the same abstract group. Correspondence of their subgroups and classes of conjugate elements is presented in Figures 2 and 3 and Table 5.

As discussed in section 2.4.1, equation $j^2 = \text{const}$ defines the reduced rotational phase space $\mathbb{S}^2$ as a sphere in the ambient space $\mathbb{R}^3$ with coordinates (j_1, j_2, j_3). The action of $O \times \mathcal{T}$ on this sphere is often represented in terms of the action of the O_h group of transformations of the $\mathbb{R}^3$ space (see Figure 7). The O_h notation, or even shorter O group notation, is used in practically all applications [18, 39, 32, 33, 34] and remains preferred (at least for the study of a purely rotational system) because geometric transformations in $\mathbb{R}^3$ are very commonly known. On the other hand, the $T_d \times \mathcal{T}$ notation properly reflects the actual symmetry of the system and is more adequate.

Any rotation C_k acting on $\mathbb{S}^2$ (as an element of the O_h group of transformations of the ambient space $\mathbb{R}^3$) has *two* fixed points, which are the two diametrically opposite points of $\mathbb{S}^2$ situated on the axis. The two points are mapped into each other by the $\mathcal{T}$ operation (which acts as inversion in $\mathbb{R}^3$) and belong to one orbit. This orbit is critical. Reversing operations $C_k \circ \mathcal{T}$ with $k > 2$ have no fixed points on $\mathbb{S}^2$. The operation $\mathcal{T}_2 = C_2 \circ \mathcal{T}$ acts in $\mathbb{R}^3$ like a symmetry plane σ orthogonal to the C_2 axis. The set of all points on $\mathbb{S}^2$ invariant with regard to $\mathcal{T}_2$ is a circle $\mathbb{S}^1$, which is the intersection of σ and $\mathbb{S}^2$.

As a simple example, consider the action of the $C_2 \times \mathcal{T}$ group on $\mathbb{S}^2$ illustrated in Figure 6

Table 7
Action of $T_d \times \mathcal{T}$ on the rotational sphere $\mathbb{S}^2$.

O_h stabilizer	C_{4v}	C_{3v}	C_{2v}	C_s	C_s'	C_1
$T_d \times \mathcal{T}$ stabilizer	$S_4 \wedge \mathcal{T}_s$	$C_3 \wedge \mathcal{T}_s$	$C_s \wedge \mathcal{T}_2$	$\mathcal{T}_2$	$\mathcal{T}_s$	C_1
Points in orbit	6	8	12	24	24	48
Conjugate stabilizers	3	4	6	3	6	1

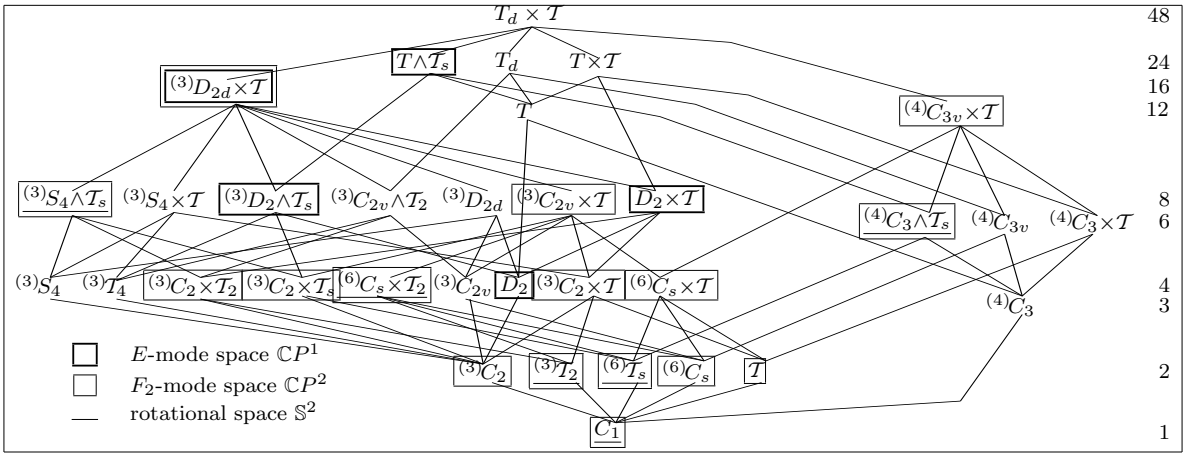

Figure 8. *Lattice of conjugate subgroups of the $T_d \times \mathcal{T}$ group. Subgroups that appear as stabilizers on the reduced phase spaces $\mathbb{S}^2$, $\mathbb{C}P^1$, and $\mathbb{C}P^2$ are underlined, bold framed, and framed, respectively. The order of all subgroups on the same row is indicated on the right of the graph; cf. Figure 3.*

(with the C_2 axis along the z axis). There are three types of orbits: a two-point orbit with stabilizer C_2, a one-dimensional stratum of two-point orbits with stabilizer $\mathcal{T}_2$, and a two-dimensional stratum with trivial stabilizer. The space of orbits is a punctured closed disc shown in Figure 6, right.

The action of $T_d \times \mathcal{T}$ on $\mathbb{S}^2$ is described in Table 7 and the space of orbits is shown in Figure 7. Out of 33 classes of the conjugate subgroups of this group, six appear as stabilizers (see Figure 8). There are 26 fixed points on $\mathbb{S}^2$, which form three critical orbits with stabilizers $S_4 \wedge \mathcal{T}_s \sim C_{4v}$, $C_3 \wedge \mathcal{T}_s \sim C_{3v}$, $C_s \wedge \mathcal{T}_2 \sim C_{2v}$. Note that, as in the case of any C_k action, each specific stabilizer in the class of conjugate stabilizers corresponds to two different points in the orbit.

4.2. *E*-mode vibrational subsystem: Action of $T_d \times \mathcal{T}$ on $\mathbb{C}P^1 \sim \mathbb{S}^2$. We find the image of the spatial symmetry group T_d in the E representation by considering the action of T_d on the plane $\mathbb{R}^2$ with coordinates (q_4, q_5) or on a complex plane with coordinates (z_4, z_5). From Table 4 we can see that operation $C_2^z = (S_4^z)^2$ acts trivially on this plane, operation C_3 rotates by $2\pi/3$ about the origin, while operations S_4^z and C_s^{xy} have the *same* action on $\mathbb{R}^2$: they reflect with respect to the axis $\{q_5 = 0\}$ passing through the origin. It follows that the image of T_d is a group D_3 (or C_{3v}).

The action of the full symmetry group $T_d \times \mathcal{T}$ on the reduced vibrational phase space $\mathbb{C}P^1$ is equivalent to that of $C_{3v} \times \mathcal{T}$. The kernel of the homomorphism $T_d \times \mathcal{T} \to C_{3v} \times \mathcal{T}$

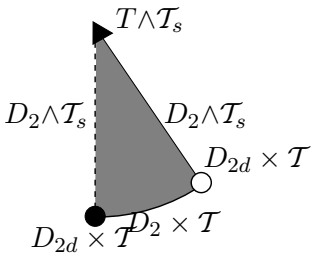

Figure 9. *Space of orbits of the $T_d\times\mathcal{T}$ symmetry group action on the E-mode reduced phase space $\mathbb{C}P^1\sim\mathbb{S}^2$. Triangle and circles mark critical orbits with stabilizers $T\wedge\mathcal{T}_s$ and $D_{2d}\times\mathcal{T}$ (C_{3v} and C_{2v} in the D_{3h} notation), respectively. One-dimensional strata with stabilizers $D_2\wedge\mathcal{T}_s$ and $D_2\times\mathcal{T}$ (σ_h) form the boundary of the variety, while generic D_2 orbits correspond to points in the interior.*

Table 8

Action of $T_d\times\mathcal{T}$ on the polyad phase space $\mathbb{C}P^1$ of the E mode; notation is explained in Table 6.

D_{3h} stabilizer	C_{3v}	C_{2v}	$C_s^{(v)}$	$C_s^{(h)}$	C_1
$(T_d\times\mathcal{T})$ stabilizer	$T\wedge\mathcal{T}_s$	$D_{2d}\times\mathcal{T}$	$D_2\wedge\mathcal{T}_s$	$D_2\times\mathcal{T}$	D_2
Number of					
points in orbit	2	3	6	6	12
conj. stabilizers	1	3	3	1	1
orbits	1	2	∞	∞	∞^2

is D_2, i.e., the order four invariant subgroup of $T_d\times\mathcal{T}$ described in Table 2. The action of $C_{3v}\times\mathcal{T}$ on the E-mode vibrational phase sphere $\mathbb{S}^2\sim\mathbb{C}P^1$ can be better visualized as the natural action of the point group D_{3h} of transformations of the Euclidean 3-space $\mathbb{R}^3$ on a sphere embedded in this space. The correspondence between the D_{3h} notation and symmetry operations of $T_d\times\mathcal{T}$ is given in Figure 4 and Table 6.

All strata of the $T_d\times\mathcal{T}$ action on the E-mode space $\mathbb{C}P^1\sim\mathbb{S}^2$ are described in Figure 9 and Table 8. The D_{3h} analogy makes understanding this stratification straightforward. We can essentially use the approach in section 4.1 and, of course, earlier results for classical C_{3v} symmetric rotational systems (see section 1), such as a triatomic molecule with equilateral equilibrium configuration. For example, any rotation in D_{3h} has two fixed points on $\mathbb{S}^2$; the particular C_3 rotation in Table 4 has fixed points with coordinates $v=(0,\pm1,0)$ or equally $(z_4,z_5)=(1,\mp i)$, which form one two-point critical orbit with stabilizer $T\wedge\mathcal{T}_s$. The stabilizer of the two other critical orbits is $D_{2d}\times\mathcal{T}$. Note that the points in the $T\wedge\mathcal{T}_s$ orbit have exactly the same stabilizer (because $T\wedge\mathcal{T}_s$ is an invariant subgroup), whereas the three points in each $D_{2d}\times\mathcal{T}$ orbit have different conjugate stabilizers.

Dynamical variables of the reduced E-mode system and local canonical coordinates near points on critical orbits on $\mathbb{C}P^1$ can be classified using irreducible representations of both $T_d\times\mathcal{T}$ and D_{3h}. Thus, vibrational angular momenta $\{v_1,v_2,v_3\}$ introduced in section 2.4.2 span the natural reducible representation $A_{2u}\oplus E_g$ of the $T_d\times\mathcal{T}$ group (see section 7), which corresponds to $A_2''\oplus E'$ of the D_{3h} group. Table 9 gives the relation between the irreducible representations of the $T_d\times\mathcal{T}$ group and its subgroup $(T_d\wedge\mathcal{T})/D_2$. This correspondence should be taken into account in order to study vibration-rotation dynamics on $\mathbb{C}P^1\times\mathbb{S}^2$, where the group $T_d\times\mathcal{T}$ acts as D_{3h} and O_h on the vibrational subspace $\mathbb{C}P^1$ and rotational subspace $\mathbb{S}^2$. We should warn the reader that D_{3h} is *not* a subgroup of O_h. We simply use standard

Table 9

Reduction of irreducible representations of $T_d \times \mathcal{T}$ ($\sim O_h$) into those of $(T_d \times \mathcal{T})/D_2$ ($\sim D_{3h}$). The correspondence is written initially for O_h and its D_{3d} subgroup and is further extended using the isomorphism $D_{3d} \leftrightarrow D_{3h}$.

$T_d \times \mathcal{T} \to$		$(T_d \times \mathcal{T})/D_2$		$T_d \times \mathcal{T} \to$		$(T_d \times \mathcal{T})/D_2$	
$\sim O_h$	$\to$	D_{3d}	$\sim D_{3h}$	$\sim O_h$	$\to$	D_{3d}	$\sim D_{3h}$
A_{1g}	$\to$	A_{1g}	A_1'	A_{1u}	$\to$	A_{1u}	A_1''
A_{2g}	$\to$	A_{2g}	A_2'	A_{2u}	$\to$	A_{2u}	A_2''
E_g	$\to$	E_g	E'	E_u	$\to$	E_u	E''
F_{1g}	$\to$	$A_{1g} \oplus E_g$	$A_1' \oplus E'$	F_{1u}	$\to$	$A_{1u} \oplus E_u$	$A_1'' \oplus E''$
F_{2g}	$\to$	$A_{2g} \oplus E_g$	$A_2' \oplus E'$	F_{2u}	$\to$	$A_{2u} \oplus E_u$	$A_2'' \oplus E''$

notation for irreducible representations of O_h and D_{3h}.

4.3. F_2-mode vibrational subsystem: Action on $\mathbb{C}P^2$. Action of several different point symmetry groups on the $\mathbb{C}P^2$ space was studied by Zhilinskiĭ [17]. An example of the extension to a larger group including the time reversal $\mathcal{T}$ was given later in [70]. We summarize the results of [17] for the symmetry groups O and T_d and then take the $\mathcal{T}$ element into account.

The action of T_d on the 3-space with coordinates (q_1, q_2, q_3), which span the irreducible representation F_2, is effective, and the image corresponds to the whole group. Of course, the same holds for (p_1, p_2, p_3) and (z_1, z_2, z_3). In order to verify that the action of $T_d \times \mathcal{T}$ on the $\mathbb{C}P^2$ space is also effective [17], we can consider the representation realized by $(z_1, z_2, z_3, \bar{z}_1, \bar{z}_2, \bar{z}_3)$, act by operations in $T_d \times \mathcal{T}$ (use (3.1a) and Table 4), and take the $\mathbb{C}P^2$ restrictions (section 2.4.3) into account. In particular, due to the common phase equivalence, points (z_1, z_2, z_3) and $(-z_1, -z_2, -z_3)$ are the same on $\mathbb{C}P^2$; i.e., the image of the 3-space inversion is identity. It follows that the images of the T_d, O, and O_h point symmetry groups are the *same* (up to an isomorphism between the stabilizers), and we can simply use the O group whose elements are proper rotations.

For any rotation axis C_k, we should consider a point in $\mathbb{C}P^2$ lying on the axis and a subspace orthogonal to the axis. The former is obviously an isolated fixed point, while the latter is a $\mathbb{C}P^1 \sim \mathbb{S}^2$ subspace of $\mathbb{C}P^2$, which contains other C_k symmetric points. As an example, take rotation about axis z_1 that can be most easily understood in the coordinates

$$z_1, \quad \zeta = \frac{1}{\sqrt{2}}(z_2 + iz_3), \qquad \zeta' = \frac{1}{\sqrt{2}}(z_2 - iz_3),$$

subject to the same restriction

$$|z_1|^2 + |\zeta|^2 + |\zeta'|^2 = 1$$

and common phase identification

$$(z_1, \zeta, \zeta') \equiv (z_1 e^{i\phi}, \zeta e^{i\phi}, \zeta' e^{i\phi})$$

as the initial (z_1, z_2, z_3) in section 2.4.3. When we rotate about z_1 by angle $\varphi \neq 0$ so that

$$(z_1, \zeta, \zeta') \to (z_1, \zeta e^{i\varphi}, \zeta' e^{-i\varphi}),$$

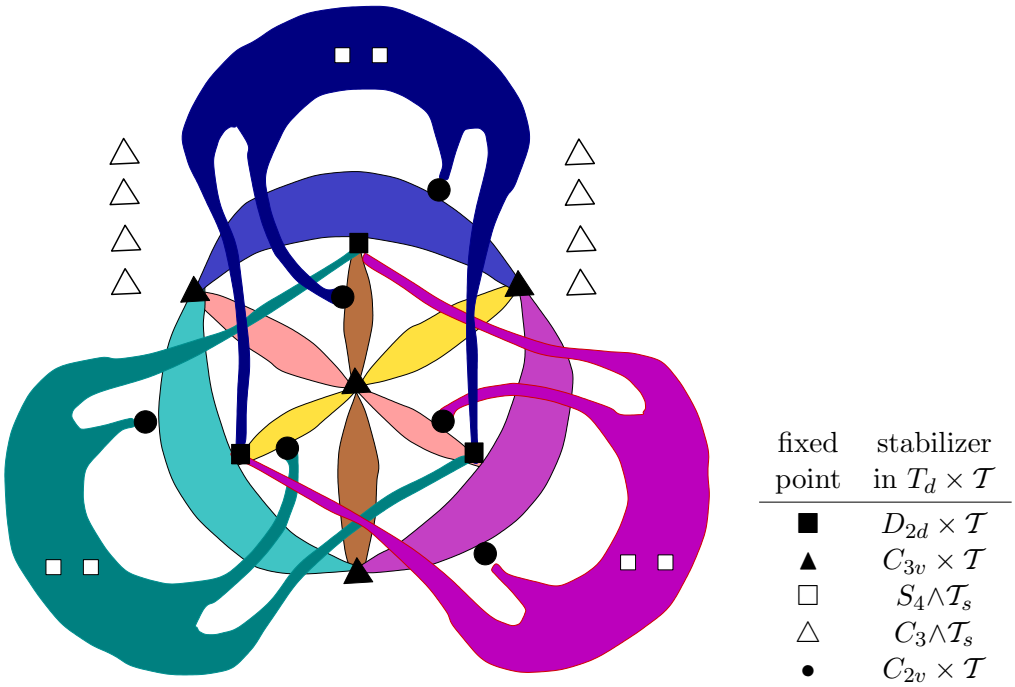

Figure 10. *Orbits of the O (and $T_d \times \mathcal{T}$) group action on the complex projective space $\mathbb{C}P^2$ according to Zhilinskiĭ [17]. Colored areas represent nine C_2-invariant spheres, which belong to the classes of three and six spheres (according to their stabilizers).*

the fixed point coordinates should satisfy equations

$$(z_1, \zeta e^{i\varphi}, \zeta' e^{-i\varphi}) = (z_1 e^{i\phi}, \zeta e^{i\phi}, \zeta' e^{i\phi}).$$

For all $\varphi \neq \pi$ (and in particular for all $\varphi = 2\pi/k$ with $k > 2$) we have three isolated solutions

$$A : \zeta = \zeta' = 0, \quad B : z_1 = \zeta = 0, \quad \text{and} \quad C : z_1 = \zeta' = 0;$$

i.e., two of the three coordinates should vanish. When $\varphi = \pi$ (rotation C_2) our equations become

$$(z_1, -\zeta, -\zeta') = (z_1 e^{i\phi}, \zeta e^{i\phi}, \zeta' e^{i\phi}).$$

We should take the point $(1, 0, 0)$ and the whole $\mathbb{C}P^1$ subspace with $z_1 = 0$. (Set $\phi = \pi$ to show explicitly that $(0, z_2, z_3)$ and $(0, -z_2, -z_3)$ is the same point of this C_2-invariant subspace.)

The action of the entire symmetry group O on the reduced phase space $\mathbb{C}P^2$ is obtained if we apply the above principle to every rotation in O. The groups T_d and O have the same action on $\mathbb{C}P^2$. The action of $T_d \times \mathcal{T}$ then can be found as an extension by adding the $\mathcal{T}$ element. Results are summarized in Figure 10 reproduced from [17] and in Tables 10–12. Action of O on $\mathbb{C}P^2$ has five critical orbits (five zero-dimensional strata) characterized in Table 10. It is important to notice that each of the three points on the D_3 orbit correspond to a different (but conjugate) stabilizer; the same is true for the four points on the D_4 orbit. In

Table 10

Zero-dimensional strata of the $\mathbb{C}P^2$ space under the action of the image of the $T_d \times \mathcal{T}$ (or $O \times \mathcal{T}$ or $O_h \times \mathcal{T}$) group in the representation spanned by bilinear combinations of vibrational coordinates q and conjugate momenta p, which transform according to the triply degenerate representation F_2 of point symmetry group T_d, O, or O_h.

Orbit stabilizer[10]		Coordinates[11]	Point stabilizer[10]	
T_d	O or O_h	on $\mathbb{C}P^2$	O or O_h	T_d
$D_{2d} \times \mathcal{T}$	$D_4 \times \mathcal{T}$	$(1,0,0)$	$D_4^{(x)} \times \mathcal{T}$	$D_{2d}^{(x)} \times \mathcal{T}$
		$(0,1,0)$	$D_4^{(y)} \times \mathcal{T}$	$D_{2d}^{(y)} \times \mathcal{T}$
		$(0,0,1)$	$D_4^{(z)} \times \mathcal{T}$	$D_{2d}^{(z)} \times \mathcal{T}$
$C_{3v} \times \mathcal{T}$	$D_3 \times \mathcal{T}$	$(1,1,1)$	$D_3^{(c)} \times \mathcal{T}$	$C_{3v}^{(c)} \times \mathcal{T}$
		$(1,-1,-1)$	$D_3^{(d)} \times \mathcal{T}$	$C_{3v}^{(d)} \times \mathcal{T}$
		$(1,-1,1)$	$D_3^{(b)} \times \mathcal{T}$	$C_{3v}^{(b)} \times \mathcal{T}$
		$(1,1,-1)$	$D_3^{(a)} \times \mathcal{T}$	$C_{3v}^{(a)} \times \mathcal{T}$
$S_4 \wedge \mathcal{T}_2$	$C_4 \wedge \mathcal{T}_2$	$(1,\pm i,0)$	$C_4^{(z)} \wedge \mathcal{T}_2^{(y)}$	$S_4^{(z)} \wedge \mathcal{T}_2^{(y)}$
		$(1,0,\pm i)$	$C_4^{(y)} \wedge \mathcal{T}_2^{(x)}$	$S_4^{(y)} \wedge \mathcal{T}_2^{(x)}$
		$(0,1,\pm i)$	$C_4^{(x)} \wedge \mathcal{T}_2^{(y)}$	$S_4^{(x)} \wedge \mathcal{T}_2^{(y)}$
$C_3 \wedge \mathcal{T}_s$	$C_3 \wedge \mathcal{T}_2^{(d)}$	$(1,\eta^2,\eta)$, $(1,\bar{\eta},\bar{\eta}^2)$	$C_3^{(a)} \wedge \mathcal{T}_2^{\perp}$	$C_3^{(a)} \wedge \mathcal{T}_s^{\parallel}$
		$(1,\eta,\eta^2)$, $(1,\bar{\eta}^2,\bar{\eta})$	$C_3^{(b)} \wedge \mathcal{T}_2^{\perp}$	$C_3^{(b)} \wedge \mathcal{T}_s^{\parallel}$
		$(1,\eta^2,\bar{\eta}^2)$, $(1,\bar{\eta}^2,\eta^2)$	$C_3^{(c)} \wedge \mathcal{T}_2^{\perp}$	$C_3^{(c)} \wedge \mathcal{T}_s^{\parallel}$
		$(1,\eta,\bar{\eta})$, $(1,\bar{\eta},\eta)$	$C_3^{(d)} \wedge \mathcal{T}_2^{\perp}$	$C_3^{(d)} \wedge \mathcal{T}_s^{\parallel}$
$C_{2v} \times \mathcal{T}$	$D_2' \times \mathcal{T}$	$(1,\pm 1,0)$	$D_2'^{(z)} \times \mathcal{T}$	$C_{2v}^{(z)} \times \mathcal{T}$
		$(1,0,\pm 1)$	$D_2'^{(y)} \times \mathcal{T}$	$C_{2v}^{(y)} \times \mathcal{T}$
		$(0,1,\pm 1)$	$D_2'^{(x)} \times \mathcal{T}$	$C_{2v}^{(x)} \times \mathcal{T}$

the case of the C_4, C_3, and D_2 orbits, one stabilizer corresponds to two different orbit points. Zero-dimensional strata of the action of the symmetry group $O \times \mathcal{T}$ and $T_d \times \mathcal{T}$ (where $\mathcal{T}$ acts as in (3.1a)) remain the same, but their stabilizers become larger. The order of the symmetry group $O \times \mathcal{T}$ is twice that of O and the order of all stabilizers is doubled. The structure of critical orbits also remains exactly the same except for the stabilizers. Each zero-dimensional stratum again consists of one orbit.

At the same time, two-dimensional invariant topological spheres $\mathbb{S}^2$ with stabilizers $C_2^{(a)}$, $a = \{x, y, z\}$, and $C_s^{(\alpha)}$, $\alpha = 1, \ldots, 6$, of the T_d action on $\mathbb{C}P^2$ (see Figure 10) become further stratified due to the action of the $\mathcal{T}$-extended group. Below we detail the action of $O \times \mathcal{T}$ (and $T_d \times \mathcal{T}$) on these invariant manifolds.

Stratification of each of the three C_2-invariant $\mathbb{S}^2$ spheres is equivalent to the natural action of the D_{2h} point symmetry group (see Figure 11, left). The generic two-dimensional

[10] We give notation for T_d, and O or O_h groups.

[11] Coordinates in terms of (z_1, z_2, z_3), $\eta = \exp(i\pi/3)$.

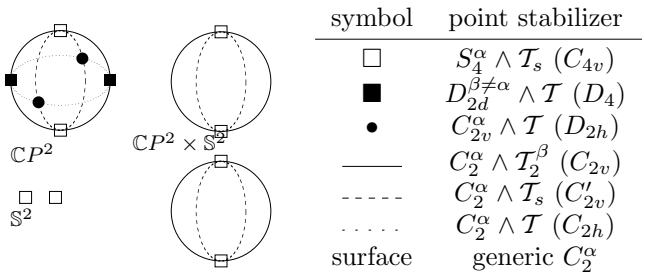

Figure 11. *Correlation between the C_2^a-invariant sphere on the $\mathbb{C}P^2$ space and C_2^a-invariant spheres on the $\mathbb{C}P^2 \times \mathbb{S}^2$ space whose coordinates on the $\mathbb{S}^2$ space (rotational sphere) are fixed to those of the $S_4^a \wedge \mathcal{T}_s$ points.*

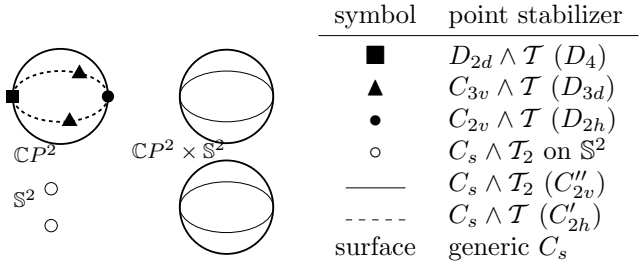

Figure 12. *Correlation between the $C_s^{(k)}$-invariant sphere on the $\mathbb{C}P^2$ space and $C_s^{(k)}$-invariant spheres on the $\mathbb{C}P^2 \times \mathbb{S}^2$ space whose coordinates on the $\mathbb{S}^2$ space (rotational sphere) are fixed to those of the $C_s^{(k)} \wedge \mathcal{T}_2$ points.*

stratum has stabilizer C_2; three isolated (critical) two-point orbits with stabilizers $D_{2d}\wedge\mathcal{T}$, $S_4\wedge\mathcal{T}_2$, and $C_{2v}\wedge\mathcal{T}$ are described in Table 10; three one-dimensional strata with stabilizers $C_2\wedge g$, where $g = \mathcal{T}$, $\mathcal{T}_2$, or $\mathcal{T}_s$, are listed in Table 11. Together with isolated fixed points, these strata form $C_2\wedge g$-invariant circles $\mathbb{S}^1$.

Stratification of the six topological $\mathbb{S}^2$ spheres with stabilizers $C_s^{(\alpha)}$ deserves special comment. Each such sphere has one exceptional two-point critical orbit with stabilizer $C_{3v}\wedge\mathcal{T}$ (see Figure 12, left). This orbit cannot be found if we consider only those symmetry operations that act within the $C_s^{(\alpha)}$-invariant sphere, its presence is due to the action of the symmetry group $T_d \times \mathcal{T}$ on the entire $\mathbb{C}P^2$ space. Disregarding the exceptional $C_{3v}\wedge\mathcal{T}$ orbit, we can identify the action of the symmetry group $T_d \times \mathcal{T}$ within each $C_s^{(\alpha)}$ sphere with the natural action of the C_{2v} point group (on a sphere in a 3-space). This action has two critical one-point orbits with global stabilizers $D_{2d}\wedge\mathcal{T}$ and $C_{2v}\wedge\mathcal{T}$ (Table 10), which lie on the C_2 axis (horizontal axis of the leftmost sphere in Figure 12) and two different one-dimensional families of orbits with stabilizers $C_s\wedge g$, where $g = \mathcal{T}$ or $\mathcal{T}_2$ (Table 11). Except for the C_{2v} and D_{2d} points, all other points form two-point orbits of the spatial subgroup C_2. The $C_s\wedge g$ invariant circles combine respective one-dimensional strata and fixed points.

All two-dimensional invariant subspaces of the $T_d \times \mathcal{T}$ group action on $\mathbb{C}P^2$ are described in Table 12. In addition to the two types of invariant spheres $\mathbb{S}^2$, this action has a number of other two-dimensional invariant subspaces whose stabilizers $\mathcal{T}$, $\mathcal{T}_2$, and $\mathcal{T}_s$ include reversing symmetries. Generic stratum on the $\mathcal{T}$, $\mathcal{T}_2$, and $\mathcal{T}_s$ invariant subspaces includes orbits with

Table 11

One-dimensional strata on the $\mathbb{C}P^2$ space under the same group action as in Table 10.

Orbit stabilizer[12]		Coordinates[13]	Point stabilizer[12]	
T_d	O or O_h	on $\mathbb{C}P^2$	O or O_h	T_d
$C_2 \wedge \mathcal{T}$	$C_2 \wedge \mathcal{T}$	$(1, \pm a, 0)$	$C_2^{(z)} \wedge \mathcal{T}$	$C_2^{(z)} \wedge \mathcal{T}$
		$(1, \pm 1/a, 0)$		
		$(1, 0, \pm a)$	$C_2^{(y)} \wedge \mathcal{T}$	$C_2^{(y)} \wedge \mathcal{T}$
		$(1, 0, \pm 1/a)$		
		$(0, 1, \pm a)$	$C_2^{(x)} \wedge \mathcal{T}$	$C_2^{(x)} \wedge \mathcal{T}$
		$(0, 1, \pm 1/a)$		
$C_2 \wedge \mathcal{T}_2$	$C_2 \wedge \mathcal{T}_2$	$(1, \pm ia, 0)$	$C_2^{(z)} \wedge \mathcal{T}_2^{(x)}$	$C_2^{(z)} \wedge \mathcal{T}_2^{(x)}$
		$(1, \pm i/a, 0)$		
		$(1, 0, \pm ia)$	$C_2^{(y)} \wedge \mathcal{T}_2^{(z)}$	$C_2^{(y)} \wedge \mathcal{T}_2^{(z)}$
		$(1, 0, \pm i/a)$		
		$(0, 1, \pm ia)$	$C_2^{(x)} \wedge \mathcal{T}_2^{(y)}$	$C_2^{(x)} \wedge \mathcal{T}_2^{(y)}$
		$(0, 1, \pm i/a)$		
$C_2 \wedge \mathcal{T}_s$	$C_2 \wedge \mathcal{T}_2^{(d)}$	$(1, \pm \eta, 0)$	$C_2^{(z)} \wedge \mathcal{T}_2^{(d)}$	$C_2^{(z)} \wedge \mathcal{T}_s^{\parallel}$
		$(1, \pm \bar{\eta}, 0)$		
		$(1, 0, \pm \eta)$	$C_2^{(y)} \wedge \mathcal{T}_2^{(d)}$	$C_2^{(y)} \wedge \mathcal{T}_s^{\parallel}$
		$(1, 0, \pm \bar{\eta})$		
		$(0, 1, \pm \eta)$	$C_2^{(x)} \wedge \mathcal{T}_2^{(d)}$	$C_2^{(x)} \wedge \mathcal{T}_s^{\parallel}$
		$(0, 1, \pm \bar{\eta})$		
$C_s \wedge \mathcal{T}$	$C_2^{(d)} \wedge \mathcal{T}$	$(1, 1, \pm a)$	$C_2^{(1)} \wedge \mathcal{T}$	$C_s^{(xy)} \wedge \mathcal{T}$
		$(1, -1, \pm a)$	$C_2^{(2)} \wedge \mathcal{T}$	$C_s^{(\overline{xy})} \wedge \mathcal{T}$
		$(1, \pm a, 1)$	$C_2^{(3)} \wedge \mathcal{T}$	$C_s^{(xz)} \wedge \mathcal{T}$
		$(1, \pm a, -1)$	$C_2^{(4)} \wedge \mathcal{T}$	$C_s^{(\overline{xz})} \wedge \mathcal{T}$
		$(1, \pm a, \pm a)$	$C_2^{(5)} \wedge \mathcal{T}$	$C_s^{(yz)} \wedge \mathcal{T}$
		$(1, \pm a, \mp a)$	$C_2^{(6)} \wedge \mathcal{T}$	$C_s^{(\overline{yz})} \wedge \mathcal{T}$
$C_s \wedge \mathcal{T}_2$	$C_2^d \wedge \mathcal{T}_2$	$(1, 1, \pm ia)$	$C_2^{(1)} \wedge \mathcal{T}_2^{(z)}$	$C_s^{(xy)} \wedge \mathcal{T}_2^{(z)}$
		$(1, -1, \pm ia)$	$C_2^{(2)} \wedge \mathcal{T}_2^{(z)}$	$C_s^{(\overline{xy})} \wedge \mathcal{T}_2^{(z)}$
		$(1, \pm ia, 1)$	$C_2^{(3)} \wedge \mathcal{T}_2^{(y)}$	$C_s^{(xz)} \wedge \mathcal{T}_2^{(y)}$
		$(1, \pm ia, -1)$	$C_2^{(4)} \wedge \mathcal{T}_2^{(y)}$	$C_s^{(\overline{xz})} \wedge \mathcal{T}_2^{(y)}$
		$(1, \pm ia, \pm ia)$	$C_2^{(5)} \wedge \mathcal{T}_2^{(x)}$	$C_s^{(yz)} \wedge \mathcal{T}_2^{(x)}$
		$(1, \pm ia, \mp ia)$	$C_2^{(6)} \wedge \mathcal{T}_2^{(x)}$	$C_s^{(\overline{yz})} \wedge \mathcal{T}_2^{(x)}$

24, 8, and 4 points, respectively. The topology of all these subspaces is $\mathbb{R}P^2$.

4.4. Rotational structure of the E mode: Action on $\mathbb{C}P^1 \times \mathbb{S}^2 \sim \mathbb{S}^2 \times \mathbb{S}^2$. The Hamiltonian that describes rotational structure of the E-mode polyads is defined on the four-dimensional reduced rotation–vibration phase space $\mathbb{C}P^1 \times \mathbb{S}^2$, the direct product of the vibrational E-mode polyad space $\mathbb{C}P^1$ (polyad sphere) and rotational sphere $\mathbb{S}^2$. We use

[12]We give notation for either the T_d, O, or O_h group.

[13]Here $a \neq 0, \pm 1, \infty$, and $\eta = e^{i\varphi}$, where $\varphi \neq k\pi/2$.

Table 12

Two-dimensional invariant subspaces of $\mathbb{C}P^2$ under the same group action as in Tables 10 and 11.

Orbit stabilizer[14]		Coordinates[15]	Point stabilizer[14]		Topology
T_d	O or O_h	on $\mathbb{C}P^2$	O or O_h	T_d	
C_2	C_2	$(1, w, 0)$	$C_2^{(z)}$	$C_2^{(z)}$	$\mathbb{S}^2$
		$(1, 0, w)$	$C_2^{(y)}$	$C_2^{(y)}$	
		$(0, 1, w)$	$C_2^{(x)}$	$C_2^{(x)}$	
C_s	$C_2^{(d)}$	$(1, 1, w)$	$C_2^{(1)}$	$C_s^{(xy)}$	$\mathbb{S}^2$
		$(1, -1, w)$	$C_2^{(2)}$	$C_s^{(\overline{xy})}$	
		$(1, w, 1)$	$C_2^{(3)}$	$C_s^{(xz)}$	
		$(1, w, -1)$	$C_2^{(4)}$	$C_s^{(\overline{xz})}$	
		$(1, w, w)$	$C_2^{(5)}$	$C_s^{(yz)}$	
		$(1, w, -w)$	$C_2^{(6)}$	$C_s^{(\overline{yz})}$	
$\mathcal{T}$	$\mathcal{T}$	$(1, a, b)$	$\mathcal{T}$	$\mathcal{T}$	$\mathbb{R}P^2$
$\mathcal{T}_2$	$\mathcal{T}_2$	$(1, a, ib)$	$\mathcal{T}_2^{(z)}$	$\mathcal{T}_2^{(z)}$	$\mathbb{R}P^2$
		$(1, ia, b)$	$\mathcal{T}_2^{(y)}$	$\mathcal{T}_2^{(y)}$	
		$(1, ia, ib)$	$\mathcal{T}_2^{(x)}$	$\mathcal{T}_2^{(x)}$	
$\mathcal{T}_s$	$\mathcal{T}_2^{(d)}$	$(1, w, w)$	$\mathcal{T}_2^{(d_1)}$	$\mathcal{T}_s^{(yz)}$	$\mathbb{R}P^2$
		$(1, w, -w)$	$\mathcal{T}_2^{(d_2)}$	$\mathcal{T}_s^{(\overline{yz})}$	
		$(1, a\eta, \eta^2)$	$\mathcal{T}_2^{(d_3)}$	$\mathcal{T}_s^{(xz)}$	
		$(1, a\eta, -\eta^2)$	$\mathcal{T}_2^{(d_4)}$	$\mathcal{T}_s^{(\overline{xz})}$	
		$(1, \eta^2, a\eta)$	$\mathcal{T}_2^{(d_5)}$	$\mathcal{T}_s^{(xy)}$	
		$(1, -\eta^2, a\eta)$	$\mathcal{T}_2^{(d_6)}$	$\mathcal{T}_s^{(\overline{xy})}$	

information on the stratification of the individual factor spaces $\mathbb{C}P^1$ (section 4.2) and $\mathbb{S}^2$ (section 4.1) in order to find the stratification of $\mathbb{C}P^1 \times \mathbb{S}^2$.

Let (v) and (r) be points on $\mathbb{C}P^1$ and $\mathbb{S}^2$, respectively, and let (v, r) denote points on the rovibrational (i.e., rotational-vibrational) space $\mathbb{C}P^1 \times \mathbb{S}^2$. The stabilizer $G_{v,r}$ of point (v, r) is an *intersection* $G_v \cap G_r$ of stabilizers on $\mathbb{C}P^1$ and $\mathbb{S}^2$. In simple terms, the symmetry of (v, r) can only be *lower* than that of its projections (v) and (r). The dimension of the stratum $\{v, r\}$ on $\mathbb{C}P^1 \times \mathbb{S}^2$ is the sum of the dimensions of strata $\{v\}$ and $\{r\}$. The stratum $\{v, r\}$ on the product space is connected if both its projections $\{v\}$ and $\{r\}$ on the two factor subspaces are connected.

Most important and basic to our analysis are critical orbits (v, r). Such orbits can either be nonconnected parts of a nonzero-dimensional stratum or belong to a stratum $\{v, r\}$ of dimension zero. These latter strata occur when both strata $\{r\}$ and $\{v\}$ have dimension zero *and* there is no stratum of nonzero dimension with stabilizer $G_r \cap G_v$.

Using the lattice of conjugate subgroups of $T_d \times \mathcal{T}$ in Figure 8, where we indicated all possible stabilizers G_v and G_r, the reader can easily find the intersections $G_v \cap G_r$ and then look up the details of the structure of the particular subgroups in Table 2. Indeed, all subgroups of a given stabilizer G are found by descending along the lattice paths which originated

[14]We give notation for either the T_d, O, or O_h group.

[15]Here a, b are real, w is a complex number, and $\eta = e^{i\varphi}$.

Table 13

Intersection (correlation) of stabilizers of the $T_d \times \mathcal{T}$ group action on the E-mode polyad phase space $\mathbb{C}P^1$ (left column) and on the rotational phase space $\mathbb{S}^2$ (top row). For information on the notation and structure of subgroups of $T_d \times \mathcal{T}$ refer to Table 2. Critical orbits on $\mathbb{C}P^1 \times \mathbb{S}^2$ are underlined.

Strata[16] on the $\mathbb{C}P^1$ space			Strata[16] on the rotational phase space $\mathbb{S}^2$					
			0D (4) $C_3 \wedge \mathcal{T}_s$	0D (3) $S_4 \wedge \mathcal{T}_s$	0D (6) $C_s \wedge \mathcal{T}_2$	1D (3) $\mathcal{T}_2$	1D (6) $\mathcal{T}_s$	2D C_1
0D		$T \wedge \mathcal{T}_s$	$\underline{C_3^{(k)} \wedge \mathcal{T}_s}$	$C_2^{\xi} \wedge \mathcal{T}_s$	$\mathcal{T}_s^{\xi_2}$	C_1	$\mathcal{T}_s^{\beta}$	C_1
0D	(3)	$D_{2d} \times \mathcal{T}$	$\mathcal{T}_s$	$\underline{S_4^{\eta} \wedge \mathcal{T}_s}$[17] $\underline{C_2^{\eta} \wedge \mathcal{T}_2^{\xi}}$[20]	$\underline{C_s \wedge \mathcal{T}_2}$[19] $\mathcal{T}_2^{\xi}$[20]	$\mathcal{T}_2^{\eta}$	$\mathcal{T}_s$[19] C_1[20]	C_1
1D	(3)	$D_2 \wedge \mathcal{T}_s$	$\mathcal{T}_s$	$C_2^{\eta} \wedge \mathcal{T}_s$[17] C_2^{ξ}[18]	$\mathcal{T}_s$[19] C_1[20]	C_1	$\mathcal{T}_s$[19] C_1[20]	C_1
1D		$D_2 \times \mathcal{T}$	C_1	$C_2^{\eta} \wedge \mathcal{T}_2^{\xi}$[20]	$\mathcal{T}_2$	$\mathcal{T}_2^{\xi}$	C_1	C_1
2D		D_2	C_1	C_2^{ξ}	C_1	C_1	C_1	C_1

at G. The highest node, where the paths descending from G_v and G_r join, is the intersection $G_v \cap G_r$, i.e., the largest common subgroup of G_v and G_r. All possible intersections are summarized in Table 13. We comment on them below starting with the low-symmetry strata.

4.4.1. Noncritical orbits. Generic points (r) on $\mathbb{S}^2$ have stabilizer $G_r = C_1$ (rightmost column in Table 13). Obviously, these points lift to points (v, r) with trivial symmetry C_1 regardless of the stabilizer G_v. The generic stratum $\{v, r\}$ is of dimension four, has stabilizer C_1, and includes 48-point orbits.

Generic points (v) on $\mathbb{C}P^1$ (bottom row in Table 13) have stabilizer D_2, which has three order-two subgroups C_2^{η} with axes $\eta = \{x, y, z\}$. Intersection of D_2 with stabilizers G_r equals C_1 in all cases except for the three conjugate subgroups $G_r^{\eta} = S_4^{\eta} \wedge \mathcal{T}_s$. Intersection $G_r^{\eta} \cap D_2$ is the particular C_2^{η} subgroup of D_2. The corresponding C_2 stratum on $\mathbb{C}P^1 \times \mathbb{S}^2$ includes 24-point orbits. Since $S_4^{\eta} \wedge \mathcal{T}_s$ points on $\mathbb{S}^2$ are critical (fixed), this stratum has dimension two.

The stabilizer $G_v = D_2 \wedge \mathcal{T}$ of the one-dimensional stratum on $\mathbb{C}P^1$ is an invariant subgroup of $T_d \times \mathcal{T}$; its intersection with subgroups G_r of the same class of conjugate subgroups of $T_d \times \mathcal{T}$ results again in conjugate subgroups. For $G_r = S_4 \wedge \mathcal{T}_s$ the intersection is $C_2 \times \mathcal{T}_2$ and the stratum $\{v, r\}$ has dimension one. If $G_r = \mathcal{T}_2^b$, where $b = \{x, y, z\}$, we have a two-dimensional

[16] For each space, strata of dimensions zero, one, and two are marked as 0D, 1D, and 2D; the number of different conjugate stabilizers in the same class of $T_d \times \mathcal{T}$ is given in parentheses. Right superscripts define concrete conjugate stabilizers: η and ξ label axes (x, y, z) for orbits on $\mathbb{C}P^1$ and $\mathbb{S}^2$, respectively; (k) and β distinguish stabilizers of orbits on $\mathbb{S}^2$ in the C_3 class and the σ class; they can take four and six values, respectively.

[17] $\eta = \xi$; axes η and ξ are the *same*.

[18] $\eta \neq \xi$; axes η and ξ are *different*.

[19] $\beta = \{\eta_1, \eta_2\}$; stabilizer of the orbits on $\mathbb{S}^2$ of index (β) includes one of the two operations of index $\{\eta_1, \eta_2\}$; see text for examples.

[20] $\beta \neq \{\eta_1, \eta_2\}$; stabilizer of the orbits on $\mathbb{S}^2$ of index (β) does not include operations of index $\{\eta_1, \eta_2\}$.

family $\{v, r\}$ of 24-point orbits with symmetry $\mathcal{T}_2^b$. If $G_r = C_s \wedge \mathcal{T}_2$, the intersection is again $\mathcal{T}_2$; i.e., isolated fixed points (r) on $\mathbb{S}^2$ with stabilizer $C_s \wedge \mathcal{T}_2$ lift to points (v, r) with stabilizer $\mathcal{T}_2$. Since the zero-dimensional stratum $C_s \wedge \mathcal{T}_2$ on $\mathbb{S}^2$ is the closure of the one-dimensional stratum $\mathcal{T}_2$ on $\mathbb{S}^2$, the entire $\mathcal{T}_2$ stratum $\{v, r\}$ is connected. As a consequence, isolated points (r) with stabilizer $C_s \wedge \mathcal{T}_2$ lift to noncritical points (v, r) on the two-dimensional stratum on $\mathbb{C}P^1 \times \mathbb{S}^2$.

When both G_v and G_r are not invariant subgroups, the symmetry of the $\{v, r\}$ stratum depends on the choice of the subgroup within the class of conjugate subgroups. In the case of $G_v = D_2 \wedge \mathcal{T}_s$ and $G_r = \mathcal{T}_s$ the intersection can be either $\mathcal{T}_s$ or C_1. As shown in Table 2, the element C_2^a, where $a = \{x, y, z\}$, of $D_2 \wedge \mathcal{T}_s$ distinguishes a particular stabilizer in the class of three conjugate subgroups. This stabilizer has two $\mathcal{T}_s$ subgroups generated by $\mathcal{T}_s^{a_1}$ and $\mathcal{T}_s^{a_2}$. If, therefore, G_r is one of these two subgroups, then its intersection with G_v is nontrivial; otherwise $G_v \cap G_r = C_1$. In the case of $G_v = D_2 \wedge \mathcal{T}_s$ and $G_r = \mathcal{T}_2$ the intersection is always trivial. On the other hand, intersection of $G_v = D_2 \wedge \mathcal{T}_s$ and $C_3 \wedge \mathcal{T}_s$ is always a nontrivial subgroup $\mathcal{T}_s$ because one of the two orthogonal symmetry planes $\mathcal{T}_s^{a_{1,2}}$ in $D_2 \wedge \mathcal{T}_s$ always contains the particular axis C_3 of $C_3 \wedge \mathcal{T}_s$. In other words, intersection of the set of two $\mathcal{T}_s$ elements in $D_2 \wedge \mathcal{T}_s$ and three $\mathcal{T}_s$ elements in $C_3 \wedge \mathcal{T}_s$ (which cross on the C_3 axis) is never empty. Observe that the $\mathcal{T}_s$ stratum $\{v, r\}$ has dimension two and is connected. All points in Table 13 that lift to this stratum become noncritical; the $\{v, r\}$ parts of dimensions zero and one form the closure.

4.4.2. Critical orbits (strata of dimension zero). Orbits that project on zero-dimensional strata of $\mathbb{C}P^1$ and $\mathbb{S}^2$ *and* have unique stabilizers are critical. The six critical orbits on $\mathbb{C}P^1 \times \mathbb{S}^2$ are characterized below.

Stabilizer on $\mathbb{C}P^1$	$T \wedge \mathcal{T}_s$	$D_{2d} \times \mathcal{T}$	$D_{2d} \times \mathcal{T}$
Stabilizer $\mathbb{C}P^1 \times \mathbb{S}^2$	$C_3 \wedge \mathcal{T}_s$	$S_4 \wedge \mathcal{T}_s$	$C_s \times \mathcal{T}_2$
Number of orbits	2	2	2
Number of points in orbit	8	6	12

We explain how to find these orbits using Table 13.

Consider the stratum $\{v\}$ with stabilizer $G_v = T \wedge \mathcal{T}_s$, which consists of one two-point orbit, and the stratum $\{r\}$ with stabilizer $G_r = C_3 \wedge \mathcal{T}_s$, which consists of one eight-point orbit. Since each of the four conjugate subgroups G_r is a subgroup of G_v, we have the zero-dimensional stratum $\{v, r\}$ with stabilizer $C_3 \wedge \mathcal{T}_s$, which includes two eight-point orbits (all points on the orbit $\{r\}$ lift to the same orbit $\{v, r\}$). If for the same $\{v\}$ we consider $\{r\}$ with stabilizer $G_r = S_4 \wedge \mathcal{T}_s$, the resulting 12-point orbit $\{v, r\}$ has the stabilizer $C_2 \times \mathcal{T}_s$ and should, therefore, be part of a one-dimensional stratum. Indeed, as can be seen from Figure 8,

$$T \wedge \mathcal{T}_s \cap S_4 \wedge \mathcal{T}_s = D_2 \wedge \mathcal{T}_s \cap S_4 \wedge \mathcal{T}_s = C_2 \times \mathcal{T}_s.$$

Consider now the stratum $\{v\}$ with stabilizer $G_v = D_{2d} \times \mathcal{T}$, which again consists of one two-point orbit. The intersection of G_v with $G_r = S_4 \wedge \mathcal{T}_s$ can be the whole G_r (i.e., G_r can be the subgroup of G_v) if both subgroups include the same element C_2^η, where axis η can be x, y, or z. In this case we have a zero-dimensional stratum $\{v, r\}$ with stabilizer $S_4 \wedge \mathcal{T}_s$, which includes two six-point orbits (all points on the six-point orbit $\{r\}$ lift to the same orbit $\{v, r\}$). If for the same $\{v\}$ we take $\{r\}$ with stabilizer $G_r = C_s \times \mathcal{T}_2$, this latter stabilizer can

Table 14

Intersection (correlation) of stabilizers of the T_d group action on the F_2-mode vibrational phase space $\mathbb{C}P^2$ (left column), on the rotational phase space $\mathbb{S}^2$ (top row, center), and on the E-mode vibrational phase space $\mathbb{C}P^1$ (top row, right). Critical orbits are underlined.

Strata[21] on $\mathbb{C}P^2$		Strata[21] on $\mathbb{S}^2$				Strata[21] on $\mathbb{C}P^1$		
		0D $S_4^{(\eta')}$ $\eta'\leq 3$	0D $C_3^{(k')}$ $k'\leq 4$	0D $C_s^{(\beta')}$ $\beta'\leq 6$	2D C_1	0D T	0D $D_{2d}^{(\eta')}$ $\eta'\leq 3$	2D D_2
0D	$D_{2d}^{(\eta)}$ $\eta\leq 3$	$\underline{S_4}$[22] $\overline{C_2}$[23]	C_1	C_s[24] C_1	C_1	D_2	$\underline{D_{2d}}$[22] $\overline{D_2}$[23]	D_2
0D	$S_4^{(\eta)}$ $\eta\leq 3$	$\underline{S_4}$[22] $\overline{C_1}$[23]	C_1	C_1	C_1	C_2	$\underline{S_4}$[22] $\overline{C_2}$[23]	C_2
0D	$C_{3v}^{(k)}$ $k\leq 4$	C_1	$\underline{C_3}$[22] $\overline{C_1}$[23]	C_s[24] C_1	C_1	$\underline{C_3}$	C_s	C_1
0D	$C_3^{(k)}$ $k\leq 4$	C_1	$\underline{C_3}$[22] $\overline{C_1}$[23]	C_1	C_1	$\underline{C_3}$	C_1	C_1
0D	$C_{2v}^{(\eta)}$ $\eta\leq 3$	C_2[22] C_1[23]	C_1	$\underline{C_s}$[24,25] $\overline{C_s}$[24] C_1	C_1	C_2	$\underline{C_{2v}}$[22] $\overline{C_2}$[23]	C_2
2D	$C_2^{(\eta)}$ $\eta\leq 3$	C_2[22] C_1[23]	C_1	C_1	C_1	C_2	C_2[22] C_2[23]	C_2
2D	$C_s^{(\beta)}$ $\beta\leq 6$	C_1	C_1	C_s[22] C_1[23]	C_1	C_1	C_s[24] C_1	C_1
4D	C_1	C_1	C_1	C_1	C_1	C_1	C_1	C_1

again be a subgroup of G_v if both share the same $C_s = \sigma$ element, which can be either σ^{η_1} or σ^{η_2} (see Table 2). Since in this case $\{r\}$ consists of one 12-point orbit, the corresponding zero-dimensional $\{v, r\}$ stratum with stabilizer $C_s \times \mathcal{T}_2$ contains two 12-point orbits.

4.5. Rotational structure of the F_2 mode: Action of T_d and $T_d \times \mathcal{T}$ on $\mathbb{C}P^2 \times \mathbb{S}^2$.

We now combine small-amplitude F_2-mode vibrations and rotation. The Hamiltonian of this system is a $(T_d \times \mathcal{T})$-invariant function on the six-dimensional reduced phase space $\mathbb{C}P^2 \times \mathbb{S}^2$. The action of the full symmetry group $T_d \times \mathcal{T}$ on $\mathbb{C}P^2 \times \mathbb{S}^2$ can be found from that on the individual spaces $\mathbb{C}P^2$ and $\mathbb{S}^2$ using the approach of the previous section; in particular, we

[21] Strata of dimension s are marked as sD, $s = 0, 1, 2, 4$. Classes of stabilizers of the strata are listed in T_d notation. Indexes η, k, β distinguish different stabilizers on $\mathbb{C}P^2$ within the same class; indexes η', k', β' are used for $\mathbb{S}^2$ or $\mathbb{C}P^1$. Refer to Table 2 for information on the notation and structure of subgroups of $T_d \times \mathcal{T}$.

[22] Identical subgroups of $T_d \times \mathcal{T}$: axes η and η', k and k', or subgroups β and β' are the *same*, i.e., $\eta \equiv \eta'$, $k \equiv k'$, or $\beta \equiv \beta'$.

[23] Different subgroups of $T_d \times \mathcal{T}$ of the same class: axes η and η', k and k', or subgroups β and β' are *different*, i.e., $\eta \neq \eta'$, etc.

[24] Subgroups $D_{2d}^{(\eta)}$, $C_{2v}^{(\eta)}$, $C_{3v}^{(k)}$ include the symmetry plane β'.

[25] β' equals η_1 or η_2; the point projects on the disconnected zero-dimensional component of the $C_s^{\eta_1}$ or $C_s^{\eta_2}$ stratum on $\mathbb{C}P^2$; see section 4.5.1.

determine intersections of stabilizers from the subgroup lattice of $T_d \times \mathcal{T}$.

Essential information can be obtained from the simpler study of the action of the spatial symmetry group T_d whose subgroup lattice is given in Figure 1. As shown in Table 14, the action of T_d on the rotation–vibration space $\mathbb{C}P^2 \times \mathbb{S}^2$ creates strata of symmetry S_4, C_2, C_3, C_s, and C_1 (generic). Some strata, notably C_s, have disconnected components of different dimension. By dimension of these strata, we mean the highest dimension of their components. The C_1 stratum has dimension six, components of other strata can be of dimension zero and two.

4.5.1. Strata and components of dimension zero (critical orbits). The S_4 stratum on $\mathbb{C}P^2 \times \mathbb{S}^2$ projects on the S_4 orbits on the rotational space $\mathbb{S}^2$ and on the D_{2d} or S_4 orbits on the vibrational space $\mathbb{C}P^2$. Each $G_r = S_4^{(\eta')}$ stabilizer has two fixed points on $\mathbb{S}^2$ (which belong to the same orbit of the T_d action). Each $G_v = D_{2d}^{(\eta)}$ stabilizer has one fixed point on $\mathbb{C}P^2$ (see Table 10). Consequently, there are two points on $\mathbb{C}P^2 \times \mathbb{S}^2$ with the same stabilizer

$$G_r \cap G_v = D_{2d}^{(\eta)} \cap S_4^{(\eta)} = S_4^{(\eta)}.$$

The six points corresponding to three different conjugate stabilizers with $\eta = x, y, z$ form one six-point orbit, which we label $A^{(4)}$. If for the same G_r we take $G_v = S_4^{(\eta)}$, we combine two points on $\mathbb{C}P^2$ (which are in the same orbit) with two points on $\mathbb{S}^2$. It is important to observe that the resulting four points on $\mathbb{C}P^2 \times \mathbb{S}^2$ belong to two different orbits: one pair belongs to orbit $B^{(4)}$ and another to orbit $C^{(4)}$. With three possible axes η taken into account, orbits B and C contain six points each.

The above description of the S_4 orbits $B^{(4)}$ and $C^{(4)}$ can be easily verified on a concrete example. Such examples are given in Table 15, where the E-mode coordinates (z_4, z_5) should at present be ignored. Consider a particular axis $\eta = z$ (axis 3). The two fixed points on the $\mathbb{C}P^2$ space have coordinates (Table 10)

$$(z_1, z_2, z_3) = (1, \pm i, 0), \tag{4.1a}$$

and the coordinates of the two fixed points on the $\mathbb{S}^2$ sphere are

$$(j_1, j_2, j_3) = (0, 0, \pm 1). \tag{4.1b}$$

(For simplicity, here and in the rest of this section, we drop normalization factors, which are not essential to our current discussion.) The group T_d acts on $\mathbb{C}P^2$ and $\mathbb{S}^2$ in such a way that any operation in T_d that interchanges the two points (4.1a) on $\mathbb{C}P^2$ interchanges the two points (4.1b) on $\mathbb{S}^2$. The C_2 rotation about axis x (axis 1) is an example:

$$C_2^x : (z_1, z_2, z_3; j_1, j_2, j_3) \to (z_1, -z_2, -z_3; j_1, -j_2, -j_3).$$

As a result, no operation in T_d maps points

$$B = (1, \pm i, 0; 0, 0, \pm 1) \quad \text{and} \quad C = (1, \pm i, 0; 0, 0, \mp 1)$$

of the $\mathbb{C}P^2 \times \mathbb{S}^2$ space into each other; these points, therefore, belong to *different* orbits.

Table 15

Fixed points of the $T_d \times \mathcal{T}$ group action on the reduced phase space $\mathbb{C}P^2 \times \mathbb{C}P^1 \times \mathbb{S}^2$.

(a) Stabilizer S_4^z (or C_4), $r_f = \sqrt{N_f}$, $r_e = \sqrt{2N_e}$, $r_j = J$.

Point	$\frac{z_1}{r_f}$	$\frac{z_2}{r_f}$	$\frac{z_3}{r_f}$	$\frac{z_4}{r_e}$	$\frac{z_5}{r_e}$	$\frac{j_1}{r_j}$	$\frac{j_2}{r_j}$	$\frac{j_3}{r_j}$
A_1	0	0	$\sqrt{2}$	1	0	0	0	1
A_1'	0	0	$\sqrt{2}$	1	0	0	0	-1
A_2	0	0	$\sqrt{2}$	0	1	0	0	1
A_2'	0	0	$\sqrt{2}$	0	1	0	0	-1
B_1	1	i	0	1	0	0	0	1
B_1'	1	$-i$	0	1	0	0	0	-1
B_2	1	i	0	0	1	0	0	1
B_2'	1	$-i$	0	0	1	0	0	-1
C_1	1	i	0	1	0	0	0	-1
C_1'	1	$-i$	0	1	0	0	0	1
C_2	1	i	0	0	1	0	0	-1
C_2'	1	$-i$	0	0	1	0	0	1

(b) Stabilizer C_3 [111], $r_f = (\sqrt{2N_f})/\sqrt{3}$, $r_e = \sqrt{N_e}$, $r_j = \sqrt{3}J$, $\chi = \exp(2\pi i/3)$.

Point	$\frac{z_1}{r_f}$	$\frac{z_2}{r_f}$	$\frac{z_3}{r_f}$	$\frac{z_4}{r_e}$	$\frac{z_5}{r_e}$	$\frac{j_1}{r_j}$	$\frac{j_2}{r_j}$	$\frac{j_3}{r_j}$
A_1	1	1	1	1	i	1	1	1
A_2	1	1	1	1	i	-1	-1	-1
B_1	1	χ	$\bar{\chi}$	1	i	1	1	1
B_2	1	χ	$\bar{\chi}$	1	i	-1	-1	-1
C_1	1	χ	$\bar{\chi}$	1	i	-1	-1	-1
C_2	1	χ	$\bar{\chi}$	1	i	1	1	1

(c) Stabilizer C_s^{xy} (or C_2), $r_f = \sqrt{N_f}$, $r_e = \sqrt{2N_e}$, $r_j = J/\sqrt{2}$.

Point	$\frac{z_1}{r_f}$	$\frac{z_2}{r_f}$	$\frac{z_3}{r_f}$	$\frac{z_4}{r_e}$	$\frac{z_5}{r_e}$	$\frac{j_1}{r_j}$	$\frac{j_2}{r_j}$	$\frac{j_3}{r_j}$
A_1	1	-1	0	1	0	1	-1	0
A_2	1	-1	0	0	1	-1	1	0

The three eight-point critical orbits of the C_3 stratum can be described analogously; cf. Table 15(b). Combination of the $C_{3v}^{(k)}$ point on $\mathbb{C}P^2$ and two $C_3^{(k)}$ points on $\mathbb{S}^2$ gives two points on the $A^{(3)}$ orbit. With all four axes C_3 taken into account ($k = 1, \ldots, 4$), the orbit has eight points. The $B^{(3)}$- and $C^{(3)}$-type orbits of the C_3 action include points (z, j) and $(z, -j)$, respectively, where (z) and (j) stand for the coordinates of the fixed point on $\mathbb{C}P^2$ and $\mathbb{S}^2$.

The two critical fixed points of the $C_s^{(\alpha)}$ action on $\mathbb{C}P^2 \times \mathbb{S}^2$ are obtained when we combine the only isolated fixed point of the $C_s^{(\alpha)}$ action on $\mathbb{C}P^2$ (see Table 10) with the two respective points on $\mathbb{S}^2$ (recall that C_s acts both on $\mathbb{C}P^2$ and on $\mathbb{S}^2$ as operation C_2 of the O group). In the particular case of $C_{2v}^{(z)}$ and its subgroup $C_s^{(xy)}$ (set $\eta = z$ and $\beta' = \eta_1 = xy$ in Table 14), we combine the $z = (1, -1, 0)$ fixed point of the $C_s^{(xy)}$ action on $\mathbb{C}P^2$ with two points $j = \pm(1, -1, 0)$ on $\mathbb{S}^2$. For six conjugate elements C_s, we obtain a 12-point orbit, which is isolated from the rest of the C_s stratum (because its projection on the $\mathbb{C}P^2$ space is isolated). This orbit is therefore critical.

4.5.2. Strata of dimension two. Action of T_d on $\mathbb{C}P^2 \times \mathbb{S}^2$ creates two strata of dimension two, C_2 and C_s. The C_s stratum has a disconnected component of dimension zero, described above. In both cases, we combine isolated fixed points on the rotational space $\mathbb{S}^2$ and points on the invariant spheres $\mathbb{S}^2 \subset \mathbb{C}P^2$. This is illustrated in Figure 11 and 12.

We describe first the C_2 stratum. Since $C_2 = S_4^2$, points with local symmetry C_2 and S_4 coincide on the rotational space $\mathbb{S}^2_j$. In the particular example of $C_2^z = (S_4^z)^2$ these points are given in (4.1b). We combine points on $\mathbb{S}^2_j$ with points on the C_2-invariant sphere in $\mathbb{C}P^2$. In our C_2^z example, these latter points are (see Table 12)

$$(z_1, z_2, z_3) = (1, w, 0), \quad \operatorname{Re} w \neq 0.$$

All points on $\mathbb{C}P^2 \times \mathbb{S}^2$ with stabilizer C_2^z are

$$(z_1, z_2, z_3;\, j_1, j_2, j_3) = (1, w, 0;\, 0, 0, \pm 1), \quad \operatorname{Re} w \neq 0.$$

Removing the above restriction on w adds four critical points $(1, \pm i, 0;\, 0, 0, \pm 1)$ with stabilizer S_4^z and produces two spheres shown in Figure 11, right. These are the only isolated critical points which remain on the C_2-invariant spheres when we add rotation; all other fixed points which lie on the C_2-invariant sphere of the purely vibrational system with phase space $\mathbb{C}P^2$ (i.e., when $j = 0$) disappear. For example, consider the two D_{2d} points $z = (1, 0, 0)$ and $(0, 1, 0)$ with stabilizers D_{2d}^x and D_{2d}^y, respectively (Table 10 and Figure 11, left). Their rotational coordinates should necessarily be $j = (1, 0, 0)$ and $(0, 1, 0)$, which project to points on $\mathbb{S}^2$ with stabilizers S_4^x and S_4^y, respectively.

A similar approach can be used to describe the C_s-invariant spheres (the two-dimensional component of the C_s stratum) in the $\mathbb{C}P^2 \times \mathbb{S}^2$ space shown in Figure 12, right. In this case, *no* critical points remain on the spheres when rotation is added and we lift from $\mathbb{C}P^2$ to $\mathbb{C}P^2 \times \mathbb{S}^2$. As an example, consider the reflection plane $x = y$ whose action is given in Table 4. This operation has two fixed points on the rotational sphere $\mathbb{S}^2_j$:

$$(j_1, j_2, j_3) = (\pm 1, \mp 1, 0).$$

(At these points, axial vector j is orthogonal to the plane $x = y$.) Operation C_s^{xy} is a combination of inversion and rotation by π about axis $x = -y$, i.e., $(1, -1, 0)$. The points on the $\mathbb{C}P^1 \sim \mathbb{S}^2$ subspace orthogonal to this axis have, therefore, coordinates (see Table 12)

$$(z_1, z_2, z_3) = (1, 1, w),$$

and the points of the two C_s-invariant spheres $\mathbb{S}^2$ in the six-dimensional space $\mathbb{C}P^2 \times \mathbb{S}^2$ are

$$(z_1, z_2, z_3;\, j_1, j_2, j_3) = (1, 1, w;\, \pm 1, \mp 1, 0).$$

Stabilizers of critical points, which are present on the C_s-invariant sphere when $j = 0$ (Figure 12, left), are such that these points become noncritical when rotation is added. Thus, the C_{2v} point with $z = (1, 1, 0)$, which lies on the C_s^{xy}-invariant sphere of our example, has the stabilizer C_2^z and must, therefore, combine with $j = (0, 0, 1)$ in order to have a higher stabilizer.

4.5.3. Extension by time reversal $\mathcal{T}$. The action of the full group $T_d \times \mathcal{T}$ on the $\mathbb{C}P^2 \times \mathbb{S}^2$ space creates more strata. For our purposes, however, it is sufficient to observe that the system of critical orbits of $T_d \times \mathcal{T}$ remains the *same*, as in the case of T_d, and to study the action of reversal operations on the invariant spheres with stabilizers C_2 and C_s.

Internal stratification of the C_2-invariant spheres in the $\mathbb{C}P^2 \times \mathbb{S}^2$ space under the action of $T_d \times \mathcal{T}$ is shown in Figure 11, right. It can be seen that the action of $T_d \times \mathcal{T}$ on these spheres is equivalent to the natural action of the C_{2v} group (whose axis C_2 is the vertical axis in Figure 11). In addition to the two isolated S_4 points, this action creates one-dimensional strata with stabilizers $C_2 \times \mathcal{T}_2$ and $C_2 \times \mathcal{T}_s$.

The C_s-invariant spheres also do not remain homogeneous when reversal operations are accounted for properly. The action of $T_d \times \mathcal{T}$ on these spheres is equivalent to that of the group C_h (whose reflection plane is the plane of Figure 12); it creates a $(C_s \wedge \mathcal{T}_2)$-invariant circle on each C_s-invariant sphere in $\mathbb{C}P^2 \times \mathbb{S}^2$.

4.6. Action on the vibrational subspace $\mathbb{C}P^2 \times \mathbb{C}P^1$. Description of combined small-amplitude E- and F_2-mode vibrations requires the six-dimensional reduced phase space $\mathbb{C}P^2 \times \mathbb{C}P^1$. The action of the $T_d \wedge \mathcal{T}$ symmetry group on the F_2-mode subspace $\mathbb{C}P^2$ and on the whole of $\mathbb{C}P^2 \times \mathbb{C}P^1$ is effective. The action of $T_d \times \mathcal{T}$ on the E-mode subspace is not effective; see Table 14: any point on this subspace is automatically D_2-invariant.

4.6.1. Critical orbits. All critical orbits on $\mathbb{C}P^2 \times \mathbb{C}P^1$ can be found and classified if we combine points from Tables 8 and 10 and determine the intersection of their stabilizers $G_f \cap G_e$ using the lattice from Figure 2, 3, or 8. To find whether the point (orbit) is critical, we consider the stratum with stabilizer $G_f \cap G_e$ and verify that we deal with an isolated point (orbit) using projections on the orbit spaces in Figures 9 and 10. As in the previous sections, we should combine points with identical stabilizers in order to determine the number of orbits and of points in the orbits. Concrete examples can be found in Table 15 if we ignore the rotational part (i.e., let $j = 0$). Results are summarized below.

Stabilizer of the orbits on			Number	Examples in
$\mathbb{C}P^2$	$\mathbb{C}P^1$	$\mathbb{C}P^2 \times \mathbb{C}P^1$	of points	Table 15
$D_{2d} \times \mathcal{T}$	$D_{2d} \times \mathcal{T}$	$D_{2d} \times \mathcal{T}$	$3+3$	$A^{(4)}_{1,2}$
$S_4 \wedge \mathcal{T}_s$	$D_{2d} \times \mathcal{T}$	$S_4 \wedge \mathcal{T}_s$	$6+6$	$(B,C)^{(4)}_{1,2}$
$C_{3v} \times \mathcal{T}$	$T \wedge \mathcal{T}_s$	$C_3 \wedge \mathcal{T}_s$	$4+4$	$A^{(3)}_{1,2}$
$C_3 \wedge \mathcal{T}_s$	$T \wedge \mathcal{T}_s$	$C_3 \wedge \mathcal{T}_s$	$8+8$	$(B,C)^{(3)}_{1,2}$
$C_{2v} \times \mathcal{T}$	$D_{2d} \times \mathcal{T}$	$C_{2v} \times \mathcal{T}$	$3+3$	$A^{(2)}_{1,2}$

Here the superscripts $^{(4)}$, $^{(3)}$, and $^{(2)}$ correspond to parts (a), (b), and (c) of Table 15; by $k+k$ we denote two k-point orbits.

4.6.2. Invariant subspaces of $\mathbb{C}P^2 \times \mathbb{C}P^1$. Three D_{2d}-invariant points on $\mathbb{C}P^2$ are the only points whose stabilizer includes D_2. Combining these points with the whole E-mode space $\mathbb{C}P^1 \sim \mathbb{S}^2$ gives three D_2-invariant spheres $\mathbb{S}^2$ in the six-dimensional space $\mathbb{C}P^2 \times \mathbb{S}^2$. Six C_s-invariant spheres on $\mathbb{C}P^2$ combined with, respectively, six D_{2d}-invariant points of the E-space give 12 C_s-invariant spheres $\mathbb{S}^2$ in $\mathbb{C}P^2 \times \mathbb{S}^2$. The stabilizer D_2 of the E-mode space $\mathbb{C}P^1 \sim \mathbb{S}^2$ has three conjugate C_2^a subgroups with $a = \{x, y, z\}$. Consequently, there are three C_2-invariant subspaces $\mathbb{S}^2_{(F)} \times \mathbb{S}^2_{(E)}$. Points with higher symmetry lie on each of the above subspaces.

4.7. Action on the full reduced phase space $\mathbb{C}P^2 \times \mathbb{C}P^1 \times \mathbb{S}^2$. In order to describe the simultaneous rotation and small amplitude E- and F_2-mode vibrations of the A_4 molecule (rotational structure of all combination polyads $n\nu_2 + m\nu_3$), we need the eight-dimensional total classical reduced phase space $\mathbb{C}P^2 \times \mathbb{C}P^1 \times \mathbb{S}^2$. In this section, we find critical (fixed) points of the $T_d \times \mathcal{T}$ action on $\mathbb{C}P^2 \times \mathbb{C}P^1 \times \mathbb{S}^2$ by combining points on the three factor spaces. Fortunately, most of the work has already been done in the previous sections. We can take critical orbits A, B, and C on $\mathbb{C}P^2 \times \mathbb{S}^2$ found in section 4.5 and combine them with critical orbits of the $T_d \times \mathcal{T}$ action on the E-mode space $\mathbb{C}P^1$ while matching the stabilizers carefully. It can be seen in the examples of Table 15 that orbits A, B, and C are duplicated in the presence of E-mode vibrations. Indexes 1 and 2 distinguish two different possible projections (z_5, z_6) on the E-mode space $\mathbb{C}P^1$. We use shorter T_d notation for stabilizers in Table 15. Extending the symmetry group T_d by the time reversal $\mathcal{T}$ does not modify the critical orbits; it merely doubles the order of stabilizers, which become $S_4 \wedge \mathcal{T}_s$, $C_3 \wedge \mathcal{T}_s$, and $C_s \times \mathcal{T}_2$. We comment briefly on these orbits.

The orbit stabilizer is defined as a class of conjugate subgroups; the point stabilizer is an individual subgroup in that class. As before, we match concrete point stabilizers. The S_4^z operation has $(1 + 2)$, 2, and 2 fixed points on the F_2-mode space $\mathbb{C}P^2$, E-mode space $\mathbb{C}P^1$, and rotational sphere $\mathbb{S}^2$, respectively. The $3 \times 2 \times 2 = 12$ points on $\mathbb{C}P^2 \times \mathbb{C}P^1 \times \mathbb{S}^2$ with the stabilizer S_4^z are listed in Table 15. To complete orbits of the T_d group action we should add points with stabilizers S_4^x and S_4^y (which are obtained from the given points using symmetry operations R such that $S_4^\alpha = R \circ S_4^z \circ R^{-1}$). The total of 36 points can split into six orbits with stabilizer S_4. In particular, points A_1 and A_1' in Table 15 belong to the same six-point orbit (which also includes two points with stabilizer S_4^y and two points with stabilizer S_4^x).

A similar argument shows that there are 12 points on $\mathbb{C}P^2 \times \mathbb{C}P^1 \times \mathbb{S}^2$ for each of the four conjugate stabilizers $C_3^{(k)}$ (Table 15(b), where points A', B', and C' are omitted for brevity). The total of $(3 \times 2 \times 2) \times 4 = 48$ points on $\mathbb{C}P^2 \times \mathbb{C}P^1 \times \mathbb{S}^2$ is made up of six eight-point orbits with stabilizer C_3.

The remaining two critical orbits on $\mathbb{C}P^2 \times \mathbb{C}P^1 \times \mathbb{S}^2$ have stabilizer C_s. We construct these orbits by taking points with stabilizer C_s^α on the $\mathbb{C}P^2 \times \mathbb{S}^2$ subspace (section 4.5) and combining them with the appropriate two D_{2d} points on the E-mode space $\mathbb{C}P^1$ (see Table 15(c)), as in the case of the stabilizer S_4. For six conjugate subgroups C_s we have 24 critical points on (the zero-dimensional component of) the C_s stratum of $\mathbb{C}P^2 \times \mathbb{C}P^1 \times \mathbb{S}^2$, which separate into two 12-point orbits.

5. Prediction of RE. This section is a reward for our painstaking study of the $T_d \times \mathcal{T}$ group action on $\mathbb{C}P^2 \times \mathbb{C}P^1 \times \mathbb{S}^2$. The reduced Hamiltonian H_{eff} is a $(T_d \times \mathcal{T})$-invariant function on $\mathbb{C}P^2 \times \mathbb{C}P^1 \times \mathbb{S}^2$ and it *must* have stationary points at all critical orbits of the $T_d \times \mathcal{T}$ action, which we found in the previous section (Table 15). Stationary points of H_{eff} are equilibria of the reduced system and are RE of the initial system with six vibrational degrees of freedom.[26]

[26]In order to simplify the analysis of the reduced system for P_4, the A_1-mode subsystem is excluded in [13] by setting $q^{A_1} = p^{A_1} = 0$ and $n_a = 0$; the model potential function was developed to cubic terms only. The number of degrees of freedom can be counted in several ways. Translational degrees of freedom can be trivially separated. Out of three rotational degrees of freedom, two can be reduced to account for the preservation of

RE correspond to families of special 3-tori in the initial phase space (see footnote 26) and are characterized *entirely* by symmetry and the values of the three integrals n_f, n_e, and j. The value of H_{eff} (energy) at RE and stability of RE are the primary characteristics of our system. Table 15 becomes, therefore, our most important result in view of practical applications. (Note that RE forming one symmetry group orbit are equivalent and it suffices to analyze stability and energy for one RE in the orbit.)

In this section, we are preoccupied with general understanding and description of possible functions H_{eff}. In particular, we want to know if such functions can have stationary points only on critical orbits, i.e., have the minimum number of stationary points. We place RE on critical group orbits and suggest possible stability. Assuming that H_{eff} is a Morse function on the space $\mathbb{C}P^2 \times \mathbb{C}P^1 \times \mathbb{S}^2$, we make sure that possible sets of stationary points satisfy Morse inequalities for this space and its invariant subspaces. We then find the simplest possible set (or sets) of RE, which correspond to the simplest Morse Hamiltonian(s) on $\mathbb{C}P^2 \times \mathbb{C}P^1 \times \mathbb{S}^2$ invariant with respect to the symmetry group of the system $T_d \times \mathcal{T}$. We can expect that at low perturbation (or excitation) our H_{eff} is such a simplest function.

The main purpose of this paper is the analysis of the complexity of the set of RE of systems combined of different subsystems. *Our first observation* in this context follows directly from the group action study in section 4. The RE set of the entire system is far from being a simple combination of the RE of the subsystems. As an example, take the F_2- and E-mode subsystems, which have 9 and 27 RE, respectively. These RE are also known as "nonlinear normal modes" [14, 15, 16]. They combine nonlinearly; there are 48 RE of the combined E–F_2 system corresponding to critical orbits on the $\mathbb{C}P^2 \times \mathbb{C}P^1$ phase space (see section 4.6).

Finding critical orbits on high-dimensional spaces constructed as a direct product of simpler spaces is greatly facilitated by tracing the correlation between critical orbits on subspaces and those on the complete space (for example, see section 4.5, Figures 11 and 12). *Our second main observation* is that the simplest $(T_d \times \mathcal{T})$-invariant Morse-type function H_{eff} with stationary points placed exclusively on critical orbits can be defined on individual subspaces $\mathbb{S}^2$, $\mathbb{C}P^1$, and $\mathbb{C}P^2$. However, when we go to a product space, such as $\mathbb{C}P^2 \times \mathbb{S}^2$, the situation becomes more complicated and there must be RE (stationary points of H_{eff}) lying on noncritical group orbits.

5.1. Consequences of local symmetry for linear stability. We can use our results on the critical orbits of the $T_d \times \mathcal{T}$ group action on $\mathbb{C}P^2 \times \mathbb{C}P^1 \times \mathbb{S}^2$ to find the position of corresponding RE and compute their energy for any given Hamiltonian H_{eff}. To find more about these RE *without* using any concrete H_{eff}, we should classify small phase space displacements x from them (coordinates on the tangent plane) according to the irreducible representations of their stabilizers. In this work, we are interested in one particular kind of group action, which

the length of the angular momentum vector and its projection on a laboratory fixed frame. This leaves six vibrational degrees of freedom and one rotational degrees of freedom, sometimes called "internal" degrees of freedom. However, we replace internal rotational degrees of freedom with two constrained oscillatory degrees of freedom, so there is a total of eight initial degrees of freedom (and a phase space of dimension 16), of which two represent one physical rotational degrees of freedom, and one representing the A_1 mode is ignored. Reduction with respect to all integrals n_a, n_f, n_e, and j leads to the reduced system on the space $\mathbb{C}P^2 \times \mathbb{C}P^1 \times \mathbb{S}^2$ with four degrees of freedom. The corresponding dynamical symmetry is T^4. If we neglect n_a by setting $q^{A_1} = p^{A_1} = 0$ *before* reduction, we restrict the initial system to seven degrees of freedom, and the dynamical symmetry is T^3.

is induced on $\mathbb{C}P^2 \times \mathbb{C}P^1 \times \mathbb{S}^2$ by spatial and reversal symmetries of the initial molecular rotation–vibration system. This action can be studied in the example of the SO(2) group (axial symmetry) and its discrete cyclic subgroups C_k (rotation by $2\pi/k$ with $k = 2, 3, 4, \dots$) acting on the initial coordinates of our system as groups of transformations.

We begin by describing a number of nondegenerate equilibria e with nontrivial stabilizers $G_e = C_k$ and corresponding G_e-invariant local quadratic Hamiltonians H_0 such that $H_0(e) = 0$. The local symmetry of e results in certain restrictions on H_0 and on the stability. We compute the Hessian matrix $\partial^2 H_0/\partial x^2$. Displacements that transform according to different rows of the same irreducible representation Γ_e form a degenerate eigenvalue block of $\partial^2 H_0/\partial x^2$. The number of negative eigenvalues of this matrix, or the *Morse index*, enters in Morse inequalities in section 5.2; the *Poincaré index* gives the sign of $\det(\partial^2 H_0/\partial x^2)$. In order to determine the stability of e, we consider H_0 as a Hamiltonian, establish local symplectic structure $\mathcal{J}$, and compute the eigenvalues of the corresponding Hamiltonian matrix $\mathcal{J}\partial^2 H_0/\partial x^2$. Hamiltonian stability and the Morse index are related unambiguously only in the case of dimension two (reduced system with one degree of freedom). The Poincaré index, which can be computed from the Morse index, gives some characteristics of linear Hamiltonian stability in systems with any degrees of freedom. Subsequently, we use our results to study the RE of our system.

5.1.1. C_k-invariant quadratic Hamiltonians on $\mathbb{R}^2$. We define the action of the rotation group SO(2) on the real variables (x_1, x_2) using the 2×2 orthogonal matrix

$$M_m(\varphi) = \begin{pmatrix} \cos m\varphi & \sin m\varphi \\ -\sin m\varphi & \cos m\varphi \end{pmatrix}, \quad m = 0, 1, 2, \dots,$$

and consider quadratic functions $H_0(x_1, x_2)$, which are invariant with respect to SO(2) or its discrete subgroups C_k (rotation by $\varphi = 2\pi/k$). For each given m we take $k > m$. Furthermore, it suffices to consider $k \le 2m$. The point $e = (x_1, x_2) = 0$ is a critical orbit and, therefore, an equilibrium of H_0. If the two displacements (x_1, x_2) about e transform as components of a two-dimensional real irreducible representation, then e can only be a minimum or a maximum of H_0 with signature $(++)$ or $(--)$ (Morse index 0 or 2), respectively, but not a saddle $(+-)$ with index 1.

Invariants of our SO(2) action are constructed using combinations

$$\xi = x_1 + ix_2 \quad \text{and} \quad \bar{\xi} = x_1 - ix_2,$$

which transform as conjugate irreducible one-dimensional complex representations $\pm m$ of SO(2). The pair (x_1, x_2) realizes a two-dimensional representation of SO(2), which is *irreducible over reals*. Descending to C_k, we should check whether this representation remains irreducible (over reals). For $m = 1$ and $m = 2$ this is the case for all $k \ne 2$ and $k \ne 4$, respectively. When $m = 2$ and $k = 4$, the image of C_4 becomes C_2. The corresponding quadratic forms are given in Table 16. We can see that the case $k = 2m$ is stable (elliptic) when $c^2 - ab < 0$ or unstable (hyperbolic) otherwise, while the $k \ne 2m$ equilibrium is always stable.

Table 16

Invariant local quadratic Hamiltonians with one and two degrees of freedom encountered in our study. The action of C_k on the phase plane $\mathbb{R}^2$ with coordinates (x_1, x_2) is given by the 2×2 orthogonal matrix $M_m(\varphi)$ with $\varphi = 2\pi/k$; the action of C_k on the phase space $\mathbb{R}^4$ with coordinates (x_1, x_2, x_3, x_4) is defined by $\mathrm{diag}(M_{m'}, M_{m''})(\varphi)$. *The action of the subgroups of $T_d \times \mathcal{T}$ on the local coordinates (x_1, x_2, y_1, y_2) is given in Table 18.*

Stabilizer	C_k-invariant quadratic form	Eigenvalues[27,28]
Case 2D: $m = 1, 2$, etc., $k > m$, and $\omega = dx \wedge dy$		
C_{2m}	$\frac{1}{2}ax^2 + \frac{1}{2}by^2 + cxy$	$\left[\pm\sqrt{c^2 - ab}\right]$, $\frac{1}{2}\{a + b \pm D_{abc}\}$
C_{2m+1}	$\frac{1}{2}a(x^2 + y^2)$	$[\pm ia]$, $\{a, a\}$
Case A: $m' = 1$, $m'' = 1$, and $\omega = dx_1 \wedge dy_1 + dx_2 \wedge dy_2$		
C_2	$\frac{1}{2}a'x_1^2 + \frac{1}{2}a''x_2^2 + \frac{1}{2}b'y_1^2 + \frac{1}{2}b''y_2^2$ + (all possible cross terms)	No restrictions
$C_k (k > 2)$	$\frac{1}{2}a(x_1^2 + x_2^2) + \frac{1}{2}b(y_1^2 + y_2^2)$ $+ c(x_1y_1 + x_2y_2) + d(x_1y_2 - x_2y_1)$	$\left[\pm\sqrt{c^2 - ab} + id, \pm\sqrt{c^2 - ab} - id\right]$ $\frac{1}{2}\left\{a + b \pm D_{abcd}\right\} \times 2$
Case A with extended symmetry $\mathcal{T}_k = C_k \times \mathcal{T}$, where $\mathcal{T} : (x_1, x_2, y_1, y_2) \to (x_1, x_2, -y_1, -y_2)$		
$\mathcal{T}_2$	$\frac{1}{2}a'x_1^2 + \frac{1}{2}a''x_2^2 + \frac{1}{2}b'y_1^2 + \frac{1}{2}b''y_2^2$ $+ cx_1x_2 + dy_1y_2$	No simple restrictions $\frac{1}{2}\left\{b' + b'' \pm D_{b'b''d}, a' + a'' \pm D_{a'a''c}\right\}$
$\mathcal{T}_k (k > 2)$	$\frac{1}{2}a(x_1^2 + x_2^2) + \frac{1}{2}b(y_1^2 + y_2^2)$	$[\pm i\sqrt{ab}] \times 2$, $\{a, b\} \times 2$
Case A with full symmetry and $\omega = dx_1 \wedge dy_1 + dx_2 \wedge dy_2$		
$C_{2v} \times \mathcal{T}$	$\frac{1}{2}a'x_1^2 + \frac{1}{2}a''x_2^2 + \frac{1}{2}b'y_1^2 + \frac{1}{2}b''y_2^2$	$\left[\pm i\sqrt{a'b'}, \pm i\sqrt{a''b''}\right]$, a', b', a'', b''
$D_{2d} \times \mathcal{T}$	$\frac{1}{2}a(x_1^2 + x_2^2) + \frac{1}{2}b(y_1^2 + y_2^2)$	$[\pm i\sqrt{ab}] \times 2$, $\{a, b\} \times 2$
$C_{3v} \times \mathcal{T}$	$\frac{1}{2}a(x_1^2 + x_2^2) + \frac{1}{2}b(y_1^2 + y_2^2)$	$[\pm i\sqrt{ab}] \times 2$, $\{a, b\} \times 2$
Case B: $m' = 1$, $m'' = 2$, and $\omega = dx_1 \wedge dy_1 + dx_2 \wedge dy_2$		
C_3	$\frac{1}{2}a'(x_1^2 + y_1^2) + \frac{1}{2}a''(x_2^2 + y_2^2)$ $+ c(x_1x_2 - y_1y_2) + d(x_1y_2 + y_1x_2)$	$\frac{1}{2}\left[i(a' - a'') \pm \Delta, i(a'' - a') \pm \Delta\right]$ $\frac{1}{2}\left\{a' + a'' \pm D_{a'a''cd}\right\} \times 2$
C_4	$\frac{1}{2}a'(x_1^2 + y_1^2) + \frac{1}{2}a''x_2^2 + \frac{1}{2}b''y_2^2 + cx_2y_2$	$[\pm ia', \pm\sqrt{c^2 - a''b''}]$ $\left\{a', a', \frac{1}{2}(a'' + b'' \pm D_{a''b''c})\right\}$
$C_k (k > 4)$	$\frac{1}{2}a'(x_1^2 + y_1^2) + \frac{1}{2}a''(x_2^2 + y_2^2)$	$[\pm ia', \pm ia'']$, $\{a', a''\} \times 2$
Case B with full symmetry and $\omega = dx_1 \wedge dy_1 + dx_2 \wedge dy_2$		
$C_3 \wedge \mathcal{T}_s$	$\frac{1}{2}a'(x_1^2 + y_1^2) + \frac{1}{2}a''(x_2^2 + y_2^2)$ $+ c(x_1x_2 - y_1y_2)$	$\frac{1}{2}\left[i(a' - a'') \pm \Delta, i(a'' - a') \pm \Delta\right]$ $\frac{1}{2}\left\{a' + a'' \pm D_{a'a''c}\right\} \times 2$
$S_4 \wedge \mathcal{T}_2$	$\frac{1}{2}a'(x_1^2 + y_1^2) + \frac{1}{2}a''x_2^2 + \frac{1}{2}b''y_2^2$	$\left[\pm ia', \pm i\sqrt{a''b''}\right]$, $\{a', a', a''b''\}$

5.1.2. C_k-invariant quadratic Hamiltonians on $\mathbb{R}^4$. We define the action of the SO(2) group on the four-plane $\mathbb{R}^4$ with coordinates (x_1, x_2, x_3, x_4) using the matrix $\left(\begin{smallmatrix} M_{m'} & 0 \\ 0 & M_{m''} \end{smallmatrix}\right)$, where the submatrices $M_{m'}$ and $M_{m''}$ act on the (x_1, x_2)-subspace and the (x_3, x_4)-subspace,

[27] Eigenvalues of the Hamiltonian and Hessian matrices are given in square [] and curly {} brackets, respectively; $\times 2$ indicates multiplicity.

[28] $\Delta = \sqrt{4(c^2 + d^2) - (a' + a'')^2}$, $D_{abcd} = \sqrt{(a - b)^2 + 4(c^2 + d^2)}$, $D_{abc} = D_{abc0}$.

respectively. (The case of the diagonal SO(2) action on $\mathbb{R}^2 \times \mathbb{R}^2$.) Invariants of this action can be readily constructed using

$$\xi = (x_1 + ix_2) \quad \text{and} \quad \eta = (x_3 + ix_4)$$

together with their conjugates $\bar{\xi}$ and $\bar{\eta}$. The four variables ξ, η, $\bar{\xi}$, $\bar{\eta}$ realize irreducible representations m', m'', $-m'$, $-m''$, respectively. We consider several situations of interest to our later study.

In the case of $m' = 1$ and $m'' = 2$, we have two quadratic SO(2) invariants $\frac{1}{2}\xi\bar{\xi}$ and $\frac{1}{2}\eta\bar{\eta}$. When SO(2) is lowered to C_3, we also have $\xi\eta$ and $\bar{\xi}\bar{\eta}$, which transform like $\exp(\pm 3i\varphi)$. Similarly, η^2 and $\bar{\eta}^2$ transform like $\exp(\pm 4i\varphi)$ and are the two extra invariants in the case of C_4.

In the case of $m' = m'' = 1$ (and generally for $m' = m''$), our SO(2) action has four quadratic invariants: the familiar $\frac{1}{2}\xi\bar{\xi}$, $\frac{1}{2}\eta\bar{\eta}$, and the cross terms $\xi\bar{\eta}$, $\eta\bar{\xi}$. The same four remain if SO(2) is lowered to C_k and $k > 2$. When $k = 2$, each coordinate x_i realizes real one-dimensional irreducible antisymmetric representation. All 10 quadratic monomials $x_j x_i$ are, therefore, C_2-invariant.

Generic C_k-invariant real quadratic forms in (x_1, x_2, x_3, x_4) constructed using the above invariants are presented in Table 16. As can be seen from this table, Hamiltonian stability of $e = (0, 0, 0, 0)$ depends on m', m'', k, and the symplectic form ω. The eigenvalues of the Hessian at $(0, 0, 0, 0)$, which are also given in Table 16, are used in the Morse theory analysis. Furthermore, we can see that additional symmetry, such as the time reversal extension for case A critical orbits (see sections 4.3, 4.5.3 and Table 15), can simplify the situation quite radically.

5.1.3. Points on $\mathbb{S}^2$ and $\mathbb{C}P^1$. Consider a nondegenerate critical point e with stabilizer G_e on the 2-sphere $\mathbb{S}^2$ or on the diffeomorphic space $\mathbb{C}P^1$. The group G_e is defined as a group of transformations of the ambient Euclidean space $\mathbb{R}^3$, which embeds $\mathbb{S}^2$ (see section 4). We want to know how G_e acts on the 2-plane $\mathbb{R}^2_{(e)}$ tangent to $\mathbb{S}^2$ or $\mathbb{C}P^1$ at e. It suffices to consider the circle group $G_e = \mathrm{SO}(2)$ and its subgroups C_k. A straightforward computation shows that the image of SO(2) and C_k in the representation spanned by the Euclidean coordinates (x, y) on $\mathbb{R}^2_{(e)}$ is again SO(2) and C_k and that $x \pm iy$ span representations ± 1. Then, following section 5.1.1, the point e on $\mathbb{S}^2$ and $\mathbb{C}P^1$ with stabilizer C_k, $k > 2$, is *always* stable; points with stabilizer C_2 can also be unstable.

5.1.4. Points on $\mathbb{C}P^2$. As before, we study a special case of the group action on the $\mathbb{C}P^2$ space induced by the natural action (vector representation) of the group SO(2) and its subgroups C_k on the complex 3-space with coordinates (z_1, z_2, z_3). This action is defined by a 3×3 orthogonal matrix M. The action on the corresponding real 6-space with coordinates $(q_1, q_2, q_3, p_1, p_2, p_3)$ is given by the matrix $\left(\begin{smallmatrix} M & 0 \\ 0 & M \end{smallmatrix}\right)$ with one copy of M acting on the q space and the other on the p space. The above action of SO(2) with the symmetry axis z_3, and of the corresponding discrete subgroups C_k with $k > 2$, on $\mathbb{C}P^2$ has three isolated fixed points (see section 4.3 and [17]):

$$A = (0, 0, 1), \qquad B = (1, \pm i, 0).$$

Table 17

Generic equilibria on $\mathbb{C}P^2$ in the presence of the natural action of the cyclic group C_k and its extensions.

Equilibrium[29]		$\partial^2 H_0$[30]	$\mathcal{J}\partial^2 H_0$[31]		Equilibrium[29]		$\partial^2 H_0$[30]	$\mathcal{J}\partial^2 H_0$[31]
A	$C_2 \times \mathcal{T}$	No simple restrictions			B	C_3	4, 2, 0	ii
	$C_{2v} \times \mathcal{T}$	4, 2, 0	ii				2	c
		3, 1	ir		B	C_4	4, 2, 0	ii
		2	rr				3, 1	ir
A	$C_k \times \mathcal{T},\ k > 2$	4, 0	ii	1:1	B	$C_k,\ k > 4$	4, 2, 0	ii
		2	rr	1:1				

(In Table 15 we use notation B, C for points of type B.) In the C_2 case, only the A-type fixed point is isolated. It is also useful to recall that the stabilizer of the A points in the case of the $T_d \times \mathcal{T}$ action on $\mathbb{C}P^2$ includes $\mathcal{T}$ (see Table 10) and that C_k can be extended easily to $\mathcal{T}_k = C_k \times \mathcal{T}$.

Any C_k-invariant Morse Hamiltonian H on $\mathbb{C}P^2$ has nondegenerate stationary points of types A and B. Let z be one of these points and let $\mathbb{C}^2_{(z)} \sim \mathbb{R}^4_{(z)}$ be the plane tangent to $\mathbb{C}P^2$ at z. This plane is a chart of $\mathbb{C}P^2$ with four real displacement coordinates (q', p', q'', p''). The zero order $H_0(q', p', q'', p'')$ of the Taylor expansion of H near z is a nondegenerate quadratic form. We study the action of C_k on (q', p', q'', p'') and find which generic forms in Table 16 correspond to H_0. Table 17 gives the summary of the results.

The action of C_k on $\mathbb{R}^4_{(z)}$ can be found by direct computation; see also section 10. The matrix of the rotation about axis z_3 by an arbitrary angle φ is

$$M(\varphi) = \begin{pmatrix} \cos\varphi & \sin\varphi & 0 \\ -\sin\varphi & \cos\varphi & 0 \\ 0 & 0 & 1 \end{pmatrix}.$$

We can see right away that four small real quantities (q_1, q_2), and (p_1, p_2), which define a displacement from point A (in the appropriate chart of $\mathbb{C}P^2$),

$$d_A = (q_1 + ip_1, q_2 + ip_2, 1)$$

transform like two copies of the real two-dimensional representation ± 1 of the group SO(2). Consequently, the forms of case A in Table 16 with (x_1, x_2, y_1, y_2) corresponding to (q_1, q_2, p_1, p_2) represent generic C_k and $(C_k \times \mathcal{T})$-invariant Morse functions locally at point A. The $C_2 \times \mathcal{T}$ form can be further simplified if we consider the full $C_{2v} \times \mathcal{T}$ stabilizer of the actual fixed point of the $T_d \times \mathcal{T}$ action. In that case H_0 has only four terms q_1^2, q_2^2, p_1^2, and p_2^2. Hamiltonian (linear) stability analysis of the A-type equilibria in the case of the full $T_d \times \mathcal{T}$ action is straightforward (see Table 17) because the linearized system separates in initial phase space coordinates and the analysis reduces to combining two systems with one degree of freedom.

[29] Type and local symmetry (stabilizer) of equilibria on $\mathbb{C}P^2$; see section 5.1.4 and Table 15 and compare to Table 16.

[30] Possible Morse index derived from the corresponding Hessian eigenvalues in Table 16.

[31] Possible eigenvalues of the Hamiltonian matrix: i and r stand for the imaginary and the real eigenvalue pair, respectively; 1:1 indicates resonance, c denotes four complex eigenvalues.

When we use the same approach for

$$d_B = (1, i + q_2 + ip_2, q_3 + ip_3) = (1, i + z_2, z_3),$$

we should project the transformed vector

$$M(\varphi)d_B = \left(e^{i\varphi} + z_2 \sin\varphi,\ ie^{i\varphi} + z_2 \cos\varphi,\ z_3\right)$$

back to the initial chart of $\mathbb{C}P^2$ and Taylor expand to the first order in (q_2, p_2, q_3, p_3),

$$\begin{aligned} M(\varphi)d_B\big|_{\text{chart}} &= \left[e^{i\varphi} + z_2 \sin\varphi\right]^{-1} M(\varphi)d_B \\ &\approx (1,\ i + e^{-2i\varphi}z_2,\ e^{-i\varphi}z_3). \end{aligned}$$

We can now see that (q_3, p_3) and (q_2, p_2) realize representations ± 1 and ± 2 of SO(2), respectively. Therefore, quadratic forms of case B in Table 16 with (x_1, y_1, x_2, y_2) corresponding to (q_2, p_2, q_3, p_3) represent generic C_k-invariant Morse functions locally at point B. For all points $B^{(k)}$ with $k > 3$, linearization separates in the initial coordinates (q_2, p_2) and (q_3, p_3). As in case A, stability analysis of these equilibria is simple. Point $B^{(3)}$ turns out to be the only interesting case, where the localized system is intrinsically four-dimensional; cf. [97].

5.1.5. Stability analysis of stationary points on $\mathbb{C}P^2$ in the presence of $T_d \times \mathcal{T}$. In the previous section, we showed that linear stability of stationary points on $\mathbb{C}P^2$ (vibrational RE) can be predicted by analyzing possible local Hamiltonians for RE whose stabilizer is an SO(2) group or a discrete cyclic subgroup C_k of this group. For the five types of vibrational RE labeled $A^{(2)}$, $A^{(3)}$, $B^{(3)}$, $A^{(4)}$, and $B^{(4)}$ (see Table 15) we take subgroups C_2, C_3, and C_4, respectively. The latter can be regarded as the principal symmetry operations of the respective stabilizers $C_{2v} \times \mathcal{T}$, $C_{3v} \times \mathcal{T}$, $C_3 \wedge \mathcal{T}$, $D_{2d} \times \mathcal{T}$, and $S_4 \wedge \mathcal{T}$. At the same time, prediction of stability of these RE can be further improved if we account for the full stabilizers.

To this end we proceed as before in section 5.1.4. We define local displacement coordinates (x_1, y_1, x_2, y_2) near the stationary point on $\mathbb{C}P^2$ and determine the action of the full stabilizer G on these coordinates. Knowing the action, we find the representation of G realized by (x_1, y_1, x_2, y_2) and construct the typical G-invariant quadratic form $H(x_1, y_1, x_2, y_2)$. We choose (x_1, y_1, x_2, y_2) so that the local 2-form is $dx_1 \wedge dy_1 + dx_2 \wedge dy_2$ and consider $H(x_1, y_1, x_2, y_2)$ as a Hamiltonian function of local linearization near the RE.

In order to define (x_1, y_1, x_2, y_2) we rotate the initial coordinates (z_1, z_2, z_3) so that in the new coordinates (z_1', z_2', z_3') the principal symmetry axis of the stabilizer becomes axis z_1'. The direction of the two other axes can be chosen as shown below:

Stabilizer	(z_1, z_2, z_3)	Map	(z_1', z_2', z_3')
$D_{2d}^{(x)} \times \mathcal{T}$	$\sqrt{2n}(1,0,0)$	E	$\sqrt{2n}(1,0,0)$
$S_4^{(x)} \wedge \mathcal{T}_2^{(y)}$	$\sqrt{n}(0,1,\mathrm{i})$	E	$\sqrt{n}(0,1,i)$
$C_{2v}^{(z)} \times \mathcal{T}$	$\sqrt{n}(1,1,0)$	M_1	$\sqrt{2n}(1,0,0)$
$C_{3v}^{[111]} \times \mathcal{T}$	$\sqrt{\frac{2}{3}n}(1,1,1)$	M_2	$\sqrt{2n}(1,0,0)$
$C_3^{[111]} \wedge \mathcal{T}_s^{\parallel}$	$\sqrt{\frac{2}{3}n}(1,\eta^2,\bar{\eta}^2)$	M_2	$\sqrt{n}e^{\mathrm{i}\pi/6}(0,1,i)$

where $z' = Mz$, $E = \mathrm{diag}(1,1,1)$,

$$M_1 = \begin{pmatrix} \frac{\sqrt{2}}{2} & \frac{\sqrt{2}}{2} & 0 \\ -\frac{\sqrt{2}}{2} & \frac{\sqrt{2}}{2} & 0 \\ 0 & 0 & 1 \end{pmatrix}, \quad \text{and} \quad M_2 = \begin{pmatrix} \frac{1}{\sqrt{3}} & \frac{1}{\sqrt{3}} & \frac{1}{\sqrt{3}} \\ \frac{1}{\sqrt{2}} & 0 & -\frac{1}{\sqrt{2}} \\ -\frac{1}{\sqrt{6}} & \frac{2}{\sqrt{6}} & -\frac{1}{\sqrt{6}} \end{pmatrix}.$$

Using the approach in section 5.1.4, we can show that the position of the RE in the new coordinates (z_1', z_2', z_3') is $(1,0,0)$ for type A and $(0,1,\pm i)$ for type B. We define displacement vectors

$$d_A = (z_1, x_1 + iy_1, x_2 + iy_2),$$

with $z_1 = \sqrt{2n - |z_2|^2 - |z_3|^2}$, and

$$d_B = (x_1 + iy_1, z_2', i\sqrt{n} + \sqrt{2}x_2 + iy_2/\sqrt{2}),$$

with $z_2' = \sqrt{n - |z_1'|^2 - |z_3'|^2}$. Note that, instead of projecting on an $\mathbb{R}^4_{(x,y)}$ chart of $\mathbb{C}P^2$ as we do in section 5.1.4, we represent the points of $\mathbb{C}P^2$ by fixing the total phase of (z_1', z_2', z_3') so that $\mathrm{Im}(z_1') = 0$ in the case of d_A and $\mathrm{Im}(z_2') = 0$ in the case of d_B (cf. section 2.4.3). Each symmetry operation R in the stabilizer G is realized initially as a linear transformation of the space $\mathbb{R}^3$ defined by a real matrix M_R. The same transformation applies to $\mathbb{C}^3$ with coordinates (z_1', z_2', z_3'). To realize this transformation on $\mathbb{C}P^2$, we should *correct* or *restore* the phase of $M_R z'$ in order to obey our phase condition. Therefore we define

$$Rd_A = \frac{[M_R\bar{z}]_1}{|[M_R\bar{z}]_1|} M_R d_A \quad \text{and} \quad Rd_B = \frac{[M_R\bar{z}]_2}{|[M_R\bar{z}]_2|} M_R d_B.$$

To find the action on (x, y) we Taylor expand Rd_A and Rd_B at $(x, y) = 0$ and compare them to the initial vectors d_A and d_B. Results are summarized in Table 18. As can be concluded from this table, displacements (x, y) realize the following representations of the respective stabilizers:

Point	Stabilizer	Representation spanned by (x, y)
$A^{(2)}$	$C_{2v} \times \mathcal{T}$	$A_{2g}(x_1) \oplus A_{2u}(y_1) \oplus B_{1g}(x_2) \oplus B_{1u}(y_2)$
$A^{(3)}$	$C_{3v} \times \mathcal{T}$	$E_g(x_1, x_2) \oplus E_u(y_1, y_2)$
$B^{(3)}$	$C_3 \wedge \mathcal{T}_s$	$E(x_1, y_1) \oplus E(x_2, -y_2)$
$A^{(4)}$	$D_{2d} \times \mathcal{T}$	$E_g(x_1, x_2) \oplus E_u(y_1, y_2)$
$B^{(4)}$	$S_4 \wedge \mathcal{T}_2$	$B_1(y_2) \oplus B_2(x_2) \oplus E(x_1, y_1)$

Here we denote irreducible representations of $\mathcal{T}$-extended groups using notation of corresponding point groups [66].

The above decomposition of representations realized by local displacements into irreducible representations makes construction of local quadratic Hamiltonians straightforward. In the case of $A^{(k)}$ and $B^{(4)}$ RE, all quadratic invariants are just linear combinations of scalar squares of displacements transforming according to different irreducible representations, such as $[E_g(x_1, x_2)]^2 = x_1^2 + x_2^2$, etc. The case of $B^{(3)}$ is the only case where a scalar product of two different displacements transforming according to the same irreducible representation E occurs. Generic local quadratic Hamiltonians for each RE are listed in Table 16. The brute-force way to find these Hamiltonians is by projecting the most general homogeneous second degree polynomial in (x_1, x_2, y_1, y_2) using the operator $|G|^{-1} \sum_{R \in G} R$, where G is the stabilizer of the RE in question.

Table 18

Action of stabilizers on local displacements from the stationary points on $\mathbb{C}P^2$.

Action of $D_{2d}^{(x)} \times \mathcal{T}$ on $E_g \oplus E_u$

R	Rx_1	Rx_2	Ry_1	Ry_2	R	Rx_1	Rx_2	Ry_1	Ry_2
E	x_1	x_2	y_1	y_2	$\mathcal{T}$	x_1	x_2	$-y_1$	$-y_2$
C_2^x	$-x_1$	$-x_2$	$-y_1$	$-y_2$	$\mathcal{T}_2^x$	$-x_1$	$-x_2$	y_1	y_2
C_2^y	$-x_1$	x_2	$-y_1$	y_2	$\mathcal{T}_2^y$	$-x_1$	x_2	y_1	$-y_2$
C_2^z	x_1	$-x_2$	y_1	$-y_2$	$\mathcal{T}_2^z$	x_1	$-x_2$	$-y_1$	y_2
σ^{yz}	x_2	x_1	y_2	y_1	$\mathcal{T}_s^{yz}$	x_2	x_1	$-y_2$	$-y_1$
$\sigma^{\overline{yz}}$	$-x_2$	$-x_1$	$-y_2$	$-y_1$	$\mathcal{T}_s^{\overline{yz}}$	$-x_2$	$-x_1$	y_2	y_1
S_4	x_2	$-x_1$	y_2	$-y_1$	$S_4\mathcal{T}$	x_2	$-x_1$	$-y_2$	y_1
S_4^{-1}	$-x_2$	x_1	$-y_2$	y_1	$S_4^{-1}\mathcal{T}$	$-x_2$	x_1	y_2	$-y_1$

Action of $C_{2v}^{(z)} \times \mathcal{T}$ on $A_{2g} \oplus A_{2u} \oplus B_{1g} \oplus B_{1u}$

R	Rx_1	Rx_2	Ry_1	Ry_2	R	Rx_1	Rx_2	Ry_1	Ry_2
E	x_1	x_2	y_1	y_2	$\mathcal{T}$	x_1	x_2	$-y_1$	$-y_2$
C_2^z	x_1	$-x_2$	y_1	$-y_2$	$\mathcal{T}_2^z$	x_1	$-x_2$	$-y_1$	y_2
σ^{xy}	$-x_1$	x_2	$-y_1$	y_2	$\mathcal{T}_s^{xy}$	$-x_1$	x_2	y_1	$-y_2$
$\sigma^{\overline{xy}}$	$-x_1$	$-x_2$	$-y_1$	$-y_2$	$\mathcal{T}_s^{\overline{xy}}$	$-x_1$	$-x_2$	y_1	y_2

Action[32] of $C_{3v}^{[111]} \times \mathcal{T}$ on $E_g \oplus E_u$

R	Rx_1	Rx_2	Ry_1	Ry_2
E	x_1	x_2	y_1	y_2
C_3	$-ax_1 - bx_2$	$bx_1 - ax_2$	$-ay_1 - by_2$	$by_1 - ay_2$
C_3^2	$-ax_1 + bx_2$	$-bx_1 - ax_2$	$-ay_1 + by_2$	$-by_1 - ay_2$
σ_{xy}	x_1	$-x_2$	y_1	$-y_2$
σ_{yz}	$-ax_1 + bx_2$	$bx_1 + ax_2$	$-ay_1 + by_2$	$by_1 + ay_2$
σ_{zx}	$-ax_1 - bx_2$	$-bx_1 + ax_2$	$-ay_1 - by_2$	$-by_1 + ay_2$
$\mathcal{T}$	x_1	x_2	$-y_1$	$-y_2$
$C_3\mathcal{T}$	$-ax_1 - bx_2$	$bx_1 - ax_2$	$ay_1 + by_2$	$-by_1 + ay_2$
$C_3^2\mathcal{T}$	$-ax_1 + bx_2$	$-bx_1 - ax_2$	$ay_1 - by_2$	$by_1 + ay_2$
$\mathcal{T}_s^{xy}$	x_1	$-x_2$	$-y_1$	y_2
$\mathcal{T}_s^{yz}$	$-ax_1 + bx_2$	$bx_1 + ax_2$	$ay_1 - by_2$	$-by_1 - ay_2$
$\mathcal{T}_s^{zx}$	$-ax_1 - bx_2$	$-bx_1 + ax_2$	$ay_1 + by_2$	$by_1 - ay_2$

Action of $S_4^{(x)} \wedge \mathcal{T}_2^{(y)}$ on $B_1 \oplus B_2 \oplus E$

R	Rx_1	Rx_2	Ry_1	Ry_2	R	Rx_1	Rx_2	Ry_1	Ry_2
E	x_1	x_2	y_1	y_2	$\mathcal{T}_2^y$	$-x_1$	$-x_2$	y_1	y_2
C_2^x	$-x_1$	x_2	$-y_1$	y_2	$\mathcal{T}_2^z$	x_1	$-x_2$	$-y_1$	y_2
S_4	y_1	$-x_2$	$-x_1$	$-y_2$	$\mathcal{T}_s^{yz}$	y_1	x_2	x_1	$-y_2$
S_4^{-1}	$-y_1$	$-x_2$	x_1	$-y_2$	$\mathcal{T}_s^{\overline{yz}}$	$-y_1$	x_2	$-x_1$	$-y_2$

Action[32] of $C_3^{[111]} \wedge \mathcal{T}_s^{\parallel}$ on $E \oplus E$

R	Rx_1	Rx_2	Ry_1	Ry_2
E	x_1	x_2	y_1	y_2
C_3	$-ax_1 - by_1$	$-ax_2 + by_2$	$bx_1 - ay_1$	$-bx_2 - ay_2$
C_3^2	$-ax_1 + by_1$	$-by_2 - ax_2$	$-bx_1 - ay_1$	$bx_2 - ay_2$
$\mathcal{T}_s^{xy}$	$ax_1 - by_1$	$ax_2 + by_2$	$-bx_1 - ay_1$	$bx_2 - ay_2$
$\mathcal{T}_s^{yz}$	$-x_1$	$-x_2$	y_1	y_2
$\mathcal{T}_s^{zx}$	$ax_1 + by_1$	$ax_2 - by_2$	$bx_1 - ay_1$	$-bx_2 - ay_2$

[32]Notation $a = 1/2$, $b = \sqrt{3}/2$.

5.2. Application of Morse theory. Simplest Morse Hamiltonians. Consider a manifold P whose topology is described by $\dim P + 1$ Betti numbers b_k. Particularly useful is the combination of these numbers, called the Euler characteristics Σ. A Morse function f on P is smooth and has only nondegenerate stationary points. Let c_k be the number of stationary points of f of Morse index k. The set of $\dim P$ Morse inequalities

$$\sum_{k=0}^{s}(-1)^{s-k}c_k \geq \sum_{k=0}^{s}(-1)^{s-k}b_k, \quad 0 \leq s < \dim P,$$

and the Euler–Poincaré equation

$$\sum_{k=0}^{\dim P}(-1)^k\, c_k = \sum_{k=0}^{\dim P}(-1)^k\, b_k = \Sigma,$$

express the relation between c_k and topological invariants b_k and Σ.

In the presence of a nonfree action of group G on P, all isolated points on the critical orbits of this action must be stationary points of f. The Morse function f with a *minimal possible* number of stationary points on P (in the presence of the specific group action) represents a class of simplest Morse functions. In the most trivial situations, such functions would have stationary points only on the isolated critical points. We should, therefore, check whether (and how) placing stationary points exclusively on the isolated points of critical orbits can satisfy the above Morse theory requirements. Table 19 gives Betti numbers for $\mathbb{S}^2$ and $\mathbb{C}P^2$ and suggests systems of stationary points on the vibrational spaces $\mathbb{C}P^2$ and $\mathbb{C}P^1$ and the rotational space $\mathbb{S}^2$ satisfying Morse theory in the presence of the $T_d \times \mathcal{T}$ group action. We begin with the simplest Morse Hamiltonians on each factor space of the total reduced phase space $\mathbb{C}P^2 \times \mathbb{C}P^1 \times \mathbb{S}^2$. Such Hamiltonians describe isolated F_2-mode or E-mode vibrational systems (polyads) or pure rotation.

5.2.1. Morse functions on the rotational space $\mathbb{S}^2$. Among the 26 fixed points of the $T_d \times \mathcal{T}$ action on $\mathbb{S}^2$ (Table 7), six points with stabilizer $S_4 \wedge \mathcal{T}$ and eight points with stabilizer $C_3 \wedge \mathcal{T}_s$ should be elliptic. The Morse conditions are satisfied if the 12 points with stabilizer $C_s \times \mathcal{T}_2$ are hyperbolic (unstable): $6 - 12 + 8 = 2$. The two possible simplest Morse Hamiltonians differ in sign: one has six maxima and eight minima while the other has this structure turned upside-down. If the internuclear adiabatic potential of the A_4 molecule can be well approximated as a sum of six pairwise interaction terms and all vibrations are frozen, then the minima are located at the six S_4 points [12] as shown in Figure 13, left.

We like to note that stationary points of simplest Morse functions of purely rotational systems (rotational RE of nonrigid bodies) should not necessarily be fixed points on $\mathbb{S}^2$. Thus in the case of the lowest possible symmetry of such systems $\mathcal{T}$ (no spatial symmetry), neither of the three pairs of equivalent RE has a fixed position on $\mathbb{S}^2$. Another example is the $C_2 \times \mathcal{T}$ system in Figure 6: four (two pairs) of its six RE can lie anywhere on the invariant circle.

5.2.2. Morse functions on the E-mode phase space $\mathbb{C}P^1$. Critical orbits of the $T_d \times \mathcal{T}$ action on $\mathbb{C}P^1$ are presented in Figure 9 and Table 8. The two equivalent $T \wedge \mathcal{T}_s$ (C_{3v}) points should be elliptic. The Morse conditions are satisfied if, out of the two three-point orbits with stabilizer $D_{2d} \times \mathcal{T}$, one contains elliptic points and the other hyperbolic points. The freedom

Table 19

Betti numbers b_k and Euler–Poincaré characteristics Σ for the spaces $\mathbb{C}P^2$ and $\mathbb{C}P^1 \sim \mathbb{S}^2$ (top). Number and type of stationary points of the simplest Morse function on the F_2-mode space $\mathbb{C}P^2$, E-mode space $\mathbb{C}P^1$, and rotational sphere $\mathbb{S}^2$ in the presence of the symmetry group $T_d \times \mathcal{T}$. The frame indicates additional stationary points of the possible nonsimplest Morse function on $\mathbb{C}P^2$.

Space	b_0	b_1	b_2	b_3	b_4	b_5	b_6	Σ
$\mathbb{C}P^1 \sim \mathbb{S}^2$	1	0	1					2
$\mathbb{C}P^2$	1	0	1	0	1			3
$\mathbb{C}P^1 \times \mathbb{S}^2$	1	0	2	0	1			4
$\mathbb{C}P^2 \times \mathbb{S}^2$	1	0	2	0	2	0	1	6

Space	c_0	c_1	c_2	c_3	c_4	c_5	c_6	Σ
$\mathbb{C}P^1$	$3D_{2d} \times \mathcal{T}$	$3D_{2d} \times \mathcal{T}$	$2T \wedge \mathcal{T}_s$					2
$\mathbb{S}^2$	$6S_4 \wedge \mathcal{T}_s$	$12C_s \wedge \mathcal{T}_2$	$8C_3 \wedge \mathcal{T}_s$					2
$\mathbb{C}P^2$	$4C_{3v} \times \mathcal{T}$	$6C_{2v} \times \mathcal{T}$	$8C_3 \wedge \mathcal{T}_s$	$6S_4 \wedge \mathcal{T}_s$	$3D_{2d} \times \mathcal{T}$			3
$\mathbb{C}P^2$	$4C_{3v} \times \mathcal{T}$	$6C_{2v} \times \mathcal{T}$	$3D_{2d} \times \mathcal{T}$ $8C_3 \wedge \mathcal{T}_s$	$\boxed{6C_s \wedge \mathcal{T}_2}$ $\boxed{6C_s \wedge \mathcal{T}_2}$	$6S_4 \wedge \mathcal{T}_s$			3
$\mathbb{C}P^2 \times \mathbb{S}^2$	$8C^{(3)}$	$12C_s$	$6C^{(4)}$ $6A^{(4)}$	$12A^{(2)}$	$8A^{(3)}$ $8B^{(3)}$	$12C_s$	$6B^{(4)}$	6

Figure 13. *Simplest purely rotational (left) and E-mode vibrational (right) Morse Hamiltonians (often called* energy surfaces*) of the* A_4 *molecule as functions on the phase spaces $\mathbb{S}^2$ and $\mathbb{S}^2 \sim \mathbb{C}P^1$. The bounding potential of the* A_4 *molecule is approximated as a sum of pairwise harmonic atom–atom interaction terms; see* [12].

of choice is limited to having two maxima and three minima or vice versa. As before, we can predict which of the two possibilities is realized in A_4 using the simple atom–atom vibrational potential of [12, 13]. It turns out that at fixed action n_e the two C_{3v}-symmetric RE have maximum energy; see Figure 13. Note that the same happens in the case of the E mode of the A_3 molecule, such as H_3^+ [19], whose equilibrium configuration is an isosceles triangle.

5.2.3. Morse functions on the F_2-mode phase space $\mathbb{C}P^2$. Among the fixed points of the $T_d \times \mathcal{T}$ action on $\mathbb{C}P^2$ (see Tables 10 and 17) only points with stabilizers $C_{2v} \wedge \mathcal{T}$ and $S_4 \wedge \mathcal{T}_2$ (D_2 and C_4 in the short notation) can have odd Morse indexes. Table 19 demonstrates how Morse inequalities for $\mathbb{C}P^2$ are satisfied if stationary points lie only on the critical orbits. We can interchange points of indexes $1 \leftrightarrow 3$ or/and $0 \leftrightarrow 4$ to obtain other possible simplest Morse functions. Table 20 shows how this simplest set of stationary points respects Morse

Table 20

Stationary points of the $(T_d \times \mathcal{T})$-invariant Morse Hamiltonians on $\mathbb{C}P^2$ (see Table 19) projected on the C_2- and C_s-invariant spheres.

Stabilizer of sphere	Stabilizer of orbit	Signature (index) on $\mathbb{C}P^2$	Signature (index) on $\mathbb{S}^2$	Number of points on $\mathbb{S}^2$
	Simplest Morse Hamiltonian:			
C_2	$D_{2d} \times \mathcal{T}$	[++++] (0)	[++] (0)	2
	$S_4 \wedge \mathcal{T}_2$	[+++−] (1)	[+−] (1)	2
	$C_{2v} \wedge \mathcal{T}$	[+−−−] (3)	[−−] (2)	2
C_s	$D_{2d} \times \mathcal{T}$	[++++] (0)	[++] (0)	1
	$C_{2v} \wedge \mathcal{T}$	[+−−−] (3)	[+−] (1)	1
	$C_{3v} \times \mathcal{T}$	[−−++] (2)	[−−] (2)	2
	Nonsimplest Morse Hamiltonian:			
C_2	$D_{2d} \times \mathcal{T}$	[+−+−] (2)	[+−] (1)	2
	$S_4 \wedge \mathcal{T}_2$	[++++] (0)	[++] (0)	2
	$C_{2v} \wedge \mathcal{T}$	[+−−−] (3)	[−−] (2)	2
C_s	$D_{2d} \times \mathcal{T}$	[+−+−] (2)	[+−] (1)	1
	$C_{2v} \wedge \mathcal{T}$	[+−−−] (3)	[+−] (1)	1
	$C_s \wedge \mathcal{T}_2$	[+++−] (1)	[++] (0)	2
	$C_{3v} \times \mathcal{T}$	[−−++] (2)	[−−] (2)	2

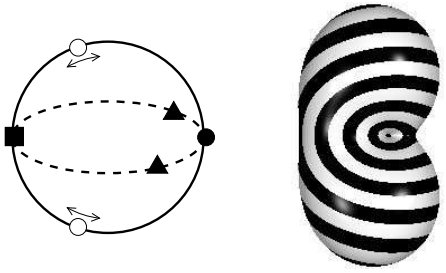

Figure 14. *Position of RE (left) and vibrational F_2-mode Hamiltonian (right) of the A_4 molecule restricted to the C_s-invariant sphere in the phase space $\mathbb{C}P^2$. White circles denote extra (nonfixed) RE; other markers correspond to fixed points in Figure 12 (left). The bounding potential of A_4 is approximated as a sum of pairwise atom–atom harmonic interaction terms [13].*

theory requirements for the C_2- or C_s-invariant spheres in Table 12 and in Figures 11 and 12 (left). It can be further verified that requirements for *all* closed invariant subspaces of $\mathbb{C}P^2$ are satisfied.

Computation with the atom–atom potential [13] (in the limit of independent vibrational and rotational motions) suggests that the simplest Morse Hamiltonian is *not* realized in real A_4 molecules. Instead we expect a Hamiltonian with 12 additional equivalent RE with stabilizer $C_s \wedge \mathcal{T}_2$, which are situated in pairs on the $(C_s \wedge \mathcal{T}_2)$-invariant main circle of the six C_s-invariant spheres, as shown in Figure 14. When the energy of the system (or the action n_f) changes, these two RE can move along the invariant circle. The set of RE of this nonsimplest system is characterized in the second to last row of Table 19 and in Table 20, bottom.

5.2.4. Morse functions on combined spaces. The Betti numbers b_k and Euler characteristics Σ for the smooth manifold P, which is a product $P' \times P''$, follow from those for factor

spaces P' and P'',

$$b_k = \sum_{i+j=k} b'_i b''_j, \quad \Sigma = \sum_{k=0}^{\dim P} (-1)^k b_k,$$

where indexes i, j, and k go from 0 to $\dim P'$, $\dim P''$, and $\dim P = \dim P' + \dim P''$, respectively. In many cases we can analyze RE on P by combining the rules for P' and P''; the most interesting case turns out to be that of $\mathbb{C}P^2 \times \mathbb{S}^2$ (F_2-mode vibration and rotation).

Satisfying Morse conditions on invariant subspaces becomes increasingly important in high dimensions. Thus, even before attempting to consider whether the "minimum" set of the 12 A^{C_2}, six $(A, B, C)^{C_4}$, and eight $(A, B, C)^{C_3}$ stationary points (see Table 15—ignore indexes $_{1,2}$) satisfies all conditions for $\mathbb{C}P^2 \times \mathbb{S}^2$, we can check if this set works for the subspaces of $\mathbb{C}P^2 \times \mathbb{S}^2$. Going back to section 4.5 and Figure 12, we conclude immediately that our set is incomplete. Indeed, we should expect at least two stationary points (a maximum and a minimum) on each of the twelve C_s-invariant spheres in $\mathbb{C}P^2 \times \mathbb{S}^2$—yet *none* of the fixed points of the $T_d \times \mathcal{T}$ action lies on these spheres. Therefore, the set of stationary points on the $\mathbb{C}P^2 \times \mathbb{S}^2$ space (rotation–vibration RE) includes necessarily at least two 12-point noncritical C_s-orbits. Adding these 24 points, the simplest Morse function on $\mathbb{C}P^2 \times \mathbb{S}^2$ can be constructed; one possibility is presented in the last row of Table 19. This function corresponds to the Coriolis-dominated structure, which we will discuss on the example in section 11.

5.3. RE in the initial phase space. RE of the A_4 molecule in the initial phase space can be largely, and in some cases *entirely*, reconstructed using the qualitative information on the symmetry group action on the reduced phase space $\mathbb{C}P^2 \times \mathbb{C}P^1 \times \mathbb{S}^2$ and stationary points of the reduced Hamiltonian. Thus all purely rotational RE of a tetrahedral molecule correspond to the stationary rotation around the symmetry axis of their stabilizers. For the $S_4 \wedge \mathcal{T}$ stabilizer we take axis C_4, and for $C_s \times \mathcal{T}_2$ we take the C_2 axis orthogonal to the symmetry plane. Vibrational RE of the E- and F_2-mode systems form families of basic periodic orbits in the initial phase space parameterized by the values of integrals n_e and n_f. Rotation–vibration RE of our system are labeled by the values of integrals j, n_e, and n_f and can be reconstructed as appropriate combinations of the periodic motions of the subsystems, which correspond to the combined stationary points on the reduced phase space $\mathbb{C}P^2 \times \mathbb{C}P^1 \times \mathbb{S}^2$ (see Table 15) and which become 3-tori (see footnote 26) in the original phase space of the system. We will characterize these RE in more detail and illustrate the results on the concrete example of the A_4 molecule introduced in section 2.3 and [13].

5.3.1. RE of the *E*-mode system. Neglecting rotation and interaction with other vibrational modes, the E-mode system can be described by the Hamiltonian

$$H = \omega_e \big[H_0 + V(q)\big], \tag{5.1a}$$

where

$$H_0 = \frac{1}{2}\sum_{i=1}^{2}(q_{E_i}^2 + p_{E_i}^2) = \frac{1}{2}(p_{E_1}^2 + p_{E_2}^2) + V_0 \tag{5.1b}$$

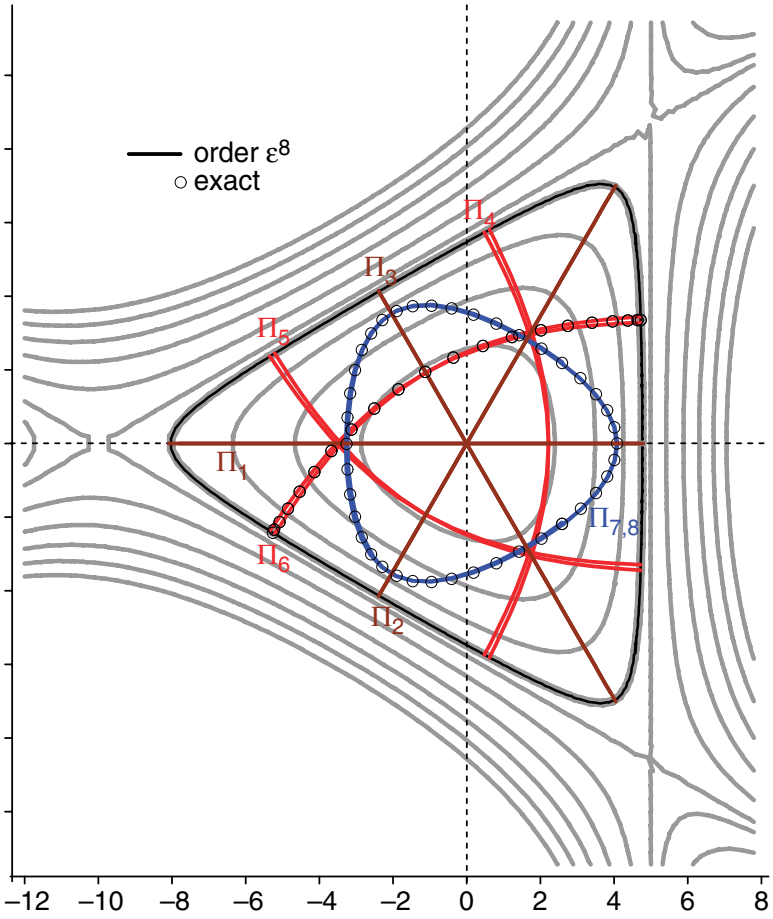

Figure 15. *Hénon–Heiles potential $V_0(q) + \varepsilon V(q)$ computed for $\varepsilon = 0.1$ and $h/h_{\text{saddle}} = 0.2, 0.45, 0.7, 0.9$ (bold contour), $1, 1.2, \ldots$ (gray). Nonlinear normal modes of the Hénon–Heiles oscillator (E-mode system) reconstructed using ϵ^8 normal form with $\varepsilon = 0.1$ and $h/h_{\text{saddle}} = 0.9$ (colored).*

is the Hamiltonian of the 1:1 harmonic oscillator, and the anharmonic part of the D_3 symmetric potential equals

$$V(q) = \varepsilon \left(\frac{1}{3} q_{E_1}^2 - q_{E_2}^2 \right) q_{E_1} + \cdots . \tag{5.1c}$$

The potential $V_0 + V$ is shown in Figure 15. We can see that to the lowest order in ε our E-mode system is equivalent to the Hénon–Heiles oscillator, which has the same symmetry $D_3 \times \mathcal{T} \sim D_{3h}$. (Note that the E-mode system of triatomic molecules with the equilateral triangle equilibrium, e.g., H_3^+ [19], also has the same symmetry and the same lowest order Hamiltonian.) In our A_4 example [13], $\varepsilon = -\frac{3\sqrt{3}}{4}\epsilon$ and $\omega_e = \omega$.

The RE of the E-mode system are, of course, reconstructed in the same way as the RE of the Hénon–Heiles oscillator [77, 14, 15, 16, 18, 19, 78]. We represent trajectories of this system at a given fixed energy h using their projection in the configuration space, a plane $\mathbb{R}_q^2$ with coordinates (q_{E_1}, q_{E_2}). To distinguish between trajectories with the same coordinate

image, we specify their direction. The boundary of the classical motion is the h-level set of $V_0(q)+V(q)$. (We consider small amplitudes and are not interested in the unbounded motion of the Hénon–Heiles system at large energies.)

The symmetry group $T_d \times \mathcal{T}$ acts on $\mathbb{R}^2_q$ (see section 4.2) like the planar point group D_3. Operations in this group $\{1, 2C_3, 3C_2\}$ act naturally on the RE projections in the $\mathbb{R}^2_q$ space. The time reversal $\mathcal{T}$ acts trivially on the coordinate space $\mathbb{R}^2_q$ while changing signs of the momenta p and thus reversing the flow of the dynamical system. It follows that $\mathcal{T}$ changes the direction of the periodic trajectories and of their image in $\mathbb{R}^2_q$. All we should do in order to reconstruct qualitatively the projection of the RE in $\mathbb{R}^2_q$ is to suggest two curves with stabilizer $T \wedge \mathcal{T}_s$ and two groups of three curves with stabilizer $D_{2d} \times \mathcal{T}$ (see critical orbits in Table 8). In [77, 14, 15, 16] these RE are called $\Pi_{7,8}$, $\Pi_{3,4,5}$, and $\Pi_{6,7,8}$, respectively.

Since the group $(T \wedge \mathcal{T}_s)/D_2 = \{1, 2C_3, 2(C_2\mathcal{T})\}$ does not include the time reversal $\mathcal{T}$ itself, the two periodic trajectories $\Pi_{7,8}$ are mapped into each other by $\mathcal{T}$ and share the same image in $\mathbb{R}^2_q$. The image is a closed C_3-invariant loop shaped as a smoothed equilateral triangle (Figure 15, right). It is easy to check that any of the three reflections C_2 also map $\Pi_7 \leftrightarrow \Pi_8$, while the operations $C_2\mathcal{T}$ leave them invariant. The trajectories $\Pi_{3,4,5}$ and $\Pi_{6,7,8}$ project on lines (degenerate loops) in $\mathbb{R}^2_q$ because their stabilizer $(D_{2d} \times \mathcal{T})/D_2 = C_2 \times \mathcal{T}$ includes time reversal $\mathcal{T}$. Such lines should necessarily begin and end on the boundary of the motion, where the trajectory has a turning point and approaches the boundary at a right angle. This leaves two possibilities (Figure 15, right): three straight lines on the three C_2 axes and three curved lines, each intersecting one of the C_2 axes at a right angle.

5.3.2. RE of the F_2-mode system. Neglecting rotation and interaction with other vibrational modes, the F_2-mode system can be described by the Hamiltonian

$$H = \omega_f \left[H_0 + \varepsilon V_1(q) + \varepsilon^2 H_2(q,p) + \cdots \right],$$

where

$$H_0 = \frac{1}{2}\sum_{i=1}^{3}(q_i^2 + p_i^2) = \frac{1}{2}(p_1^2 + p_2^2 + p_3^2) + V_0$$

is the Hamiltonian of the 1:1:1 harmonic oscillator and

$$V_1(q) = q_1 q_2 q_3$$

is the lowest order anharmonic part of the T_d symmetric potential. The potential $V_0 + \varepsilon V_1$ illustrated in Figure 16 appears as a direct three-dimensional analogue of the two-dimensional Hénon–Heiles potential in (5.1c). However, the (small) fourth degree term

$$V_2(q) = q_1^4 + q_2^4 + q_3^4$$

should also be included for the more general description of the reduced system [98]. (Note that any T_d symmetric potential can be written as a polynomial in V_0, V_1, and V_2.) In the concrete potential of the A_4 molecule [13], we have

$$V(q) = V_0 + \epsilon \frac{3}{2\,(2)^{1/4}} V_1 + \epsilon^2 \left(\frac{7\sqrt{2}}{64} V_2 - \frac{5\sqrt{2}}{16} V_0^2 \right),$$

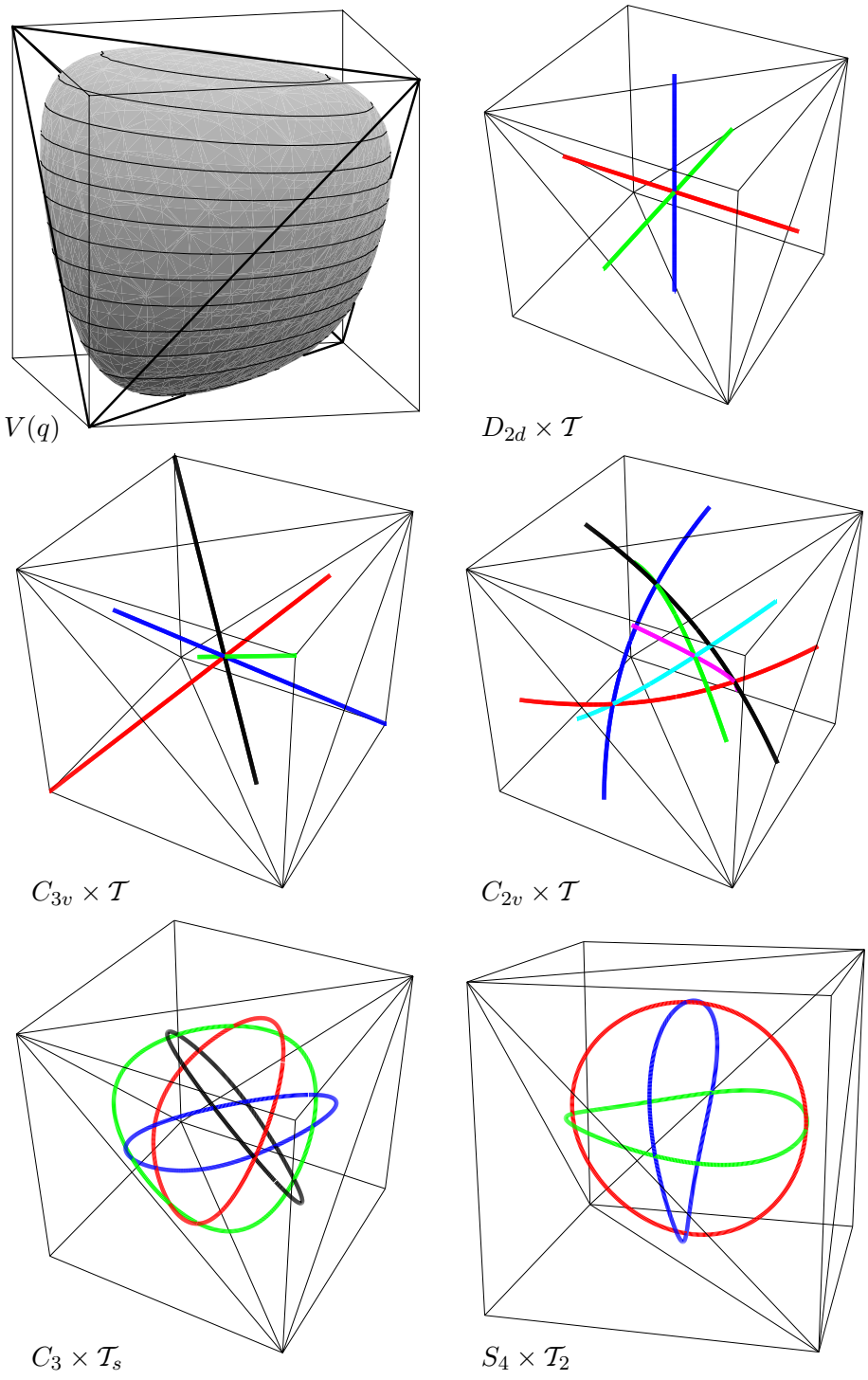

Figure 16. *Qualitative representation of the equipotential surface of the F_2-mode system (top left). Nonlinear normal modes (RE) of the three-dimensional analogue of the Hénon–Heiles oscillator (F_2-mode system) reconstructed for $\epsilon = 1$ and energy $H_0 = 0.118$.*

while $\omega_f = \sqrt{2}\omega_e$. The molecular F_2-mode Hamiltonian H_2 also contains the kinematic term $\epsilon^2 \frac{1}{8}[\mathbf{p} \times \mathbf{q}]^2$ related to the angular momentum induced by the F_2-mode vibrations.

The RE of the F_2-mode system in Figure 16 (cf. Figure 8 in [18] and [98]) can be reconstructed qualitatively using the method in the previous section. We project trajectories of this system in the configuration space $\mathbb{R}^3_q$, where they stay inside a tetrahedral cavity bounded by the h-level of $V(q)$; see Figure 16, top left. We classify curves in this cavity by their stabilizers. RE with stabilizers $D_{2d} \times \mathcal{T}$, $C_{3v} \times \mathcal{T}$, and $C_{2v} \times \mathcal{T}$ (D_4, D_3, and D_2 in the shorthand notation of section 4.3) are $\mathcal{T}$-invariant. They project to lines in $\mathbb{R}^3_q$, which are passed in both directions. Like $\Pi_{1,2,3}$ of the Hénon–Heiles system, the $D_{2d} \times \mathcal{T}$ and $C_{3v} \times \mathcal{T}$ RE lie on the corresponding symmetry axes C_4 and C_3. The $C_{2v} \times \mathcal{T}$ RE lie in the symmetry planes C_s and are slightly curved; they resemble, therefore, $\Pi_{4,5,6}$. RE with stabilizers $S_4 \times \mathcal{T}_s$ and $C_3 \wedge \mathcal{T}_s$ are similar to the "circular" RE $\Pi_{7,8}$. They project on closed directed curves in $\mathbb{R}^3_q$. In the crudest approximation, these RE can be represented as circles lying in the plane orthogonal to the respective axes C_4 and C_3. The $S_4 \times \mathcal{T}_s$ RE develops a characteristic "bow tie" twist (see Figure 16), which brings the circular symmetry down precisely to $S_4 \times \mathcal{T}_s$. The $C_3 \wedge \mathcal{T}_s$ RE has a triangular shape similar to that of $\Pi_{7,8}$ and bends slightly out of plane like the trim on a skullcap. We can further observe that the energy–action characteristics of the F_2-mode RE (see Table 19 and sections 5.1.4 and 5.2.3) also shows a certain similarity to the E-mode system: At given fixed action n_f, the energy of "circular" RE tends to be higher than that of "linear" RE.

5.4. Quantum predictions. Quantum manifestations of RE are very familiar to physicists working on highly excited rotating molecules [31, 32, 33, 34, 18]. Within our more general context we should consider these manifestations for reduced phase spaces of dimension greater than two and products of two (or more) reduced phase spaces with two (or more) dynamical integrals of motion. The latter are quantized, and the corresponding quantum numbers label polyads or multiplets of quantum levels whose internal structure (at given fixed values of integrals) is analyzed using RE. In our system we have three dynamical integrals j, n_e, and n_f, and three corresponding quantum numbers J, N_e, and N_f, which all take integer values.

5.4.1. Systems with one dynamical integral. The most well-known quantum "signature" of classical RE is the presence of quantum states localized predominantly near one particular stable RE (a basic stable periodic orbit). In the simplest situation, all nodes of the quantum wavefunction lie along the periodic orbit, and the number of nodes N (up to Maslov's correction μ negligible in the classical limit of large N) equals $(2\pi)^{-1}$ times the action integral taken along the orbit that in turn equals the value of the dynamical integral n for the particular RE and energy h,

$$N + \mu = n(h) = \frac{1}{2\pi} \oint_{H(p,q)=h} p\, dq,$$

where $\mu = K/2$ for a K-dimensional harmonic oscillator. The energy of such a state is as close to h, i.e., to the classical maximum or minimum energy, as possible. With excitation of oscillations about the RE growing, the nodal pattern becomes less trivial and localization disappears eventually.

Stable RE manifest themselves clearly in the structure of the energy levels. The energy level structure largely depends on the dimension of the reduced phase space P and the symmetry present. The reduced system near a stable RE on P can be represented as a nonlinear oscillator of dimension $\frac{1}{2}\dim P$. If the area of classical stability in the phase space is sufficiently large (compared to $\hbar$) we can even observe a "family" of states. If $\frac{1}{2}\dim P > 1$, the harmonic oscillator frequencies can be (partially) degenerate due to the local symmetry of the RE. In the case of k equivalent RE, our reduced system is represented locally as a k-well oscillator. The depth of the wells (or the height of the barrier) is determined by the stability of the RE. We observe k-level quasi-degenerate quantum states or *clusters*. The cluster, which is closest in energy to the classical RE limit, has the smallest splitting.

We should well distinguish the quasi-degeneracy of quantum states caused by the degeneracy of the local oscillator system and by the presence of several equivalent (by symmetry) stable RE, respectively. We also recall that the presence of the symmetry group with multidimensional (degenerate) irreducible representations can further complicate the analysis of the energy level patterns because quantum states with wavefunctions transforming according to rows of the same irreducible representation are strictly degenerate.

5.4.2. Examples of simple cluster structures. The most well-known molecular example of the correspondence between quantum energy levels and classical RE is the structure of individual (isolated) rotational multiplets (section 1.2). In this case $P \sim \mathbb{S}^2$, $\frac{1}{2}\dim P = 1$. We observe simple regular sequences of rotational clusters. Near the limiting RE energy, the system of almost equidistant sequences resembles a k-well one-dimensional harmonic oscillator; the energy separation between the RE and the closest (first) cluster is approximately half the distance between the clusters, i.e., half-quantum.

The $2J+1$ multiplet of the ground vibrational state of a spherical top molecule [31, 32, 33, 34, 79] has six-fold and eight-fold clusters corresponding to stable RE (stable stationary axes of rotation) with stabilizers C_4 and C_3, respectively. The energy region near the unstable RE with stabilizer C_s separates the two cluster systems. In the case of A_4 (section 5.2) the six-fold clusters lie at the bottom energies.

Asymmetric top molecules, such as H_2O, have three paired RE. The RE in each pair correspond to classical rotation about one of the principal inertia axes in two different directions and are related by time reversal. Four RE (in two pairs) are stable and rotational levels form respective two-fold clusters (doublets).

A similar cluster structure is known for vibrational systems with $P \sim \mathbb{S}^2$, such as the E-mode system in H_3^+ [19], and in A_4 (section 5.2 and 5.3.1). Vibrational polyads of these systems are labeled by quantum number $N_e = 0, 1, \ldots$ and contain $N_e + 1$ levels (to complete the rotational analogy use $J_e = \frac{1}{2}N_e$); two-fold and three-fold clusters lie near the top and bottom polyad energies, respectively. These E-mode clusters are formed when vibrational excitation is high enough to have at least five quantum states in the polyad ($N_e > 4$). Other vibrational systems with reduced phase space $\mathbb{S}^2$ include a number of triatomic molecules with nearly 1:1 resonant stretching vibrations, notably H_2O and O_3 [22, 23, 24, 25, 26, 27]. The so-called *local modes* of these molecules are nothing else but a pair of stable equivalent RE, which bifurcates (very early) from the initial "normal mode" RE as the polyad quantum number n rises. The corresponding "local mode states" form doublets; they are commonly

associated with vibrations localized on the particular atom–atom bond.

5.4.3. Quantum F_2-mode system. So far in this section, we have summarized the fundamentals of quantum interpretation of RE that are largely known. New aspects begin here. The reduced phase space $P \sim \mathbb{C}P^2$ of the F_2-mode system is a compact space of real dimension four, and $\frac{1}{2}\dim P = 2$. This means that we have a finite number of quantum states in each *polyad* with quantum number $N_f = 0, 1, \ldots$ and that the number of states is given by a polynomial in N_f of degree 2. More precisely, the polyads of the 1:1:1 oscillator have $\frac{1}{2}(N_f+1)(N_f+2)$ states.

Predicting and understanding the internal structure of the F_2-mode polyads begins with the RE analysis. Taking into account Morse theory requirements for $\mathbb{C}P^2$ (see section 5.1.4 and Table 17) and its C_s- and C_2-invariant symplectic subspaces $\mathbb{S}^2$ (section 5.2.3) we can suggest stability of the set of RE in the second to last row of Table 19. One possibility is given below.

RE	Stabilizer	Signature	Stability		Type
$6C_4$	$S_4 \wedge \mathcal{T}_2$	$[----]$	ii		$B, C^{(4)}$
$12C_s$	$C_s \wedge \mathcal{T}_2$	$[---+]$	ir		Not fixed
$8C_3$	$C_3 \wedge \mathcal{T}_s$	$[++--]$	c		$B, C^{(3)}$
$3D_4$	$D_{2d} \wedge \mathcal{T}$	$[+-+-]$	rr	1:1	$A^{(4)}$
$6D_2$	$C_{2v} \wedge \mathcal{T}$	$[-+++]$	ir		$A^{(2)}$
$4D_3$	$C_{3v} \wedge \mathcal{T}$	$[++++]$	ii	1:1	$A^{(3)}$

Here, as in Table 17, we use i and r to mark imaginary and real eigenvalue pairs of the local linearized Hamiltonian; c stands for four complex eigenvalues.

Using only N_f and energy H is insufficient to untangle the rich energy level spectrum of the polyad. Since the system is not integrable (there is no third global integral), all we can do is label localized states of different kinds with different sets of additional "good" quantum numbers. When the local approximation separates into the i and/or r subsystems, quantum analysis becomes straightforward. Thus, near the two stable (elliptic) RE, which are denoted ii, our system can be represented as a two-dimensional oscillator.

At the minimum polyad energy $H(A^{(3)})$ we have an oscillator with four equivalent equilibria or "wells." Near each equilibrium it is described as a two-dimensional D_3 symmetric oscillator with 1:1 resonant harmonic frequencies. In other words, we encounter a four-fold analogue of the Hénon–Heiles system. Provided that the $A^{(3)}$ RE is sufficiently stable (the wells are deep) we may expect to find a series of "small polyads" labeled by an additional "good" quantum number $\tilde{N} = 0, 1, \ldots \ll N_f$. The structure is similar to that already discussed for the E-mode system, albeit the number of levels is quadrupled. In particular, the first level with $\tilde{N} = 0$ (the lowest level in the polyad) is a four-fold cluster. At the maximum polyad energy $H(B^{(4)})$ we find a six-well two-dimensional oscillator. The wells are C_4 symmetric and have two frequencies which are, in general, incommensurate. The level system associated with the $B^{(4)}$ RE can be described using two additional local quantum numbers $\tilde{N}'$ and $\tilde{N}''$; the first level (the highest level in the polyad) is a six-fold cluster.

5.4.4. Combined systems with several dynamical integrals. Multiplets of combined systems are labeled with several quantum numbers. For example, rotation–vibration multiplets of the F_2-mode system are labeled with a pair of numbers (J, N_f) and contain $\frac{1}{2}(N_f+1)(N_f+2)(2J+1)$ states. The structure of such multiplets can be analyzed using our results for

the individual subsystems, the principles of combining rotational and vibrational RE, and, of course, the set of critical orbits of the $T_d \times \mathcal{T}$ action given in Table 15. The new idea here is that we can continue to distinguish between the two kinds of motion, rotation and vibration, while both of them are treated classically.

In typical molecules, vibrational and rotational quanta differ by a magnitude, and the common experimental situation is that $J \gg N_f$. In this limit, it is often possible to separate the whole rotational–vibrational polyad into bands, branches, or, in the terminology of [80],[33] *vibrational components* and consider the latter for different J at fixed N_f (or/and N_e). How do RE reflect this band structure? The answer is simple: points in Table 15 with the *same* rotational coordinates (j_1, j_2, j_3) give different classical limits within the same component. Thus the F_2-mode system has three kinds of bands A, B, and C.

We recall that F_2-mode vibrations induce angular momentum $\boldsymbol{\pi}$. Rotational multiplets of the F_2-mode polyads are split into branches due to the Coriolis coupling of $\mathbf{J}$ and $\boldsymbol{\pi}$ and are labeled with the additional "good" quantum number R of the angular momentum $\mathbf{J} + \boldsymbol{\pi}$ [81]. The $N_f = 1$ fundamental state has $\boldsymbol{\pi} = 1$. This state splits into three branches with $R = J - 1,\ J,\ J + 1$, which diverge linearly as J increases. The "circular" RE of type B, C (see section 5.3.2) have maximal angular momentum $\boldsymbol{\pi}$ and are the classical limit for the $R = J \pm 1$ branches; the A-type RE have zero momentum and give the limit of the $R = 0$ branch. Provided that we add the two extra nonfixed RE of symmetry $C_s \wedge \mathcal{T}_2$ (see section 5.2.4), each classical limit branch has three types of RE with shorthand labels C_4, C_2, and C_3; the internal structure of branches can be analyzed like that of an isolated rotational state in section 5.2.1.

Similar analysis for the E-mode system shows that it has two types of branches A_1 and A_2 (see Table 15—ignore the F_2 part (z_1, z_2, z_3) and use time reversal where necessary). In particular, the $N_e = 1$ state has two branches. The splitting between them is determined by higher order rotation–vibration interactions.

The number of vibrational states and, correspondingly, the number of quantum branches, increases with vibrational excitation. The number of critical orbits and of corresponding rotational–vibrational RE remains the same. Quantum branches that lie at "intermediate energies" far from the limit given by the RE can be considered in the same way as quantum states at intermediate energies of purely vibrational polyads (sections 5.4.2 and 5.4.3), i.e., as states with more complex vibrational localization. The RE analysis of the rovibrational structure is simpler for low vibrational polyads.

The number of quantum states in each band and possible intersections of bands (vibrational components) which can change this number is the subject of further qualitative study of bands. This study is beyond the scope of the present basic RE analysis. We mention only that each band can be assigned a topological index (Chern index) [82], which gives the difference between the number of states $2J + 1$ of an isolated rotational multiplet and the number of states in the band. The sum of these indexes over all components of the polyad equals zero. Thus the number of states in the Coriolis branches of the F_2-mode fundamental state equals $2R + 1$ and the indexes are ± 2 and 0. In the E-mode polyads the indexes can equal only 2 or 4 modulo 6 [80].

[33] Note that the index introduced in this work equals one-half of the Chern index introduced in [82].

6. Dynamical invariants of the reduced system. In the previous sections we analyzed the action of the symmetry group on the reduced phase space of our system and predicted its RE entirely on the basis of this analysis. We defined RE explicitly (Table 15) in terms of coordinates $(z, \bar{z})$ of the initial system (2.1). Any given reduced Hamiltonian H_{eff} can be expressed in terms of $(z, \bar{z})$ and the energy–action characteristics of fixed RE can be computed. Stability of RE can be determined using local expansions of H_{eff}. Those RE whose position on the reduced phase space changes (as a function of energy or parameters) are found as conditional extrema of $H_{\text{eff}}(z, \bar{z})$ on the reduced phase space.

The use of initial coordinates $(z, \bar{z})$ has, however, obvious limitations. These coordinates are not well suited to studying dynamics on the reduced phase space $\mathbb{C}P^2 \times \mathbb{C}P^1 \times \mathbb{S}^2$. The more appropriate way to analyze the reduced system is in terms of dynamically invariant functions, which can be constructed of $(z, \bar{z})$ [44]. In the following sections we show how invariant polynomials in $(z, \bar{z})$ can be used to describe the reduced system. We will use invariants to (i) express the reduced Hamiltonian H_{eff} most compactly and unambiguously, (ii) define nonlinear coordinates on the reduced phase space $\mathbb{C}P^2 \times \mathbb{C}P^1 \times \mathbb{S}^2$, (iii) describe the action of the symmetry group $T_d \times \mathcal{T}$ on this space, (iv) describe the dynamics of the reduced system, and (v) characterize RE in terms of both their position on $\mathbb{C}P^2 \times \mathbb{C}P^1 \times \mathbb{S}^2$ and stability.

We consider appropriate dynamical symmetry and its reduction in order to introduce dynamical invariants of degree 2 in $(z, \bar{z})$ (section 6.2 and Table 21), which generate the ring of all invariant polynomials. All terms in H_{eff} can be expressed as various powers of these generators. In section 6.3 we describe the structure of the ring of invariant polynomials using the Molien generating function, and later in section 6.4 we define an integrity basis in order to represent uniquely each invariant polynomial in this ring. In particular, all remaining dependence on the A_1 variables is expressed as a power series in the 1-oscillator action n_a. This happens because the A_1 vibration does not change the geometry of the molecule.

6.1. Reduction of the initial rovibrational system and normal form H_{eff}. The zero order Hamiltonian of our system is a sum of three harmonic oscillators,

$$H_0 = \omega_{A_1} n_a + \omega_E n_e + \omega_{F_2} n_f + 0j, \tag{6.1a}$$

where n_a, n_e, n_f, and j represent oscillators with degeneracy 1, 2, 3, and 2, respectively. Explicit definition in terms of initial symplectic variables $(z, \bar{z})$ is given in Table 21. The first three oscillators describe the A_1, E, and F_2 vibrational modes, respectively. The reduced rotational subsystem is lifted to an auxiliary degenerate two-oscillator system with dynamical variables $(z_6, z_7, \bar{z}_6, \bar{z}_7)$, which is more convenient in computations.

The complete initial rotation–vibration Hamiltonian H is a power series in dynamical variables $(z, \bar{z})$,

$$H = H_0 + \epsilon H_1 + \epsilon^2 H_2 + \cdots, \tag{6.1b}$$

where ϵ is a smallness parameter, and different perturbation terms are characterized below.

Table 21

Generators of the dynamical symmetry group action describing dynamics on $\mathbb{C}P^2 \times \mathbb{C}P^1 \times \mathbb{S}^2$.

	Definition		Definition
n_a	$\frac{1}{2}(z_a\bar{z}_a)$	n_f	$\frac{1}{2}(z_1\bar{z}_1 + z_2\bar{z}_2 + z_3\bar{z}_3)$
j	$\frac{1}{4}(z_6\bar{z}_6 + z_7\bar{z}_7)$	x_3	$\frac{1}{2}(z_1\bar{z}_1 - z_2\bar{z}_2)$
j_2	$\frac{1}{4}(z_6\bar{z}_7 + z_7\bar{z}_6)$	n_3	$\frac{1}{2}(z_3\bar{z}_3)$
j_3	$\frac{1}{4}(z_6\bar{z}_7 - z_7\bar{z}_6)i$	s_1	$\frac{1}{2}(z_2\bar{z}_3 + z_3\bar{z}_2)$
j_1	$\frac{1}{4}(z_6\bar{z}_6 - z_7\bar{z}_7)$	t_1	$\frac{1}{2}(z_2\bar{z}_3 - z_3\bar{z}_2)i$
n_e	$\frac{1}{2}(z_4\bar{z}_4 + z_5\bar{z}_5)$	s_2	$\frac{1}{2}(z_1\bar{z}_3 + z_3\bar{z}_1)$
v_1	$-\frac{1}{4}(z_4\bar{z}_5 - z_5\bar{z}_4)i$	t_2	$\frac{1}{2}(z_3\bar{z}_1 - z_1\bar{z}_3)i$
v_2	$\frac{1}{4}(z_5\bar{z}_5 - z_4\bar{z}_4)$	s_3	$\frac{1}{2}(z_1\bar{z}_2 + z_2\bar{z}_1)$
v_3	$\frac{1}{4}(z_4\bar{z}_5 + z_5\bar{z}_4)$	t_3	$\frac{1}{2}(z_1\bar{z}_2 - z_2\bar{z}_1)i$

Order	Degree	Type of the term
ϵ	z^3	Cubic anharmonic terms
ϵ^2	z^4	Quartic anharmonic terms
	$z^2 j$	Coriolis interaction
	j^2	"Rigid rotor" rotation

When the frequencies ω_{A_1}, ω_E, and ω_{F_2} are incommensurate, n_a, n_e, and n_f can be regarded as three approximate integrals of motion with values N_a (see footnote 26), N_e, and N_f, respectively. The fourth integral j with the value J is the amplitude of the total angular momentum, which is strictly conserved.

We can now reduce (normalize) perturbations H_1, H_2, etc. in (6.1b) by removing all terms which do not Poisson commute with integrals n_f, n_e, and j. (Note that a priori $\{H, j\} = 0$ since j is a strict integral.) In other words, we reduce the action of the dynamical 4-torus symmetry group $\mathbb{T}^4$ (see footnote 26) on the initial 16-dimensional phase space with coordinates $(z, \bar{z})$. This group is defined by the flow of four Hamiltonian vector fields X_{n_f}, X_{n_e}, X_{n_a}, and X_j. The normalized Hamiltonian H_{eff}, also called the reduced and/or effective Hamiltonian, or simply the normal form, is invariant with regard to this flow.

6.2. Invariant polynomials of the oscillator symmetry. The dynamical symmetry of each oscillator subsystem has the form

$$\varphi : \mathbb{R}^1 \times C_k \to C_k : (t, z) \to \exp(it)\, z, \tag{6.2a}$$

where dimension k can be 3 (F_2 mode), 2 (E mode and rotation), or 1 (A_1 mode). The conjugate vector $\bar{z}$ transforms, of course, as follows:

$$(t, \bar{z}) \to \exp(-it)\, \bar{z}. \tag{6.2b}$$

It follows that all monomials in $(z, \bar{z})$ that are invariant with respect to φ are of even total degree and have the same degree in z and $\bar{z}$, e.g., $z_i\bar{z}_j$, $z_i z_j \bar{z}_m \bar{z}_l$, etc. Furthermore, all invariant polynomials can be expressed using quadratic monomials of the form $z\bar{z}$ (or similar homogeneous polynomials of degree 2), which *generate* the multiplicative ring $\mathcal{R}$ of all polynomials

invariant with respect to φ. Since φ is a flow of the vector field of the linearized system with Hamiltonian

$$H_0 = \frac{1}{2} z\bar{z} = \frac{1}{2}(z_1\bar{z}_1 + z_2\bar{z}_2 + \cdots + z_k\bar{z}_k),$$

all polynomials in this ring Poisson commute with H_0, which is an integral of motion for the reduced system.

Generators are defined explicitly in Table 21. In the case of the rotational subsystem, the generators are the familiar components j_1, j_2, and j_3 of the angular momentum whose amplitude j is a constant. Since the reduced phase space of the 1:1 oscillator and that of the rotator are diffeomorphic, $\mathbb{C}P^1 \sim \mathbb{S}^2$, the generators v_1, v_2, and v_3 for the E-mode polyads can also be considered as components of an angular momentum with fixed amplitude $\frac{1}{2}n_e$ [69]. The reduced F_2-mode oscillator system is described by nine linearly independent generators. The integral of motion n_f, and polynomials x_3 and n_3, are combinations of the actions of the individual oscillators,

$$n_k = \frac{1}{2} z_k\bar{z}_k, \quad k = 1, 2, 3.$$

Invariants s and t can be considered as inner and exterior products of 2-vectors,

$$s_\alpha = \frac{1}{2}(z_\beta, \bar{z}_\beta) \cdot (z_\gamma, \bar{z}_\gamma), \qquad t_\alpha = \frac{i}{2}(z_\beta, \bar{z}_\beta) \wedge (z_\gamma, \bar{z}_\gamma).$$

This construction of invariants goes back to Weyl [83].

6.3. Generating function for oscillator symmetry. Once the action of the dynamical symmetry on the initial phase space C_k of the k-oscillator is defined explicitly in (6.2) we can compute the Molien generating function $g(\lambda)$, a heuristic tool [48, 49, 50, 84] suggesting certain structural characteristics of the ring of invariant polynomials in $(z, \bar{z})$. The function $g(\lambda)$ can be obtained directly from the Molien theorem [83]

$$g(\lambda) = \frac{1}{2\pi} \int_0^{2\pi} \frac{dt}{\det(1 - \lambda U_t)}, \tag{6.3}$$

where the $2k \times 2k$ matrix U_t represents the action of the dynamical symmetry in (6.2) on both $z_1, \ldots, z_k$ and $\bar{z}_1, \ldots, \bar{z}_N$, i.e., on all phase space variables used to construct invariants. We can see from (6.2) that U_t is a diagonal matrix

$$U_t = \operatorname{diag}(\underbrace{e^{it}, \ldots, e^{it}}_{k \text{ times}}, \underbrace{e^{-it}, \ldots, e^{-it}}_{k \text{ times}}), \tag{6.4}$$

and that

$$g(\lambda) = \frac{1}{2\pi} \int_0^{2\pi} \frac{dt}{(1 - \lambda e^{it})^k (1 - \lambda e^{-it})^k}. \tag{6.5}$$

After changing to the complex unimodular variable

$$\theta = \exp(it), \quad dt = \frac{d\theta}{i\theta}, \tag{6.6}$$

the integral (6.5) becomes a Cauchy integral

$$g(\lambda) = \frac{1}{2\pi i} \oint_{|\theta|=1} \frac{\theta^{k-1} d\theta}{(1-\lambda\theta)^k (\theta-\lambda)^k}. \tag{6.7}$$

Here we note that the formal real variable λ is used in Taylor series expansions of $g(\lambda)$ and the value of λ can be assumed arbitrarily small. In particular, we can have $|\lambda^{-1}| > 1$. Since our integral has a single pole $\theta = \lambda$ of order $k \geq 1$ within the unit circle $|\theta| = 1$, the Cauchy integral formula yields

$$g(\lambda) = \frac{1}{(k-1)!} \frac{\partial^{k-1}}{\partial \theta^{k-1}} \frac{\theta^{k-1}}{(1-\lambda\theta)^k} \bigg|_{\theta=\lambda}, \tag{6.8}$$

and in particular,[34]

$$g_{C_1/S_1}(\lambda) = 1/(1-\lambda^2), \tag{6.9a}$$

$$g_{C_2/S_1}(\lambda) = (1+\lambda^2)/(1-\lambda^2)^3, \tag{6.9b}$$

$$g_{C_3/S_1}(\lambda) = (1+4\lambda^2+\lambda^4)/(1-\lambda^2)^5, \tag{6.9c}$$

$$g_{C_k/S_1}(\lambda) = \sum_{s=0}^{k-1} \binom{k-1}{s}^2 \lambda^{2s} \Big/ (1-\lambda^2)^{2k-1}. \tag{6.9d}$$

Here the formal variable λ represents any of the variables z and $\bar{z}$. Since all invariants are of even degree in z and $\bar{z}$, the degree in λ is also even. We can, therefore, change to variable

$$\mu = \lambda^2,$$

which represents generators in Table 21. We can also omit one factor $(1-\lambda^2)$ in the denominator of (6.9) that represents the principal oscillator invariant. Then

$$g_{\mathbb{C}P^1}(\mu) = (1+\mu)/(1-\mu)^2, \tag{6.10a}$$

$$g_{\mathbb{C}P^2}(\mu) = (1+4\mu+\mu^2)/(1-\mu)^4. \tag{6.10b}$$

6.4. Integrity basis. All functions invariant with respect to the dynamical symmetry (6.2a), and in particular the reduced Hamiltonian (the normal form) H_{eff} in (2.4), can be expressed in terms of generator invariants in Table 21. Coefficients c_k in the Taylor series for the corresponding Molien function $g(\lambda)$ at $\lambda = 0$ give the total number of linearly independent invariant polynomials of degree k. Even though the generators themselves are linearly independent, there are algebraic relations between them and the representation of c_k invariants of degree k in terms of such generators is not unique.

For example, the components of the angular momentum obey the relation

$$j_1^2 + j_2^2 + j_3^2 = j^2 = \text{const}.$$

[34] Alternative derivation of generating functions (6.9) was given in [84].

Due to this relation, the ring of all invariant polynomials generated multiplicatively by (j_1, j_2, j_3) is not free. To express any member of this ring unambiguously we can use monomials of the type $j_1^a j_2^b j_3^c$, where a and b are arbitrary nonnegative integers and c equals 0 or 1. In other words, the ring generated by (j_1, j_2, j_3) has the structure [48, 49, 50]

$$\mathcal{R}(j_1, j_2) \bullet \{1, j_3\},$$

where $\mathcal{R}$ is a polynomial ring generated freely by j_1 and j_2. This structure is described by the Molien generating function

$$g_j = (1 + \mu_j)/(1 - \mu_j)^2, \tag{6.11}$$

where the formal variable μ_j represents any of (j_1, j_2, j_3), the two denominator factors $(1-\mu_j)$ suggest two main (or *principal*) invariants of degree 1 in (j_1, j_2, j_3), while numerator terms 1 and μ_j suggest *auxiliary* invariants of degrees 0 and 1. Such decomposition of generators into principal and auxiliary is called *integrity basis*.[35] Our example shows that the choice of such basis is not unique. Thus we can equally use (j_2, j_3) and j_1. Similarly, all E-mode invariant polynomials constitute the ring

$$\mathcal{R}(v_2, v_3) \bullet \{1, v_1\}$$

described by the generating function

$$g_e = (1 + \mu_e)/(1 - \mu_e)^2. \tag{6.12}$$

Note that v_1 changes sign under time reversal $\mathcal{T}$, while v_2 and v_3 are $\mathcal{T}$-invariant. Choosing v_1 as an auxiliary (numerator) invariant is convenient for further symmetrization with respect to $\mathcal{T}$.

The choice of the integrity basis is more difficult in the case of the 1:1:1 oscillator system (F_2 mode) with the reduced space $\mathbb{C}P^2$.[36] There are nine quadratic relations ("sygyzies" of the first order) among the generators,

$$t_1^2 + s_1^2 - 4n_3n_2 = 0, \quad t_1t_2 - s_1s_2 + 2s_3n_3 = 0, \qquad s_2t_3 + s_3t_2 + 2n_1t_1 = 0, \tag{6.13a}$$

$$t_2^2 + s_2^2 - 4n_3n_1 = 0, \quad t_1t_3 - s_1s_3 + 2s_2n_2 = 0, \qquad s_1t_3 + s_3t_1 + 2n_2t_2 = 0, \tag{6.13b}$$

$$t_3^2 + s_3^2 - 4n_1n_2 = 0, \quad t_2t_3 - s_2s_3 + 2s_1n_1 = 0, \qquad s_1t_2 + s_2t_1 + 2n_3t_3 = 0, \tag{6.13c}$$

as well as other relations of higher degree. The Molien generating function

$$g_f = (1 + 4\mu_f + \mu_f^2)/(1 - \mu_f)^4, \tag{6.14}$$

with μ_f representing any of the generators $\{x_3, n_3, s, t\}$, suggests that all four principal invariants can be chosen from $\{x_3, n_3, s, t\}$ and that there should be four auxiliary invariants of

[35] Such decomposition is known as integrity basis [83], homogeneous system of parameters [110], or Hironaka decomposition [111].

[36] The number of principal and auxiliary invariants and their degrees in $(z, \bar{z})$ can be deduced from the Molien generating function. This function, however, does not suggest the explicit construction of the generators, which may not be unique or may not be possible at all.

degree 1 and one of degree 2. The choice of four main invariants is far from arbitrary. One possible representation of the structure of this ring is

$$\mathcal{R}(x_3, s_1, s_2, s_3) \bullet \{1, n_3, n_3^2, t_1, t_2, t_3\}.$$

If we use this integrity basis, relations (6.13) should, of course, be rewritten in order to replace n_1 and n_2 as

$$n_1 = \tfrac{1}{2}(n_f - n_3 + x_3), \qquad n_2 = \tfrac{1}{2}(n_f - n_3 - x_3).$$

To obtain an unambiguous expression of the reduced rotation–vibration Hamiltonian H_{eff} defined on $\mathbb{C}P^2 \times \mathbb{C}P^1 \times \mathbb{S}^2$, we should combine the three integrity bases introduced above. The direct multiplication of the three rings is described by the generating function

$$g = g_f g_e g_j = \frac{1 + \mu_f + 3\bar{\mu}_f + \mu_f^2}{(1-\mu_f)^4} \frac{1 + \bar{\mu}_e}{(1-\mu_e)^2} \frac{1 + \bar{\mu}_j}{(1-\bar{\mu}_j)^2},$$

where μ and $\bar{\mu}$ stand for $\mathcal{T}$-invariants and $\mathcal{T}$-covariants. We can use main invariants

$$\mathcal{R}(x_3, s_1, s_2, s_3, v_2, v_3, \underline{j_1}, \underline{j_2})$$

and auxiliary invariants

$$\begin{aligned}\{1, &\underline{v_1}, \underline{j_3}, n_3, n_3^2, \underline{t_1}, \underline{t_2}, \underline{t_3}, v_1 j_3, \underline{n_3 v_1}, \underline{n_3^2 v_1},\\ &t_1 v_1, t_2 v_1, t_3 v_1, \underline{n_3 j_3}, \underline{n_3^2 j_3}, t_1 j_3, t_2 j_3, t_3 j_3,\\ &n_3 v_1 j_3, n_3^2 v_1 j_3, \underline{t_1 v_1 j_3}, \underline{t_2 v_1 j_3}, \underline{t_3 v_1 j_3}\ \}.\end{aligned}$$

All polynomials in the above integrity basis are chosen to be either invariant or pseudoinvariant (change sign) with respect to the time reversal $\mathcal{T}$; the pseudoinvariants are underlined. This helps further symmetrization in section 7. Of course, we should multiply our ring by all integrals $\mathcal{R}(n_f, n_e, j)$. More rigorously, we should first express the normalized Hamiltonian $\mathcal{H}_{\text{nf}}$ in terms of the above integrity basis *and* $\mathcal{R}(n_f, n_e, j)$, and only then we replace n_f, n_e, j with their constant values N_f, N_e, and J, and thus obtain the *reduced* Hamiltonian H_{eff}.

7. Dynamical invariants symmetrized with respect to finite symmetries. While the integrity basis introduced above in section 6.4 serves the purpose of dynamical (oscillator) symmetry reduction, further modifications should, in principle, follow in order to take the finite symmetry of our system into account. In particular, a symmetrized basis allows us to express (2.4) using the *minimum* number of (linearly independent) terms whose coefficients can be treated by spectroscopists as free phenomenological (or "adjustable") parameters.

7.1. Symmetry properties of dynamical invariants. We first find the action of the symmetry group $T_d \times \mathcal{T}$ on the generators in Table 21. Before considering $T_d \times \mathcal{T}$, we explain the action of two basic symmetry elements, the rotation C_k and the time reversal $\mathcal{T}$.

7.1.1. Spatial axial symmetry. Consider a rotation C_φ of the Euclidean 3-space about axis 1 by angle φ, which equals $2\pi/k$ in the case of the discrete operation C_k with $k = 2, 3, \ldots$. The action of C_φ on the coordinates (q_1, q_2, q_3) is defined by the familiar 3×3 orthogonal matrix

$$\left(\begin{array}{c|c} 1 & 0 \\ \hline 0 & M(2\varphi) \end{array}\right), \quad M(\varphi) = \begin{pmatrix} \cos\varphi & \sin\varphi \\ -\sin\varphi & \cos\varphi \end{pmatrix}. \tag{7.1}$$

Components of the angular momentum (j_1, j_2, j_3) also transform according to this matrix.

To understand the action of C_φ on the E-mode reduced space $\mathbb{C}P^1$, consider the rotation of the complex plane with coordinates (z_4, z_5) defined by matrix $M(\varphi)$ in (7.1) (recall that we rotate the (q_4, q_5) and (p_4, p_5) planes simultaneously) and show that the corresponding rotation of the 3-space with coordinates (v_1, v_2, v_3) defined in Table 21 is given by the 3×3 matrix in (7.1). It follows that for the 2-sphere $\mathbb{S}^2$, which is defined as $v_1^2 + v_2^2 + v_3^2 = \frac{1}{4}N_e^2$ and is isomorphic to $\mathbb{C}P^1$, axis v_1 is the corresponding symmetry axis of rotation. It can be equally verified that (due to the particular choice of variables (j_1, j_2, j_3) in Table 21) similar rotation of the (z_6, z_7) plane corresponds to the symmetry axis j_3.

To find how C_φ acts on the $\mathbb{C}P^2$ space, we can rotate the complex space C_3 with coordinates (z_1, z_2, z_3) using the matrix

$$\left(\begin{array}{c|c} M(\varphi) & 0 \\ \hline 0 & 1 \end{array}\right),$$

where $M(\varphi)$ is the 2×2 matrix in (7.1), and show by a direct calculation that the action of this operation on the invariants

$$\left(\frac{x_3}{\sqrt{2}}, \frac{s_3}{\sqrt{2}}\right), \quad \left(\frac{s_2}{\sqrt{2}}, \frac{s_1}{\sqrt{2}}\right), \quad \left(\frac{t_1}{\sqrt{2}}, \frac{t_2}{\sqrt{2}}\right), \quad n_3, \quad t_3,$$

is given by the matrix $\operatorname{diag}(M(2\varphi), M(\varphi), M(\varphi), 1, 1)$, i.e., that these invariants realize representations of the SO(2) group of indexes ± 2, ± 1, ± 1, 0, and 0, respectively.

7.1.2. Time reversal symmetry $\mathcal{T}$ (or Z_2). Recalling the action of $\mathcal{T}$ on the initial vibrational variables $(z, \bar{z})$, we can see that vibrational generators v_2, v_3, s_1, s_2, s_3, x_3, and n_3 defined in Table 21 are invariants of the Z_2 action, while v_1, t_1, t_2, and t_3 are covariants,

$$(s_1, s_2, s_3) \to (s_1, s_2, s_3), \tag{7.2a}$$

$$(x_3, n_3, v_2, v_3) \to (x_3, n_3, v_2, v_3), \tag{7.2b}$$

$$(t_1, t_2, t_3, v_1) \to (-t_1, -t_2, -t_3, -v_1). \tag{7.2c}$$

Integrity basis polynomials in section 6.4 are chosen as either $\mathcal{T}$-invariant or $\mathcal{T}$-covariant (antisymmetric or antisymmetric with respect to $\mathcal{T}$). We can easily symmetrize this basis with respect to $\mathcal{T}$ by taking squares of the principal $\mathcal{T}$-covariants $\underline{j_1}$ and $\underline{j_2}$ and excluding all auxiliary covariants. The corresponding transformation of the generating function $g_f g_e g_j$ [48, 49, 50] begins with multiplying by

$$(1 + \lambda)^2/(1 + \lambda)^2 = (1 + \bar{\mu}_j)^2/(1 + \bar{\mu}_j)^2$$

(to transform the denominator) followed by expanding the numerator and sorting out all numerator terms which represent $\mathcal{T}$-invariants. The resulting generating function

$$\frac{1+\mu+19\mu^2+6\mu^3+19\mu^4+\mu^5+\mu^6}{(1-\mu)^6(1-\mu^2)^2}, \tag{7.3}$$

where μ replaces any of formal variables $\{\mu_f,\mu_e,\mu_j\}$ and $\{\bar\mu_f,\bar\mu_e,\bar\mu_j\}$ for $\mathcal{T}$-invariants and $\mathcal{T}$-covariants, respectively, describes polynomials on the phase space $\mathbb{C}P^2\times\mathbb{C}P^1\times\mathbb{S}^2$, which are invariant with regard to both dynamical and time reversal symmetry. The detailed expression for the numerator of (7.3) shows the origin of the auxiliary integrity basis invariants:

$$\begin{aligned}&1+\mu_f+\mu_f^2+3\bar\mu_f\bar\mu_e+3\bar\mu_e\bar\mu_j+9\bar\mu_f\bar\mu_j+3\bar\mu_j^2\\&+3\mu_f\bar\mu_j^2+3\mu_f\bar\mu_e\bar\mu_j+3\mu_f^2\bar\mu_e\bar\mu_j+3\mu_f^2\bar\mu_j^2\\&+9\bar\mu_f\bar\mu_e\bar\mu_j^2+3\bar\mu_f\bar\mu_j^3+\bar\mu_e\bar\mu_j^3+\mu_f\bar\mu_e\bar\mu_j^3+\mu_f^2\bar\mu_e\bar\mu_j^3.\end{aligned}$$

7.1.3. Finite symmetry $T_d\times\mathcal{T}$. The action of $T_d\times\mathcal{T}$ on the dynamical variables in Table 21 can, in principle, be found on the basis of sections 7.1.1 and 7.1.2 if we introduce an appropriately rotated coordinate frame to study each particular axial symmetry element of the T_d group. Otherwise we can consider tensor products

$$\left[z^E\times\bar z^E\right]^\Gamma \quad\text{and}\quad \left[z^{F_2}\times\bar z^{F_2}\right]^{\Gamma'}$$

of vectors $z^{F_2}=(z_1,z_2,z_3)$ and $z^E=(z_4,z_5)$ that transform according to irreducible representations Γ or Γ' of T_d (and $T_d\times\mathcal{T}$) and express these products in terms of invariants in Table 21. A straightforward calculation using Clebsch–Gordan coefficients for cubic groups [85, 86, 87, 88, 89, 90, 91, 92, 93][37] gives

$$\begin{aligned}n_e&=\frac{\sqrt2}{2}\left[z^E\times\bar z^E\right]^{A_1},\\ v_1&=-i\frac{\sqrt2}{4}\left[z^E\times\bar z^E\right]^{A_2},\\ (v_2,v_3)&=\frac{\sqrt2}{4}\left[z^E\times\bar z^E\right]^{E},\\ n_f&=\frac{\sqrt3}{2}\left[z^{F_2}\times\bar z^{F_2}\right]^{A_1},\\ \left(\frac{3n_3-n_f}{\sqrt3},x_3\right)&=-\frac{1}{\sqrt2}\left[z^{F_2}\times\bar z^{F_2}\right]^{E},\\ (t_1,t_2,t_3)&=-\frac{i}{\sqrt2}\left[z^{F_2}\times\bar z^{F_2}\right]^{F_1},\\ (s_1,s_2,s_3)&=-\frac{1}{\sqrt2}\left[z^{F_2}\times\bar z^{F_2}\right]^{F_2}.\end{aligned}$$

[37] Our parameters $h_{ff}^{\Omega(K,\Gamma)}$ correspond to $t_{ff}^{\Omega(K,\Gamma)}$ in [92] times a constant (see [13]). The values of parameters are in spectroscopic units of energy, cm^{-1}.

The transformation properties of the generators now can be obtained explicitly from the matrices in Table 4 and equations in section 7.1.2. In particular, (t_1, t_2, t_3) and (s_1, s_2, s_3) realize irreducible representations F_{1u} and F_{2g} of $T_d \times \mathcal{T}$. We can further note that the components of the 3-vectors q^{F_2}, p^{F_2}, and $z^{F_2} = q^{F_2} - ip^{F_2}$ transform according to the irreducible representation of index 1 of the 3-space rotation group SO(3). We can also show that

$$n_f, \quad (t_1, t_2, t_3), \quad \text{and} \quad \left(s_1, s_2, s_3, \frac{3n_3 - n_f}{\sqrt{3}}, x_3\right)$$

transform according to the irreducible representations of SO(3) of indexes 0, 1, and 2, respectively.

Variables (j_1, j_2, j_3) are components of the total angular momentum, which is an axial vector transforming according to the irreducible representation 1 of the SO(3) group and F_1 of the O group. We can see from (3.1c) that (j_1, j_2, j_3) realize an irreducible representation F_{1u} of $T_d \times \mathcal{T}$. (This O_h-like notation should not be confused with F_{1g}, which is the representation of the *spatial group* $O_h \subset O(3)$ realized by (j_1, j_2, j_3).)

7.2. Symmetrized integrity basis. Once the symmetry properties of the dynamical variables are established, the integrity basis in sections 6 and 7.1.2 can be symmetrized with regard to the finite group $T_d \times \mathcal{T}$ and can be used to describe the ring of all polynomials invariant with regard to $T_d \times \mathcal{T}$.

7.2.1. Symmetrized basis for the rotational subsystem. The ring $\mathcal{R}$ of polynomials in $\{j_1, j_2, j_3\}$ invariant with respect to the action of $T_d \times \mathcal{T}$ has the same structure as the ring of polynomials in $\{x, y, z\}$ invariant with respect to the action of the O_h group of transformations of $\mathbb{R}^3$. In both cases we construct an integrity basis using the components of the triply degenerate irreducible representation F_{1u} realized by $\{j_1, j_2, j_3\}$. The Molien generating function $g(A_{1g}, F_{1u}; \lambda)$ in Table 22 indicates that the ring $\mathcal{R}$ is freely generated by three invariants j^2, r_4, and r_6 of degree 2, 4, and 6, respectively. (In molecular literature these invariants have several definitions, such as Ω_4 and Ω_6 in [31, 79] and $R^{4(4,A_1)}$ and $R^{6(6,A_1)}$ in [85, 86, 87, 88, 89].) Thus, up to degree 6 in j, a purely rotational effective Hamiltonian of a tetrahedral (or octahedral) molecule has only *six* parameters corresponding to terms j^2, j^4, r_4, j^6, $j^2 r_4$, and r_6.

To express terms in the reduced rotation–vibration Hamiltonian we also need to construct Γ-covariants (i.e., polynomials that transform according to representation Γ) for all irreducible representations Γ of $T_d \times \mathcal{T}$. Corresponding Molien generating functions $g(\Gamma, F_{1u}; \lambda)$ have, of course, the same denominator as $g(A_{1g}, F_{1u}; \lambda)$ but also have a numerator $\mathrm{num}(\Gamma)$ which describes auxiliary Γ-covariants. The ring of Γ-covariants is a product of freely generated $\mathcal{R}(j^2, r_4, r_6)$ and a finite set of numerator Γ-covariants. One possible explicit choice of these covariants is suggested in Table 22. (See [94] for the discussion of integrity bases for point groups.)

Table 22

Molien functions and possible explicit definition for invariants ($\Gamma = A_{1g}$) *and* Γ*-covariants of the action of the* O_h *group (and of the isomorphic group* $T_d \times \mathcal{T}$*) constructed from the components* $\{x, y, z\}$ *of the triply degenerate irreducible representation* F_{1u}.

K[38]	Γ	num(Γ)[39]	Invariants and Γ-covariants[40]
0	A_{1g}	1	$x^2+y^2+z^2$
4			$x^4+y^4+z^4$
6			$x^2y^2z^2$
9	A_{1u}	λ^9	$xyz(x^2-y^2)(y^2-z^2)(z^2-x^2)$
6	A_{2g}	λ^6	$(x^2-y^2)(y^2-z^2)(z^2-x^2)$
3	A_{2u}	λ^3	xyz
2	E_g	$\lambda^2+\lambda^4$	$\{\sqrt{3}(y^2-z^2),\ y^2+z^2-2x^2\}$
4			$\{\sqrt{3}(y^4-z^4),\ y^4+z^4-2x^4\}$
5	E_u	$\lambda^5+\lambda^7$	$xyz\{y^2+z^2-2x^2,\ \sqrt{3}(z^2-y^2)\}$
7			$xyz\{y^4+z^4-2x^4,\ \sqrt{3}(z^4-y^4)\}$
4	F_{1g}	$\lambda^4+\lambda^6+\lambda^8$	$\{(y^2-z^2)yz, (z^2-x^2)zx, (x^2-y^2)xy\}$
6			$\{(z^4-x^4)zx, (z^4-x^4)zx, (x^4-y^4)xy\}$
8			$\{(x^6-y^6)xy, (z^6-x^6)zx, (x^6-y^6)xy\}$
1	F_{1u}	$\lambda+\lambda^3+\lambda^5$	$\{x,\ y,\ z\}$
3			$\{x^3,\ y^3,\ z^3\}$
5			$\{x^5,\ y^5,\ z^5\}$
2	F_{2g}	$\lambda^2+\lambda^4+\lambda^6$	$\{yz,\ zx,\ xy\}$
4			$\{x^2yz,\ y^2zx,\ z^2xy\}$
6			$\{x^4yz,\ y^4zx,\ z^4xy\}$
3	F_{2u}	$\lambda^3+\lambda^5+\lambda^7$	$\{x(y^2-z^2),\ y(z^2-x^2),\ z(x^2-y^2)\}$
5			$\{x^2(y^2-z^2),\ y^2(z^2-x^2),\ z^2(x^2-y^2)\}$
7			$\{x^4(y^2-z^2),\ y^4(z^2-x^2),\ z^4(x^2-y^2)\}$

7.2.2. Symmetrized basis for the E-mode subsystem. The three components $\{v_1, v_2, v_3\}$ of the induced vibrational angular momentum of the E-mode transform according to the reducible representation $A_1'' \oplus E'$ of D_{3h} (v_1 transforms according to A_1'' and $\{v_2, v_3\}$ span the doubly degenerate irreducible representation E'). The structure of the integrity basis for the invariant and Γ-covariant polynomials in $\{v_1, v_2, v_3\}$, i.e., for the functions on the vibrational E-mode phase space $\mathbb{C}P^1 \sim \mathbb{S}^2$, is described by the Molien functions $g(A_1', A_1'' \oplus E'; \mu, \lambda)$ and $g(\Gamma, A_1'' \oplus E'; \mu, \lambda)$ in Table 23.

Table 23 also suggests the explicit form of the integrity basis polynomials. One of the principal second degree invariants is, of course, the oscillator integral $\frac{1}{2}n_e = v_1^2 + v_2^2 + v_3^2$. We also note that the cubic invariant $v_2^3 - 3v_2v_3^2$ represents the three-fold symmetry and that the reduced vibrational E-mode Hamiltonian should go up to degree 6 in the initial variables

[38] Maximum index of the irreducible representation of SO(3).

[39] Molien function for Γ-covariants $g(\Gamma, F_{1u}; \lambda)$ equals

$$\frac{\text{num}(\Gamma)}{(1-\lambda^2)(1-\lambda^4)(1-\lambda^6)} = \text{num}(\Gamma)\, g(A_{1g}, F_{1u}; \lambda).$$

[40] Axes $\{x, y, z\}$ correspond to symmetry axes C_4.

Table 23

Molien functions and possible explicit definition for invariants and Γ*-covariants of the action of the* D_{3h} *group (and of the isomorphic group* $(T_d \times \mathcal{T})/D_2$*) constructed from the components* $z \oplus \{x, y\}$ *of the representation* $A_1'' \oplus E'$*.*

Γ	num(Γ)[41,42]	Invariants and Γ-covariants[43,44]
A_1'	1	$x^2 + y^2 + z^2$, z^2, $x^3 - 3xy^2$
A_1''	μ	z
A_2'	λ^3	$3yx^2 - y^3$
A_2''	$\lambda^3\mu$	$z(3yx^2 - y^3)$
E'	$\lambda + \lambda^2$	$\{x, y\}$, $\{y^2 - x^2, 2xy\}$
E''	$\mu(\lambda + \lambda^2)$	$\{zy, -zx\}$, $\{2xyz, z(x^2 - y^2)\}$

Table 24

Molien generating functions for invariants ($\Gamma = A_{1g}$) *and* Γ*-covariants of the action of the* O_h *group (and of the isomorphic group* $T_d \times \mathcal{T}$*) constructed from the components* $\{x, y, z\}$ *of the triply degenerate irreducible representation* F_{2g}*.*

Γ[45]	num(Γ)[46,47]
A_{1g}	$1 + \lambda^3 + \lambda^4 + \lambda^5 + \lambda^6 + \lambda^9$
A_{2g}	$2\lambda^3 + \lambda^4 + \lambda^5 + 2\lambda^6$
E_g	$\lambda + 2\lambda^2 + \lambda^3 + 2\lambda^4 + 2\lambda^5 + \lambda^6 + 2\lambda^7 + \lambda^8$
F_{1g}	$\lambda^2 + 3\lambda^3 + 5\lambda^4 + 5\lambda^5 + 3\lambda^6 + \lambda^7$
F_{2g}	$\lambda + 2\lambda^2 + 3\lambda^3 + 3\lambda^4 + 3\lambda^5 + 3\lambda^6 + 2\lambda^7 + \lambda^8$
A_{1u}	$\lambda^3 + \lambda^4 + 2\lambda^5 + \lambda^6 + \lambda^9$
A_{2u}	$\lambda^2 + \lambda^3 + \lambda^4 + \lambda^5 + \lambda^6 + \lambda^7$
E_u	$\lambda^2 + 2\lambda^3 + 3\lambda^4 + 3\lambda^5 + 2\lambda^6 + \lambda^7$
F_{1u}	$\lambda + \lambda^2 + 3\lambda^3 + 4\lambda^4 + 4\lambda^5 + 3\lambda^6 + \lambda^7 + \lambda^8$
F_{2u}	$2\lambda^2 + 3\lambda^3 + 4\lambda^4 + 4\lambda^5 + 3\lambda^6 + 2\lambda^7$

(q, p) in order to represent adequately the symmetry of the system.

7.2.3. Symmetrized basis for the F_2-mode subsystem. Generating functions for the invariants and covariants of the O and T_d group action on the $\mathbb{C}P^2$ are given in [84]. The generating function for the invariants has the form

$$\frac{1 + 2\lambda^3 + 3\lambda^4 + 3\lambda^5 + 2\lambda^6 + \lambda^9}{(1 - \lambda^2)^2(1 - \lambda^3)(1 - \lambda^4)}. \tag{7.4a}$$

[41] Molien function for Γ-covariants $g(\Gamma, A_1'' \oplus E'; \mu, \lambda)$ equals

$$\frac{\text{num}(\Gamma)}{(1 - \lambda^2)(1 - \lambda^3)(1 - \mu^2)} = \text{num}(\Gamma)\, g(A_1', A_1'' \oplus E'; \mu, \lambda).$$

[42] Formal variables μ and λ represent z and $\{x, y\}$, respectively.
[43] In the case of the E-mode $\{z, x, y\} = \{v_1, v_2, v_3\}$.
[44] Axes z and x correspond to symmetry axes C_3 and C_2.
[45] g and u label $\mathcal{T}$ symmetric and $\mathcal{T}$ antisymmetric representations.
[46] All functions have the same denominator as in (7.4b).
[47] The formal variable λ represents $z\bar{z}$, where z is any of (z_1, z_2, z_3).

The corresponding integrity basis is further simplified due to the $\mathcal{T}$-symmetrization, which removes half of the auxiliary (numerator) invariants. The function (7.4a) becomes

$$\frac{1+\lambda^3+\lambda^4+\lambda^5+\lambda^6+\lambda^9}{(1-\lambda^2)^2(1-\lambda^3)(1-\lambda^4)}. \tag{7.4b}$$

Generating functions for covariants are given in Table 24.

Coefficients c_k of terms λ^k in the formal series expansion of the generating functions in Table 24 equal the number of linearly independent polynomials of the kind $z^k\bar{z}^k$. Thus expansion of the function (7.4b)

$$1+2\lambda^2+2\lambda^3+5\lambda^4+5\lambda^5+\cdots \tag{7.5a}$$

suggests that there are two linearly independent $(T_d\times\mathcal{T})$-invariant terms $z^3\bar{z}^3$. This does not include polynomials built with powers of the scalar n_f that can be taken into account if we divide (7.4b) by one more $(1-\lambda)$. Then the corresponding formal series

$$1+\lambda+3\lambda^2+5\lambda^3+10\lambda^4+15\lambda^5+\cdots \tag{7.5b}$$

indicates five terms of degree 3, of which three should, obviously, contain n_f. In fact there is n_f^3 and two terms of the kind $n_f z^2\bar{z}^2$.

The generators of the rings of T_d and $(T_d\times\mathcal{T})$-invariants and covariants can be constructed from the polynomials of the forms

$$\begin{bmatrix} abc \\ pqr \end{bmatrix} = z_1^a z_2^b z_3^c \bar{z}_1^p \bar{z}_2^q \bar{z}_3^r + \left\{ \begin{array}{c} \text{column} \\ \text{permutations} \end{array} \right\} \tag{7.6a}$$

and

$$\begin{pmatrix} abc \\ pqr \end{pmatrix} = \begin{bmatrix} abc \\ pqr \end{bmatrix} + \begin{bmatrix} pqr \\ abc \end{bmatrix}. \tag{7.6b}$$

In particular, $n_f = \frac{1}{2}\left[\begin{smallmatrix}100\\100\end{smallmatrix}\right]$. The Molien functions in Table 24 characterize heuristically the structure of these rings. The denominator of the function (7.4b) tells us that there are two $z^2\bar{z}^2$, one $z^3\bar{z}^3$, and one $z^4\bar{z}^4$ principal integrity basis invariants, which can enter in any degree in the expression for other invariants and covariants. The concrete choice of these four principal invariants,

$$\begin{bmatrix} 110 \\ 110 \end{bmatrix}, \quad \begin{bmatrix} 200 \\ 020 \end{bmatrix}, \quad \begin{bmatrix} 111 \\ 111 \end{bmatrix}, \quad \begin{pmatrix} 400 \\ 022 \end{pmatrix}, \tag{7.7a}$$

and five nontrivial auxiliary (numerator) invariants,

$$\begin{pmatrix} 300 \\ 120 \end{pmatrix}, \begin{pmatrix} 301 \\ 121 \end{pmatrix}, \begin{pmatrix} 410 \\ 032 \end{pmatrix}, \begin{pmatrix} 411 \\ 033 \end{pmatrix}, \begin{pmatrix} 702 \\ 144 \end{pmatrix} - \begin{pmatrix} 612 \\ 054 \end{pmatrix}, \tag{7.7b}$$

is suggested in [84].

7.2.4. Symmetrized basis for the complete system. Once we take all symmetries into consideration and *combine* the three subsystems, the integrity basis becomes very complicated. Resulting symmetrized principal polynomials and a large number of auxiliary polynomials require high powers of dynamical variables and will not be used here. Instead, we will study both the group action of $T_d \times \mathcal{T}$ and the dynamics of the reduced system in terms of simpler dynamical invariants in Table 21. In the next section we briefly describe the tensorial basis, which we use to express the effective Hamiltonian H_{eff} (normal form).

7.2.5. Tensorial bases used in molecular literature. Instead of using an integrity basis of the kind described above, spectroscopists represent their effective Hamiltonians using tensorial bases constructed by the rules of the tensorial product of the finite symmetry group of the system. For example, the F_2-mode Coriolis term is constructed as

$$\left[i\left[z^{F_2} \times \bar{z}^{F_2}\right]^{F_1} \times j^{F_1}\right]^{A_1} = -\frac{\sqrt{2}}{\sqrt{3}}(t, j).$$

(This term is invariant with regard to a larger group SO(3).) Such bases guarantee completeness but cannot exclude the possibility of linear dependence among terms of a given order. At low orders, where such dependencies are few or nonexistent, this is tolerable. Explicit construction of all linearly independent terms of a given degree using the standard coupling scheme of tensors adopted in molecular spectroscopy is often nontrivial. The difficulty increases rapidly with degree. Of course, all spectroscopic tensors can be expressed using generators in Table 21. Some of the most frequently used terms [13] are given in Tables 25 and 26.

8. Group action, fixed points, and invariant subspaces. The action of the symmetry group of our system $T_d \times \mathcal{T}$ on the reduced phase space $\mathbb{C}P^2 \times \mathbb{C}P^1 \times \mathbb{S}^2$ is not free. Our main interest is in the *fixed points* of this action and in the subspaces of $\mathbb{C}P^2 \times \mathbb{C}P^1 \times \mathbb{S}^2$, which are invariant with regard to the spatial symmetry group T_d and are therefore dynamically invariant.

In section 4 we analyzed the action of $T_d \times \mathcal{T}$ using complex dynamical variables z of the initial system (see section 2.2). Below we obtain the same results using the dynamical invariants in Table 21 and their symmetry properties. These invariants serve both as dynamical variables of the reduced system and as polynomial "coordinates" on the reduced phase space $\mathbb{C}P^2 \times \mathbb{C}P^1 \times \mathbb{S}^2$. We use invariants in order to remove the dynamical symmetry $G_{\text{dyn}} = \mathbb{T}^4$ (see footnote 26 and section 6.1) and to avoid the ambiguity of the $(z, \bar{z})$ coordinates. (Indeed, the values of generators in Table 21 specify uniquely a G_{dyn} orbit, which corresponds to a distinct point on $\mathbb{C}P^2 \times \mathbb{C}P^1 \times \mathbb{S}^2$.) At the same time, we cannot label orbits of the finite group $T_d \times \mathcal{T}$ because our polynomials are not symmetrized with regard to $T_d \times \mathcal{T}$. Instead we find concrete fixed points (and invariant subspaces) for concrete stabilizer subgroups of $T_d \times \mathcal{T}$. Results are summarized in Tables 27 and 28.

8.1. Fixed points in the presence of spatial axial symmetry. We return to the general discussion of the axial symmetry in section 7.1.1. The action of any spatial rotation C_k with $k = 2, 3, \ldots, \infty$ on the $\mathbb{C}P^1$ space and on the isomorphic 2-sphere $\mathbb{S}^2$ has *two* fixed points. These points lie on the symmetry axis. Thus in the j_3 axis example,

$$j_1 = j_2 = 0, \quad j_3 = \pm J.$$

Table 25

Expression of spectroscopic tensors used in effective rotation–vibration Hamiltonians for the E and F_2 modes in terms of dynamical invariants.

H^{0}_{ff}	n_f
H^{0}_{ee}	n_e
$H^{1(1,F_1)}_{ff}$	$-\frac{\sqrt{2}}{\sqrt{3}}(t_3j_3 + t_2j_2 + t_1j_1)$
J^2	j^2
$V^{A_1}_{eeee}$	$2\left(\frac{1}{4}n_e^2 - v_1^2\right)$
V^{E}_{eeee}	$\sqrt{2}\left(\frac{1}{4}n_e^2 + v_1^2\right)$
$V^{A_1}_{ffff}$	$\frac{1}{3}(s_1^2 + s_2^2 + s_3^2) + n_3^2 - \frac{2}{3}n_fn_3 + \frac{1}{3}x_3^2$
V^{E}_{ffff}	$\frac{\sqrt{2}}{6}\left(\frac{3}{2}n^2 + \frac{3}{2}n_3^2 + \frac{1}{2}x_3^2 - n_fn_3 - s_1^2 - s_2^2 - s_3^2\right)$
$V^{F_2}_{ffff}$	$\frac{1}{2\sqrt{3}}(n_f^2 - x_3^2 + 2n_fn_3 - 3n_3^2)$
$V^{F_1}_{efef}$	$\frac{1}{2\sqrt{3}}n_fn_e + \frac{1}{2\sqrt{3}}(3n_3 - n_f)v_2 + \frac{1}{2}x_3v_3$
$V^{F_2}_{efef}$	$\frac{1}{2\sqrt{3}}n_fn_e - \frac{1}{2\sqrt{3}}(3n_3 - n_f)v_2 - \frac{1}{2}x_3v_3$
$H^{2(0,A_1)}_{ff}$	$-\frac{4}{3}n_fj^2$
$H^{2(2,E)}_{ff}$	$\sqrt{2}(3n_3 - n_f + x_3)j_2^2 - 2\sqrt{2}\left(n_3 - \frac{1}{3}n_f\right)j^2$ $+\sqrt{2}(3n_3 - n_f - x_3)j_1^2$
$H^{2(2,F_2)}_{ff}$	$-\frac{4}{\sqrt{3}}(s_1j_3j_2 + s_2j_3j_1 + s_3j_2j_1)$
$H^{2(0,A_1)}_{ee}$	$-\frac{2\sqrt{2}}{\sqrt{3}}n_ej^2$
$H^{2(2,E)}_{ee}$	$2\sqrt{6}\,v_2\left(\frac{2}{3}j^2 - j_2^2 - j_1^2\right) + 2\sqrt{2}\,v_3(j_1^2 - j_2^2)$
$H^{3(3,A_2)}_{ee}$	$-16\sqrt{3}\,v_1j_3j_2j_1$
J^4	j^4
$H^{4(4,A_1)}$	$16\frac{\sqrt{10}}{\sqrt{3}}\left(j_2^4 + j_1^4 + j_2^2j_1^2 - j^2(j_1^2 + j_2^2) + \frac{1}{5}j^4\right)$

In the complex coordinates (z_6, z_7) these points can be represented as $(1, 0)$ and $(0, 1)$. The analysis is the same for the E-mode space.

Rotation C_k with $k > 2$ acting on the $\mathbb{C}P^2$ space has *three* fixed points. The action of this operation on the dynamical invariants is described in section 7.1.1 for the case of rotation about z_3 (take $\varphi < \pi$ because $k > 2$). In this case, we find that

$$x_3 = s_3 = s_2 = s_1 = t_1 = t_2 = 0$$

at the fixed points. Substitution into (6.13) gives

$$(1 - \eta)\eta = (1 - \eta)t_3 = \eta^2 - t_3^2 = 0,$$

Table 26

Relation between low degree polynomials constructed in terms of integrity basis and spectroscopic tensorial terms. Only leading terms are taken into account (i.e., classical limit commutativity of variables is assumed).

$\begin{bmatrix}100\\100\end{bmatrix}$	$2H^0_{ff}$
$\begin{bmatrix}100\\100\end{bmatrix}^2$	$4V^{A_1}_{ffff}+4\sqrt{2}V^{E}_{ffff}+4\sqrt{3}V^{F_2}_{ffff}$
$\begin{bmatrix}110\\110\end{bmatrix}$	$2\sqrt{3}V^{F_2}_{ffff}$
$\begin{bmatrix}200\\020\end{bmatrix}$	$8V^{A_1}_{ffff}-4\sqrt{2}V^{E}_{ffff}$
$\begin{bmatrix}100\\100\end{bmatrix}^3$	$8\sqrt{3}\left(V^{EF_2,EF_2}_{fff,fff}+V^{F_2F_2,F_2F_2}_{fff,fff}+V^{A_1F_2,A_1F_2}_{fff,fff}\right)$
	$+24\sqrt{3}V^{EF_1,EF_1}_{fff,fff}+8V^{F_2A_1,F_2A_1}_{fff,fff}$
$\begin{bmatrix}100\\100\end{bmatrix}\begin{bmatrix}110\\110\end{bmatrix}$	$4V^{F_2A_1,F_2A_1}_{fff,fff}+8\sqrt{3}V^{EF_1,EF_1}_{fff,fff}+4\sqrt{3}V^{F_2F_2,F_2F_2}_{fff,fff}$
$\begin{bmatrix}100\\100\end{bmatrix}\begin{bmatrix}200\\020\end{bmatrix}$	$8\sqrt{3}\left(2V^{A_1F_2,A_1F_2}_{fff,fff}-V^{EF_1,EF_1}_{fff,fff}-V^{EF_2,EF_2}_{fff,fff}\right)$
$\begin{bmatrix}111\\111\end{bmatrix}$	$\frac{4}{3}V^{F_2A_1,F_2A_1}_{fff,fff}$
$\begin{pmatrix}300\\120\end{pmatrix}$	$4\sqrt{3}\left(4V^{A_1F_2,A_1F_2}_{fff,fff}-V^{F_2F_2,F_2F_2}_{fff,fff}-2V^{EF_2,EF_2}_{fff,fff}\right)$

where $n_1 = n_2 = \frac{1}{2}\eta \geq 0$ and of course $n_3 = N_f - \eta \geq 0$. This system has three solutions, all isolated fixed points on $\mathbb{C}P^2$, with $(t_3/N_f, \eta/N_f)$ equal to $(0,0)$, $(1,1)$, and $(1,-1)$, respectively. The first solution is invariant with regard to time reversal $\mathcal{T}$, while the other two constitute one $\mathcal{T}$ orbit. In the complex coordinates (z_1, z_2, z_3) these points can be represented as $(1,0,0)$ and $(0,1,\pm i)$.

In the special case of the C_2 rotation we can only assert that

$$s_2 = s_1 = t_1 = t_2 = 0.$$

This leaves two possibilities: an isolated fixed point

$$n_3 = N_f, \quad n_1 = n_2 = t_3 = s_3 = 0,$$

and a 2-sphere defined as

$$n_3 = 0, \quad t_3^2 + s_3^2 + x_3^2 = N_f^2.$$

In the original (z_1, z_2, z_3) coordinates, the former is again the point $(1,0,0)$, while the latter is the $\mathbb{C}P^1$ subspace of $\mathbb{C}P^2$, where $z_3 = 0$.

Table 27

Points in the critical orbits of the $T_d \times \mathcal{T}$ group action on the reduced phase space $\mathbb{C}P^2 \times \mathbb{C}P^1 \times \mathbb{S}^2$ characterized by values of dynamical invariants in Table 21. Points are listed without their time reversal ($\mathcal{T}$) companions; upper and lover signs in the $\pm$ and $\mp$ notation correspond to different orbits with subscript indices 1 and 2, respectively. Matrices of stabilizers S_4^z, $C_3^{[111]}$, and C_s^{xy} are given in Table 4.

Orbit	$\frac{x_3}{N_f}$	$\frac{s_1}{N_f}$	$\frac{s_2}{N_f}$	$\frac{s_3}{N_f}$	$\frac{n_3}{N_f}$	$\frac{t_1}{N_f}$	$\frac{t_2}{N_f}$	$\frac{t_3}{N_f}$	$\frac{v_1}{N_e}$	$\frac{v_2}{N_e}$	$\frac{v_3}{N_e}$	$\frac{j_1}{J}$	$\frac{j_2}{J}$	$\frac{j_3}{J}$	Stabilizer
$A_{1,2}^{(2)}$	0	0	0	-1	0	0	0	0	0	$\mp\frac{1}{2}$	0	$\frac{1}{\sqrt{2}}$	$\frac{-1}{\sqrt{2}}$	0	C_s^{xy}
	0	0	0	1	0	0	0	0	0	$\mp\frac{1}{2}$	0	$\frac{1}{\sqrt{2}}$	$\frac{1}{\sqrt{2}}$	0	
	$\frac{1}{2}$	0	-1	0	$\frac{1}{2}$	0	0	0	0	$\pm\frac{1}{4}$	$\pm\frac{\sqrt{3}}{4}$	$\frac{1}{\sqrt{2}}$	0	$\frac{-1}{\sqrt{2}}$	
	$\frac{1}{2}$	0	1	0	$\frac{1}{2}$	0	0	0	0	$\pm\frac{1}{4}$	$\pm\frac{\sqrt{3}}{4}$	$\frac{1}{\sqrt{2}}$	0	$\frac{1}{\sqrt{2}}$	
	$-\frac{1}{2}$	1	0	0	$\frac{1}{2}$	0	0	0	0	$\pm\frac{1}{4}$	$\mp\frac{\sqrt{3}}{4}$	0	$\frac{1}{\sqrt{2}}$	$\frac{1}{\sqrt{2}}$	
	$-\frac{1}{2}$	-1	0	0	$\frac{1}{2}$	0	0	0	0	$\pm\frac{1}{4}$	$\mp\frac{\sqrt{3}}{4}$	0	$\frac{1}{\sqrt{2}}$	$\frac{-1}{\sqrt{2}}$	
$A_{1,2}^{(3)}$	0	$\frac{2}{3}$	$\frac{2}{3}$	$\frac{2}{3}$	$\frac{1}{3}$	0	0	0	$\mp\frac{1}{2}$	0	0	$\frac{1}{\sqrt{3}}$	$\frac{1}{\sqrt{3}}$	$\frac{1}{\sqrt{3}}$	$C_3^{[111]}$
	0	$\frac{2}{3}$	$-\frac{2}{3}$	$-\frac{2}{3}$	$\frac{1}{3}$	0	0	0	$\mp\frac{1}{2}$	0	0	$\frac{1}{\sqrt{3}}$	$\frac{-1}{\sqrt{3}}$	$\frac{-1}{\sqrt{3}}$	
	0	$-\frac{2}{3}$	$\frac{2}{3}$	$-\frac{2}{3}$	$\frac{1}{3}$	0	0	0	$\mp\frac{1}{2}$	0	0	$\frac{-1}{\sqrt{3}}$	$\frac{1}{\sqrt{3}}$	$\frac{-1}{\sqrt{3}}$	
	0	$-\frac{2}{3}$	$-\frac{2}{3}$	$\frac{2}{3}$	$\frac{1}{3}$	0	0	0	$\mp\frac{1}{2}$	0	0	$\frac{-1}{\sqrt{3}}$	$\frac{-1}{\sqrt{3}}$	$\frac{1}{\sqrt{3}}$	
$B_{1,2}^{(3)}$	0	$-\frac{1}{3}$	$-\frac{1}{3}$	$-\frac{1}{3}$	$\frac{1}{3}$	$\frac{1}{\sqrt{3}}$	$\frac{1}{\sqrt{3}}$	$\frac{1}{\sqrt{3}}$	$\mp\frac{1}{2}$	0	0	$\frac{1}{\sqrt{3}}$	$\frac{1}{\sqrt{3}}$	$\frac{1}{\sqrt{3}}$	$C_3^{[111]}$
	0	$-\frac{1}{3}$	$\frac{1}{3}$	$\frac{1}{3}$	$\frac{1}{3}$	$\frac{1}{\sqrt{3}}$	$\frac{-1}{\sqrt{3}}$	$\frac{-1}{\sqrt{3}}$	$\mp\frac{1}{2}$	0	0	$\frac{1}{\sqrt{3}}$	$\frac{-1}{\sqrt{3}}$	$\frac{-1}{\sqrt{3}}$	
	0	$\frac{1}{3}$	$-\frac{1}{3}$	$\frac{1}{3}$	$\frac{1}{3}$	$\frac{-1}{\sqrt{3}}$	$\frac{1}{\sqrt{3}}$	$\frac{-1}{\sqrt{3}}$	$\mp\frac{1}{2}$	0	0	$\frac{-1}{\sqrt{3}}$	$\frac{1}{\sqrt{3}}$	$\frac{-1}{\sqrt{3}}$	
	0	$\frac{1}{3}$	$\frac{1}{3}$	$-\frac{1}{3}$	$\frac{1}{3}$	$\frac{-1}{\sqrt{3}}$	$\frac{-1}{\sqrt{3}}$	$\frac{1}{\sqrt{3}}$	$\mp\frac{1}{2}$	0	0	$\frac{-1}{\sqrt{3}}$	$\frac{-1}{\sqrt{3}}$	$\frac{1}{\sqrt{3}}$	
$C_{1,2}^{(3)}$	0	$-\frac{1}{3}$	$-\frac{1}{3}$	$-\frac{1}{3}$	$\frac{1}{3}$	$\frac{-1}{\sqrt{3}}$	$\frac{-1}{\sqrt{3}}$	$\frac{-1}{\sqrt{3}}$	$\mp\frac{1}{2}$	0	0	$\frac{1}{\sqrt{3}}$	$\frac{1}{\sqrt{3}}$	$\frac{1}{\sqrt{3}}$	$C_3^{[111]}$
	0	$-\frac{1}{3}$	$\frac{1}{3}$	$\frac{1}{3}$	$\frac{1}{3}$	$\frac{-1}{\sqrt{3}}$	$\frac{1}{\sqrt{3}}$	$\frac{1}{\sqrt{3}}$	$\mp\frac{1}{2}$	0	0	$\frac{1}{\sqrt{3}}$	$\frac{-1}{\sqrt{3}}$	$\frac{-1}{\sqrt{3}}$	
	0	$\frac{1}{3}$	$-\frac{1}{3}$	$\frac{1}{3}$	$\frac{1}{3}$	$\frac{1}{\sqrt{3}}$	$\frac{-1}{\sqrt{3}}$	$\frac{1}{\sqrt{3}}$	$\mp\frac{1}{2}$	0	0	$\frac{-1}{\sqrt{3}}$	$\frac{1}{\sqrt{3}}$	$\frac{-1}{\sqrt{3}}$	
	0	$\frac{1}{3}$	$\frac{1}{3}$	$-\frac{1}{3}$	$\frac{1}{3}$	$\frac{1}{\sqrt{3}}$	$\frac{1}{\sqrt{3}}$	$\frac{-1}{\sqrt{3}}$	$\mp\frac{1}{2}$	0	0	$\frac{-1}{\sqrt{3}}$	$\frac{-1}{\sqrt{3}}$	$\frac{1}{\sqrt{3}}$	
$A_{1,2}^{(4)}$	0	0	0	0	1	0	0	0	0	$\mp\frac{1}{2}$	0	0	0	1	S_4^z
	1	0	0	0	0	0	0	0	0	$\pm\frac{1}{4}$	$\mp\frac{\sqrt{3}}{4}$	1	0	0	S_4^x
	-1	0	0	0	0	0	0	0	0	$\pm\frac{1}{4}$	$\pm\frac{\sqrt{3}}{4}$	0	1	0	S_4^y
$B_{1,2}^{(4)}$	0	0	0	0	0	0	0	1	0	$\mp\frac{1}{2}$	0	0	0	1	S_4^z
	$-\frac{1}{2}$	0	0	0	$\frac{1}{2}$	1	0	0	0	$\pm\frac{1}{4}$	$\mp\frac{\sqrt{3}}{4}$	1	0	0	S_4^x
	$\frac{1}{2}$	0	0	0	$\frac{1}{2}$	0	1	0	0	$\pm\frac{1}{4}$	$\pm\frac{\sqrt{3}}{4}$	0	1	0	S_4^y
$C_{1,2}^{(4)}$	0	0	0	0	0	0	0	-1	0	$\mp\frac{1}{2}$	0	0	0	1	S_4^z
	$-\frac{1}{2}$	0	0	0	$\frac{1}{2}$	-1	0	0	0	$\pm\frac{1}{4}$	$\mp\frac{\sqrt{3}}{4}$	1	0	0	S_4^x
	$\frac{1}{2}$	0	0	0	$\frac{1}{2}$	0	-1	0	0	$\pm\frac{1}{4}$	$\pm\frac{\sqrt{3}}{4}$	0	1	0	S_4^y

8.2. Fixed points of the $T_d \times \mathcal{T}$ group action.

8.2.1. Stabilizer S_4. Orientation of the S_4^z axis in Table 4 corresponds to the one used in section 8.1 for the general case of a C_k axis; solutions for fixed points with stabilizer C_4 on the F_2-mode space $\mathbb{C}P^2$ and on the rotational space $\mathbb{S}^2$ are already given above in section 8.1. On the E-mode space $\mathbb{C}P^1 \sim \mathbb{S}^2$; the image of the S_4^z operation is a rotation about axis v_2 by

Table 28
Invariant subspaces of $\mathbb{C}P^2 \times \mathbb{C}P^1 \times \mathbb{S}^2$ with stabilizers C_s^{xy} and C_2^z.

Stabilizer	Values of dynamical variables and defining equation(s)	Orbit size	Topology
C_2^z	$\frac{x_3}{N_f}\ \frac{s_1}{N_f}\ \frac{s_2}{N_f}\ \frac{s_3}{N_f}\ \frac{n_3}{N_f}\ \frac{t_1}{N_f}\ \frac{t_2}{N_f}\ \frac{t_3}{N_f}\ \frac{v_1}{N_e}\ \frac{v_2}{N_e}\ \frac{v_3}{N_e}\ \frac{j_1}{J}\ \frac{j_2}{J}\ \frac{j_3}{J}$		
	$0\ \ 0\ \ 0\ \ 0\ \ 1\ \ 0\ \ 0\ \ 0\ \ \nu_1\ \ \nu_2\ \ \nu_3\ \ 0\ \ 0\ \ 1$	6	
	$\nu_1^2 + \nu_2^2 + \nu_3^2 = \frac{1}{4}$		S_2
C_2^z	$\xi\ \ 0\ \ 0\ \ \sigma\ \ 0\ \ 0\ \ 0\ \ \tau\ \ \nu_1\ \ \nu_2\ \ \nu_3\ \ 0\ \ 0\ \ 1$	6	
	$\tau^2 + \sigma^2 + \xi^2 = 1,\quad \nu_1^2 + \nu_2^2 + \nu_3^2 = \frac{1}{4}$		$S_2 \times S_2$
C_s^{xy}	$0\ \ \sigma\ \ \sigma\ \ \eta\ \ 1-\eta\ \ \tau\ \ -\tau\ \ 0\ \ 0\ \ \frac{1}{2}\ \ 0\ \ \frac{1}{\sqrt{2}}\ \ \frac{-1}{\sqrt{2}}\ \ 0$	12	
	$2\tau^2 + 2\sigma^2 + (2\eta - 1)^2 = 1$		S_2
	$0\ \ \sigma\ \ \sigma\ \ \eta\ \ 1-\eta\ \ \tau\ \ -\tau\ \ 0\ \ 0\ \ -\frac{1}{2}\ \ 0\ \ \frac{1}{\sqrt{2}}\ \ \frac{-1}{\sqrt{2}}\ \ 0$	12	

angle π. Consequently, at the two fixed points on this space, $v_1 = v_3 = 0$.

8.2.2. Stabilizer C_2. We can consider the C_2^z stabilizer using directly the results in section 8.1. There is a fixed point and an invariant 2-sphere in $\mathbb{C}P^2$ and two fixed points on the rotational sphere $\mathbb{S}^2$ (the fixed points are the same as in the case of S_4^z). Furthermore, the whole E-mode space $\mathbb{C}P^1 \sim \mathbb{S}^2$ is invariant because operations C_2^z, C_2^x, and C_2^y act trivially on this space. There is, therefore, no restriction on (v_1, v_2, v_3). On the full reduced space $\mathbb{C}P^2 \times \mathbb{C}P^1 \times \mathbb{S}^2$ we can have a point, an invariant 2-sphere, or an $\mathbb{S}^2 \times \mathbb{S}^2$ space.

8.2.3. Stabilizer C_3. In the case of C_3, we also expect three fixed points on $\mathbb{C}P^2$ and two points on $\mathbb{C}P^1$ and $\mathbb{S}^2$ each. We first recall that (j_1, j_2, j_3) transform according to the irreducible representation F_1 of the T_d group. Considering the matrix representation of F_1 for the particular operation $C_3^{[111]}$ in Table 4, we can see immediately that a point on the rotational sphere $\mathbb{S}^2$ remains invariant (stable) with respect to this operation only if

$$j_1 = j_2 = j_3.$$

Furthermore, since

$$j_1^2 + j_2^2 + j_3^2 = j^2 = J^2,$$

the two possible solutions for the fixed points on $\mathbb{S}^2$ are

$$j_1 = j_2 = j_3 = \pm J/\sqrt{3}.$$

These two points form one $\mathcal{T}$ orbit. There are four axes C_3 (four conjugate subgroups C_{3v} of the T_d group) and there is one orbit of the action of the full group $T_d \times \mathcal{T}$ that includes all eight points on $\mathbb{S}^2$ with stabilizer C_3.

Vibrational E-mode polynomials v_1 and (v_2, v_3) are chosen so that they transform according to the irreducible representations A_2 and E of T_d (see section 7). When the E-mode reduced phase space is defined using equation

$$v_1^2 + v_2^2 + v_3^2 = \frac{1}{4} n_e^2 = \frac{1}{4} N_e^2$$

as a 2-sphere in the ambient 3-space with coordinates (v_1, v_2, v_3), the action of the C_3 operation is equivalent to the C_3 rotation about axis v_1. (This illustrates the abstract statement that the image of the T_d group in this case is a dihedral group D_3.) The two points that are invariant with regard to this operation lie on the v_1 axis (on the diametrically opposite ends),

$$v_1 = \pm\frac{1}{2}N_e, \quad v_2 = v_3 = 0.$$

Since v_1 has the symmetry A_2, these points are mapped into each other by operations S_4 and C_s of T_d and, therefore, they are equivalent and form one two-point orbit. Operation $\mathcal{T}$ also maps these points into each other.

To find the fixed points on $\mathbb{C}P^2$ with stabilizer $C_3^{[111]}$, we note that polynomials (s_1, s_2, s_3) and (t_1, t_2, t_3) transform according to the irreducible representations F_2 and F_1 of the T_d group, respectively. From matrices in Table 4 we conclude that at the fixed points on $\mathbb{C}P^2$,

$$s_1 = s_2 = s_3 = \sigma N_f, \qquad t_1 = t_2 = t_3 = \tau N_f, \tag{8.1a}$$

where σ and τ are dimensionless. We further note that at the same fixed point (with stabilizer $C_3^{[111]}$) polynomials

$$\left(\frac{3n_3 - n_f}{\sqrt{3}},\, x_3\right),$$

which transform according to the irreducible representation E, should vanish, i.e.,

$$3n_3 - n_f = x_3 = n_1 - n_2 = 0, \tag{8.1b}$$

and since $n_1 + n_2 + n_3 = N_f$ we obtain

$$n_1 = n_2 = n_3 = \frac{1}{3}N_f. \tag{8.1c}$$

Substituting conditions (8.1) into relations (6.13) produces equations

$$\left\{(1 + 3\sigma)\tau = 0, \quad \sigma^2 + \tau^2 = \frac{4}{9}, \quad \sigma^2 - \tau^2 = \frac{2}{3}\sigma\right\}$$

with two kinds of solutions:

$$(\tau, \sigma) = \left(0, \frac{2}{3}\right) \quad \text{and} \quad \left(\pm\frac{1}{\sqrt{3}}, -\frac{1}{3}\right).$$

Combining fixed points on $\mathbb{S}^2$, $\mathbb{C}P^1$, and $\mathbb{C}P^2$ for the *same* stabilizer, i.e., the group generated by the $C_3^{[111]}$ operation in Table 4, we obtain the fixed points on $\mathbb{C}P^2 \times \mathbb{C}P^1 \times \mathbb{S}^2$ listed in Table 27.

8.2.4. Stabilizer C_s. In the case of C_s, solution for the fixed points on the rotational sphere $\mathbb{S}^2$ and on the E-mode space $\mathbb{C}P^1 \sim \mathbb{S}^2$ is again quite simple. Indeed, using F_1 and E matrices of the C_s^{xy} example in Table 4 we find that these fixed points are defined as

$$j_1 = -j_2, \quad j_3 = 0 \quad \text{and} \quad v_1 = 0, \quad v_3 = 0.$$

On the F-mode space $\mathbb{C}P^2$ we look for a fixed point and a C_s-invariant sphere (see section 8.1). In the particular case of the C_s^{xy}-invariant points we find that

$$t_3 = 0, \quad t_1 = -t_2 = \tau N_f, \quad s_1 = s_2 = \sigma N_f, \quad x_3 = 0.$$

Using the notation

$$n_1 = n_2 = \frac{\eta}{2} N_f \geq 0, \quad n_3 = (1-\eta) N_f \geq 0, \quad s_3 = s N_f,$$

we obtain from relations (6.13) that

$$\begin{aligned} \tau^2 + \sigma^2 &= 2(1-\eta)s = 2(1-\eta)\eta, \\ \eta^2 - s^2 &= \tau(\eta - s) = \sigma(\eta - s) = 0. \end{aligned}$$

These equations have two kinds of solutions: an isolated point with

$$\eta = 1, \quad s = -1, \quad \sigma = \tau = 0,$$

which is listed in Table 27, and a 2-sphere defined by

$$\eta = s, \quad 2\tau^2 + 2\sigma^2 + (2\eta - 1)^2 = 1.$$

8.3. Orbits of the $T_d \times \mathcal{T}$ action. To find the *orbits* of equivalent fixed points of the $T_d \times \mathcal{T}$ action we take the fixed points found in the previous section for concrete stabilizers in Table 4 and act on them by all symmetry operations of $T_d \times \mathcal{T}$. We use the symmetry properties of dynamical invariants (generators in Table 21) described in section 7.1.3. These invariants are not symmetrized with regard to $T_d \times \mathcal{T}$ and their values (which play the role of "coordinates" on $\mathbb{C}P^2 \times \mathbb{C}P^1 \times \mathbb{S}^2$) differ for the points in the orbit. On the contrary, the value and behavior of any $T_d \times \mathcal{T}$ invariant function, such as the reduced Hamiltonian H_{eff}, remains the same.

Table 27 presents orbits of the $T_d \times \mathcal{T}$ action on $\mathbb{C}P^2 \times \mathbb{C}P^1 \times \mathbb{S}^2$. The list of fixed points in each orbit starts with the particular point found in section 8.2. Since time reversal images of points can be easily found using (7.2), we omit them for brevity so that each orbit in Table 27 has twice the number of points listed. For example, the orbit $A_1^{(4)}$ with stabilizer $S_4 \times \mathcal{T}$ has six equivalent fixed points, which correspond to three conjugate symmetry operations S_4^z, S_4^x, and S_4^y of the T_d group. The other six-point orbit $A_2^{(4)}$ differs from $A_1^{(4)}$ in the way the F_2- and E-mode coordinates are combined.

Invariant subspaces in Table 28 also are representatives of orbits of equivalent subspaces. There are six 2-spheres with stabilizer C_2, six $\mathbb{S}^2 \times \mathbb{S}^2$ spaces with the same stabilizer, and two different orbits of twelve 2-spheres with stabilizer C_s. Explicit coordinate representations for all these spaces can be obtained in the same way as obtained for the fixed points.

Table 29

Further stratification of the invariant subspaces of $\mathbb{C}P^2 \times \mathbb{C}P^1 \times \mathbb{S}^2$ *with stabilizers* C_s^{xy} *and* C_2^z *(Table 28) due to residual group action.*

Stabilizer	Equations	Topology
$C_2^z \times \mathcal{T}_2$	$v_1 = 0$	S_1
$C_2^z \times \mathcal{T}_s$	$v_2 = 0$	S_1
$C_2^z \times \mathcal{T}_2$	$v_1 = x_3 = \xi = 0$	$T_2 = S_1 \times S_1$
$C_2^z \times \mathcal{T}_s$	$v_2 = s_3 = \sigma = 0$	$T_2 = S_1 \times S_1$
$C_s^{xy} \times (\mathcal{T}_2, \mathcal{T}_s)$	$\sigma = 0$	S_1

8.4. Residual group action on invariant subspaces. Invariant subspaces of the T_d group action on $\mathbb{C}P^2 \times \mathbb{C}P^1 \times \mathbb{S}^2$, which are characterized in Table 28, are not homogeneous spaces with regard to the $T_d \times \mathcal{T}$ action. This has, of course, important consequences for the dynamics, which we will analyze later.

First we can verify whether some of the fixed points of the $T_d \times \mathcal{T}$ group action in Table 27 lie on any of the invariant subspaces. The presence of fixed points indicates that there is some nontrivial residual action of $T_d \times \mathcal{T}$ on the subspace. Continuing the C_2^z example in Table 28, we find that two points $A_1^{(4)}$ and $A_2^{(4)}$ lie on the C_2-invariant E-mode sphere, and four points $B_1^{(4)}$, $B_2^{(4)}$, $C_1^{(4)}$, and $C_2^{(4)}$ lie on the C_2-invariant space $\mathbb{S}^2 \times \mathbb{S}^2$. In the particular case of C_2^z, the residual T_d action is equivalent to the rotation by π about axes t_3 and v_2 in the respective ambient 3-spaces.

A complete study of all residual symmetries can be easily done by selecting all operations of the $T_d \times \mathcal{T}$ group which map invariant subspaces into themselves. Such selection is, of course, greatly simplified by the fact that many invariants take definite fixed values (see Table 28). Thus when studying symmetry operations acting on the invariant space $\mathbb{S}^2 \times \mathbb{S}^2$ with stabilizer C_2^z, we consider only those operations of $T_d \times \mathcal{T}$ which leave j_3 invariant (such as rotations around axis 3) or change its sign (such as reflections C_s in the planes containing axis 3). In the latter case, we should add the $\mathcal{T}$ operation to restore the sign of j_3. Another simplifying observation is that invariants used as coordinates on the subspaces often transform according to (rows of) different irreducible representations of the T_d group. In that case the residual group can have only one-dimensional representations.

Residual group action of $T_d \times \mathcal{T}$ on the invariant subspaces of the action of the spatial group T_d on $\mathbb{C}P^2 \times \mathbb{C}P^1 \times \mathbb{S}^2$ is characterized in Table 30. We can see that the residual action on the C_2 and C_s invariant spaces is equivalent to that of a C_{2v} and a C_h group, respectively. (As before we use point group analogies of groups which include reversing operations $\mathcal{T}$, $\mathcal{T}_s$, or $\mathcal{T}_2$.) Due to the presence of this residual action, invariant subspaces contain lower-dimensional strata in addition to just fixed points; see Tables 29 and 30.

9. Dynamics of the reduced system. Classical equations of motion for the reduced system can, in principle, be obtained using initial dynamical variables $(z, \bar{z})$ and the Poisson bracket

$$\{z, \bar{z}\} = \{q + ip, q - ip\} = -2i$$

Table 30

Residual action of $T_d \times \mathcal{T}$ on the dynamical invariants used to represent invariant subspaces in Table 28; note that $\mathcal{T}_2$ and $\mathcal{T}_s$ stand for $C_2 \circ \mathcal{T}$ and $C_s \circ \mathcal{T}$, respectively.

Spaces with stabilizer C_2^z

Dynamical invariants		Classes of $T_d \times \mathcal{T}$ I, C_2	$\mathcal{T}_2$	S_4	$\mathcal{T}_s$
$F_{1u}^{(3)}$	t_3, j_3	1	1	1	1
$E_g^{(1)}$	v_2, n_3	1	1	1	1
$E_g^{(2)}$	x_3, v_3	1	1	−1	−1
$F_{2g}^{(3)}$	s_3	1	−1	−1	1
A_{2u}	v_1	1	−1	−1	1

2-sphere with stabilizer C_s^{xy}

Dynamical invariants		Classes I, C_s	$\mathcal{T}_2$
$E_g^{(1)}$	v_2, n_3	1	1
F_{1u}	$\frac{t_1 - t_2}{\sqrt{2}}, \frac{j_1 - j_2}{\sqrt{2}}$	1	1
F_{2g}	$\frac{s_1 + s_2}{\sqrt{2}}$	1	−1

if we consider the reduced Hamiltonian H_{eff} as a function of $(z, \bar{z})$. These equations of motion should preserve all symplectic symmetries of H_{eff}, i.e., remain invariant with regard to the dynamical (oscillator) symmetry and to the action of the spatial group T_d described in section 7. We can, therefore, represent them in terms of invariants in Table 21 and thus obtain equations of motion on $\mathbb{C}P^2 \times \mathbb{C}P^1 \times \mathbb{S}^2$. A more elegant approach is to study the Poisson algebra generated by the invariants and then obtain the same equations directly.

9.1. Poisson algebra of dynamical invariants. Invariants in Table 21 generate a multiplicative ring $\mathcal{R}$ of polynomials invariant with regard to the oscillator symmetry. The Poisson bracket of any two generators in Table 21 is itself a dynamically invariant polynomial function, which is a member of $\mathcal{R}$. We say that $\mathcal{R}$ has a Poisson structure. Invariant polynomials in Table 21 generate a Poisson algebra and can be used as dynamical variables. The integrals j, n_e, and n_f are Casimirs. To compute the structure of the algebra, we can return to the $(z, \bar{z})$ representation.

For the E-mode invariants and, of course, for the angular momentum components, we obtain the standard algebra so(3),

$$\{j_\alpha, j_\beta\} = \epsilon_{\alpha\beta\gamma}\, j_\gamma, \quad \{v_\alpha, v_\beta\} = \epsilon_{\alpha\beta\gamma}\, v_\gamma,$$

and the Euler–Poisson equations,

$$\frac{d}{dt} j_\alpha = \{H_{\text{eff}}, j_\alpha\} = \frac{\partial H_{\text{eff}}}{\partial j_\gamma} j_\beta - \frac{\partial H_{\text{eff}}}{\partial j_\beta} j_\gamma. \tag{9.1a}$$

Dynamics on the $\mathbb{C}P^2$ space is described by the system of equations for eight invariant polynomials, which can be considered as independent dynamical variables. Since all these polynomials are quadratic in $(z, \bar{z})$, their Poisson brackets are also quadratic and can be expressed as their linear combinations. Resulting Poisson algebra is characterized in Table 31. Given the structure matrix $\mathcal{M}$ in this table, equations of motion can be written as

$$\dot{\theta} = \mathcal{M}^T \nabla_\theta H_{\text{eff}}, \tag{9.1b}$$

where θ is a vector $\theta = (x_3, s_1, s_2, s_3, n_3, t_1, t_2, t_3)$ and $\mathcal{M}^T = -\mathcal{M}$.

Table 31

Poisson algebra of the invariants describing dynamics on $\mathbb{C}P^2 \times \mathbb{C}P^1 \times \mathbb{S}^2$ (F_2- and E-mode polyads and rotational subsystem). Here $x_1 = n_2 - n_3$, $x_3 = n_1 - n_2$, $x_2 = n_3 - n_1$, and $x_1 + x_2 + x_3 = 0$.

	s_1	s_2	s_3	n_3	t_1	t_2	t_3
x_3	$-t_1$	$-t_2$	$2t_3$	0	s_1	s_2	$-2s_3$
s_1		$-t_3$	t_2	t_1	$2x_1$	$-s_3$	s_2
s_2			$-t_1$	$-t_2$	s_3	$2x_2$	$-s_1$
s_3				0	$-s_2$	s_1	$2x_3$
n_3					s_1	$-s_2$	0
t_1						t_3	$-t_2$
t_2							t_1

	j_2	j_3
j_1	j_3	$-j_2$
j_2		j_1

	v_2	v_3
v_1	v_3	$-v_2$
v_2		v_1

9.2. Canonical variables in the limit of linearization. In section 8.2 we found RE, or equilibria of the reduced system, as isolated fixed points (critical orbits) of the $T_d \times \mathcal{T}$ action. To study dynamics near these RE, and in particular to determine their stability, we should linearize H_{eff} near them. Linearization in terms of $(z, \bar{z})$ variables was already introduced in section 5.1.4.

Similarly to finding coordinates of RE in section 8.2, linearizing near an RE can be understood on the example of a C_k symmetric RE whose symmetry axis is oriented as in section 7.1.1. Axis S_4^z (or C_4) has such an orientation, and coordinates of the RE $A_{1,2}^{(4)}$ and $B_{1,2}^{(4)}$ on the $\mathbb{C}P^2$ space and rotational sphere $\mathbb{S}^2$ (see Table 27) define, in fact, fixed points and RE for *any* C_k^z action on these spaces with $k = 3, 4, \ldots, \infty$.

Consider first the familiar simple case of the rotational sphere $\mathbb{S}^2$ described by (j_1, j_2, j_3) or by scaled variables

$$\tilde{j}_i = \frac{j_i}{\sqrt{J}}, \quad i = 1, 2, 3. \tag{9.2}$$

At the fixed point $j_3 = J$, the only nonzero Poisson bracket is $\{j_1, j_2\} = j_3$ (Table 31), and consequently the scaled variables $(\tilde{j}_1, \tilde{j}_2)$ become the standard canonical coordinate–momentum pair in the limit of linearization near the relative equilibrium with $j_3 = J$. Near the second fixed point on $\mathbb{S}^2$ with $j_3 = -J$ (which is the time reversal image of the first point) canonical variables will be $(\tilde{j}_2, \tilde{j}_1)$; i.e., $\tilde{j}_2$ will play the role of coordinate and $\tilde{j}_1$ the role of conjugate momentum.

The E-mode space $\mathbb{C}P^1$ is isomorphic to a sphere $\mathbb{S}^2$ defined in the ambient 3-space with coordinates (v_1, v_2, v_3). We should scale these coordinates as follows:

$$\tilde{v}_i = \frac{v_i\sqrt{2}}{\sqrt{N_e}}, \quad i = 1, 2, 3. \tag{9.3}$$

The S_4^z operation acts on the E-mode sphere as rotation by π about axis v_2; the two fixed points with $v_2 = \pm N_e/2$ lie on this axis. In the limit of linearization near these points we use canonical coordinates $(\tilde{v}_1, \tilde{v}_3)$ and $(\tilde{v}_3, \tilde{v}_1)$.

On the F_2-mode space $\mathbb{C}P^2$ we proceed in a similar fashion [97]. We compute the Poisson structure in Table 31 at each relative equilibrium and then find canonical variables of the

Table 32

Standard canonical coordinates and conjugate momenta for the linearization near RE with stabilizer S^z_4.

Space	Mode[48]	$A_1^{(4)}$	$B_1^{(4)}$	$\overline{B}_1^{(4)}$
$\mathbb{C}P^2$	F_2	$\tilde{t}_1, \tilde{s}_1$	$\frac{\tilde{s}_2 - \tilde{t}_1}{\sqrt{2}}, \frac{\tilde{s}_1 - \tilde{t}_2}{\sqrt{2}}$	$\frac{\tilde{s}_1 + \tilde{t}_2}{\sqrt{2}}, \frac{\tilde{s}_2 + \tilde{t}_1}{\sqrt{2}}$
		$\tilde{s}_2, \tilde{t}_2$	$\tilde{x}_3, \tilde{s}_3$	$\tilde{s}_3, \tilde{x}_3$
$\mathbb{C}P^1$	E	$\tilde{v}_1, \tilde{v}_3$	$\tilde{v}_1, \tilde{v}_3$	$\tilde{v}_1, \tilde{v}_3$
$\mathbb{S}^2$	rot	$\tilde{j}_1, \tilde{j}_2$	$\tilde{j}_1, \tilde{j}_2$	$\tilde{j}_2, \tilde{j}_1$

linearization limit. After changing to scaled variables

$$\tilde{a}_i = \frac{a_i}{\sqrt{2N_f}}, \quad a = s, t, n, x, \quad i = 1, 2, 3, \tag{9.4}$$

we obtain the results in Table 32.

Another way to proceed is to find coordinates near each RE on $\mathbb{C}P^2$ without demanding that these coordinates be canonical. The set of coordinate invariants $\zeta_i^{(c)}$ $(i = 1, \ldots, 4)$ that we use is selected from among the invariants n_i, s_i, and t_i $(i = 1, 2, 3)$ such that the syzygy relations (6.13), together with the constraint $n_1 + n_2 + n_3 = N_f$, can be solved in order to express the remaining invariants $\zeta_i^{(r)}$ $(i = 1, \ldots, 5)$ in terms of $\zeta_i^{(c)}$ and N_f.

We find a set of invariants with the above property by checking that the conditions of the implicit function theorem are satisfied. Specifically, let F_i $(i = 1, \ldots, 9)$ be the left-hand sides of the syzygy relations (6.13) and $F_{10} = n_1 + n_2 + n_3 - N_f$. The invariants $\zeta_i^{(r)}$ are selected in such a way that the 10×5 matrix

$$\frac{\partial(F_i)}{\partial(\zeta_j^{(r)})} \tag{9.5}$$

has rank 5. Then $\zeta_i^{(r)}$ can be expressed in terms of $\zeta_i^{(c)}$ and N_f. There is usually more than one choice for $\zeta_i^{(c)}$, but not all choices are equally acceptable. Since we need to actually solve the equations $F_i = 0$, we must try to find a set $\zeta_i^{(c)}$ such that the solution takes a simple form. This can be done only by inspecting the solutions in each case.

For example, for the $A^{(4)}$ point $(1, 0, 0)$ with stabilizer $D_{2d}^{(x)} \times \mathcal{T}$, we find that $\zeta^{(c)} = (s_2, s_3, t_2, t_3)$ is a suitable set of invariants. The values of these invariants on the specific RE are $\zeta^{(c)*} = (0, 0, 0, 0)$. We define the displacement vector

$$d_i^{A^{(4)}} = \zeta_i = \zeta_i^{(c)} - \zeta_i^{(c)*}, \quad i = 1, \ldots, 4.$$

Notice that near the RE we can express all the invariants in terms of the displacements ζ_i.

An important difference with regard to the previous discussion is that the displacements here are not necessarily canonically conjugate variables. It is therefore important to calculate the linearized Poisson structure near each RE. In order to do this we calculate each Poisson bracket $\{\zeta_i, \zeta_j\}$ using the invariants, and then we express the result as a function of the

[48] Notation as in Table 21 with $n \equiv N_f$.

Table 33

Dynamically invariant local coordinates at the RE on the F_2-mode space $\mathbb{C}P^2$.

Type of RE		Poisson algebra[49]
$A^{(4)}$	$D_{2d}^{(x)} \times \mathcal{T}$	$s_2=\zeta_1$, $s_3=\zeta_2$, $t_2=\zeta_3$, $t_3=\zeta_4$: $\{\zeta_2,\zeta_3\}=-2n$, $\{\zeta_3,\zeta_4\}=2n$, $\{\zeta_2,\zeta_4\}=0$
$A^{(2)}$	$C_{2v}^{(z)} \times \mathcal{T}$	$n_2-\frac{1}{2}n=\zeta_1$, $s_1=\zeta_2$, $t_1=\zeta_3$, $t_3=\zeta_4$: $\{\zeta_2,\zeta_3\}=0$, $\{\zeta_3,\zeta_4\}=n$, $\{\zeta_2,\zeta_4\}=0$
$A^{(3)}$	$C_{2v}^{(z)} \times \mathcal{T}$	$s_2-2n/3=\zeta_1$, $s_3-2n/3=\zeta_2$, $t_2=\zeta_3$, $t_3=\zeta_4$: $\{\zeta_2,\zeta_3\}=0$, $\{\zeta_3,\zeta_4\}=2n/3$, $\{\zeta_2,\zeta_4\}=0$
$B^{(3)}$	$C_3^{[111]} \wedge \mathcal{T}_s^{\parallel}$	$s_2+n/3=\zeta_1$, $s_3+n/3=\zeta_2$, $t_2-n/\sqrt{3}=\zeta_3$, $t_3-n/\sqrt{3}=\zeta_4$: $\{\zeta_2,\zeta_3\}=-n/\sqrt{3}$, $\{\zeta_3,\zeta_4\}=-n/3$, $\{\zeta_2,\zeta_4\}=n/3$, $\{\zeta_4,\zeta_4\}=n/\sqrt{3}$
$B^{(4)}$	$S_4^{(x)} \wedge \mathcal{T}_2^{(y)}$	$n_3-\frac{1}{2}n=\zeta_1$, $s_1=\zeta_2$, $s_2=\zeta_3$, $t_2=\zeta_4$: $\{\zeta_2,\zeta_3\}=-n$, $\{\zeta_3,\zeta_4\}=0$, $\{\zeta_2,\zeta_4\}=0$, $\{\zeta_4,\zeta_4\}=n$

displacements ζ_i, keeping terms only up to first order. We can follow the above program for all the RE. The results are summarized in Table 33. Observe that for most cases in this table it is immediately obvious how to define standard canonically conjugate variables. Thus in the case of the $A^{(3)}$ point, we can define canonically conjugate variables (ξ,η),

$$\xi_1=\alpha\zeta_2,\ \eta_1=\alpha\zeta_3,\ \xi_2=\alpha\zeta_4,\ \eta_2=\alpha\zeta_1,\quad \alpha=\sqrt{\tfrac{3}{2N_f}},$$

such that the local 2-form is $d\xi_1\wedge d\eta_1+d\xi_2\wedge d\eta_2$. The only case where the proper definition of the canonical variables is not obvious is the case of the $B^{(3)}$ point.

To conclude this section, we should add one important remark. The above canonical (or noncanonical) variables can *only* be used to study *linear* Hamiltonian equations of the reduced system near the RE. This limitation is due to the fact that the symplectic form near the RE has a standard matrix $\left(\begin{smallmatrix}0 & 1\\ -1 & 0\end{smallmatrix}\right)$ only to the first order (in the limit of linearization). When nonlinear equations of motion near the RE are sought (e.g., when bifurcations of the RE are studied) this form should be further "flattened" in higher orders; see section V.8.2 of [11].

9.3. Dynamics on invariant subspaces of $\mathbb{C}P^2\times\mathbb{C}P^1\times\mathbb{S}^2$. In section 8.4 and Table 28 we describe three possible types of subspaces of the reduced phase space $\mathbb{C}P^2\times\mathbb{C}P^1\times\mathbb{S}^2$ that

[49] Notation as in Table 21 with $n\equiv N_f$.

are invariant with regard to the (symplectic) action of the spatial group T_d and are therefore dynamically invariant subspaces of the reduced system. These subspaces are either 2-spheres $\mathbb{S}^2 \sim \mathbb{C}P^1$ or a product of 2-spheres $\mathbb{S}^2 \times \mathbb{S}^2$. Dynamics on each $\mathbb{S}^2$ can be described by Euler–Poisson equations. The corresponding "angular momentum" algebras so(3) are constructed below.

The construction is most straightforward in the case of the C_2-invariant $\mathbb{S}^2$ subspace of $\mathbb{C}P^2$ (which can be represented using complex coordinates (z_1, z_2) and $z_3 = 0$). We can see from Tables 21 and 28 that the three so(3) components can be chosen as

$$(Y_1, Y_2, Y_3) = \left(\frac{s_3}{2}, \frac{t_3}{2}, \frac{x_3}{2}\right).$$

Restricting the Poisson algebra in Table 31 to the C_2^z-invariant sphere defined in Table 28 shows that this is indeed so(3),

$$\{Y_\alpha, Y_\beta\} = \epsilon_{\alpha\beta\gamma} Y_\gamma,$$

with Casimir

$$Y_1^2 + Y_2^2 + Y_3^2 = \left(\frac{N_f}{2}\right)^2.$$

Dynamics on the $\mathbb{S}^2 \times \mathbb{S}^2$ invariant subspace in Table 28 is described using an so(3) × so(3) algebra. The second so(3) is generated by (v_1, v_2, v_3), commutes with (Y_1, Y_2, Y_3), and has the Casimir

$$v_1^2 + v_2^2 + v_3^2 = \left(\frac{N_e}{2}\right)^2.$$

Dynamical variables for the C_s^{xy}-invariant sphere in Table 28 are obtained analogously. Restricting the Poisson algebra in Table 31, we find polynomials

$$\begin{aligned}(X_1, X_2, X_3) &= \left(\frac{t_1 - t_2}{2\sqrt{2}}, \frac{s_1 + s_2}{2\sqrt{2}}, \frac{2s_3 - N_f}{2}\right) \\ &= \left(\frac{\tau}{\sqrt{2}}, \frac{\sigma}{\sqrt{2}}, \frac{2\eta - 1}{2}\right) N_f,\end{aligned}$$

which form the so(3) algebra, such that

$$X_1^2 + X_2^2 + X_3^2 = \left(\frac{N_f}{2}\right)^2, \quad \{X_i, X_j\} = \epsilon_{ijk} X_k.$$

10. Existence and stability of RE. RE are special stationary solutions of the equations of motion (9.1), which in many cases are defined entirely by symmetry and exist for any generic small symmetry-preserving perturbation. Isolated fixed points of the $T_d \times \mathcal{T}$ group action on the reduced phase space $\mathbb{C}P^2 \times \mathbb{C}P^1 \times \mathbb{S}^2$ found in section 8 are necessarily stationary solutions of (9.1) and are therefore representing RE. We show how to determine the stability of these RE using the reduced Hamiltonian H_{eff} defined as a function on $\mathbb{C}P^2 \times \mathbb{C}P^1 \times \mathbb{S}^2$. Subsequently, we search for other RE, which are not fixed by the action of the finite symmetry group.

10.1. Linear stability of fixed RE. Fixed RE of our system correspond to fixed points of the group action found in sections 8.1 and 8.2 (see Table 10, 15, and 27). Stability of these RE was already analyzed in section 5.1.4, where we studied analytical Poincaré surfaces of section using initial phase space variables $(z, \bar{z})$. Here we use invariants in Table 21 to study RE stability directly on $\mathbb{C}P^2 \times \mathbb{C}P^1 \times \mathbb{S}^2$, i.e., *without* lifting back to the initial phase space. As before, we can explain our approach in the example of axial symmetry with axis C_k oriented as C_4^z (see sections 8.1 and 9.2).

Analysis on $\mathbb{C}P^2$ is the most difficult [97]. Using canonical variables of the linearization limit found in section 9.2 and Table 32, we come to the problem of determining linear stability of a stationary point in different canonical planes. Each such plane has its origin at the relative equilibrium, and the stabilizer C_k of the RE acts as a rotation $C_{k'}$ about the origin. In general, the actions of C_k on the initial 3-space and on the particular canonical plane can differ. We have shown in section 7 that these actions are the same, and $k = k'$ for all planes except (x_3, s_3), where $k' = k/2$.

In the case of C_3 and C_k with $k > 4$, canonical coordinate–momentum pairs in each of the four symplectic planes transform according to a pair of conjugate complex representations of the symmetry group (which correspond to two representations of the SO(2) group of indexes $\pm m$). Variables x_3 and s_3 in the case of C_4 and all variables in the case of C_2 transform according to different real one-dimensional irreducible representations.

In order to take into account the full symmetry group $T_d \times \mathcal{T}$, as in section 5.1.5 we should find the action of the stabilizer of each RE on the local variables ζ_i, defined in section 9.2. As before, we need to define the action of the elements R of the stabilizer G of each RE on the displacement vector $d = \{\zeta_i\}_{i=1,\dots,4}$. For this we act with R on the original complex variables (z_1, z_2, z_3). This action induces a linear action L_R on the invariants, and a nonlinear action N_R on the displacements ζ_i. The last action is computed by expressing ζ_i in terms of the invariants $\zeta_i^{(r)}$, acting on them with L_R, and expressing the result again in terms of the displacements ζ_i. The action $N_R^{(1)}$ is then defined as the linearization of N_R.

The results are presented in Table 34. We can find from this table that the reducible representation of each stabilizer spanned by the variables ζ_i is decomposed into exactly the same irreducible representations as the representation of the stabilizer spanned by the local variables (x_1, x_2, y_1, y_2) of section 5.1.5.

10.2. Finding additional stationary points on invariant subspaces. In sections 8.4 and 9.3 and in Tables 28 and 30 we describe subspaces of $\mathbb{C}P^2 \times \mathbb{C}P^1 \times \mathbb{S}^2$ whose stabilizers are purely spatial subgroups of $T_d \times \mathcal{T}$. Such subgroups are symplectic and the subspaces are dynamically invariant subspaces of the reduced system. To find equations of motion on these subspaces we can simply restrict the reduced Hamiltonian H_{eff} using Table 28 and express it in terms of dynamical variables (Y_1, Y_2, Y_3) or (X_1, X_2, X_3), defined in Table 33, and/or (v_1, v_2, v_3). Equations of motion then can be generated using the respective so(3) algebras. Before a general solution is attempted, resulting equations first can be restricted to the one-dimensional strata of the residual group action (see section 8.4). All stationary points found should satisfy Morse conditions for the respective subspace.

As explained in section 5, we should study the C_s-invariant subspace, which is a 2-sphere with no critical orbits of the symmetry group action (no RE fixed by symmetry). This sphere

Table 34

Action of stabilizers on dynamically invariant local coordinates on $\mathbb{C}P^2$ defined in Table 33.

Action of $D_{2d}^{(x)} \times \mathcal{T}$ on $E_g \oplus E_u$ for the $A^{(4)}$ RE

R	$R\zeta_1$	$R\zeta_2$	$R\zeta_3$	$R\zeta_4$	R	$R\zeta_1$	$R\zeta_2$	$R\zeta_3$	$R\zeta_4$
E	ζ_1	ζ_2	ζ_3	ζ_4	$\mathcal{T}$	ζ_1	ζ_2	$-\zeta_3$	$-\zeta_4$
C_2^x	$-\zeta_1$	$-\zeta_2$	$-\zeta_3$	$-\zeta_4$	$C_2^x\mathcal{T}$	$-\zeta_1$	$-\zeta_2$	ζ_3	ζ_4
C_2^y	ζ_1	$-\zeta_2$	ζ_3	$-\zeta_4$	$C_2^y\mathcal{T}$	ζ_1	$-\zeta_2$	$-\zeta_3$	ζ_4
C_2^z	$-\zeta_1$	ζ_2	$-\zeta_3$	ζ_4	$C_2^z\mathcal{T}$	$-\zeta_1$	ζ_2	ζ_3	$-\zeta_4$
σ^{yz}	ζ_2	ζ_1	$-\zeta_4$	$-\zeta_3$	$\sigma^{yz}\mathcal{T}$	ζ_2	ζ_1	ζ_4	ζ_3
$\sigma^{\overline{yz}}$	$-\zeta_2$	$-\zeta_1$	ζ_4	ζ_3	$\sigma^{\overline{yz}}\mathcal{T}$	$-\zeta_2$	$-\zeta_1$	$-\zeta_4$	$-\zeta_3$
S_4^x	$-\zeta_2$	ζ_1	ζ_4	$-\zeta_3$	$S_4^x\mathcal{T}$	$-\zeta_2$	ζ_1	$-\zeta_4$	ζ_3
$(S_4^x)^{-1}$	ζ_2	$-\zeta_1$	$-\zeta_4$	ζ_3	$(S_4^x)^{-1}\mathcal{T}$	ζ_2	$-\zeta_1$	ζ_4	$-\zeta_3$

Action of $S_4^{(x)} \wedge \mathcal{T}_2^{(y)}$ on $B_1 \oplus B_2 \oplus E$ for the $B^{(4)}$ RE

R	$R\zeta_1$	$R\zeta_2$	$R\zeta_3$	$R\zeta_4$	R	$R\zeta_1$	$R\zeta_2$	$R\zeta_3$	$R\zeta_4$
E	ζ_1	ζ_2	ζ_3	ζ_4	$\sigma^{yz}\mathcal{T}$	$-\zeta_1$	ζ_2	$-\zeta_4$	$-\zeta_3$
C_2^x	ζ_1	ζ_2	$-\zeta_3$	$-\zeta_4$	$\sigma^{\overline{yz}}\mathcal{T}$	$-\zeta_1$	ζ_2	ζ_4	ζ_3
S_4^x	$-\zeta_1$	$-\zeta_2$	ζ_4	$-\zeta_3$	$C_2^y\mathcal{T}$	ζ_1	$-\zeta_2$	ζ_3	$-\zeta_4$
$(S_4^x)^{-1}$	$-\zeta_1$	$-\zeta_2$	$-\zeta_4$	ζ_3	$C_2^z\mathcal{T}$	ζ_1	$-\zeta_2$	$-\zeta_3$	ζ_4

Action of $C_{2v}^{(z)} \times \mathcal{T}$ on $A_{2g} \oplus A_{2u} \oplus B_{1g} \oplus B_{1u}$ for the $A^{(2)}$ RE

R	$R\zeta_1$	$R\zeta_2$	$R\zeta_3$	$R\zeta_4$	R	$R\zeta_1$	$R\zeta_2$	$R\zeta_3$	$R\zeta_4$
E	ζ_1	ζ_2	ζ_3	ζ_4	$\mathcal{T}$	ζ_1	ζ_2	$-\zeta_3$	$-\zeta_4$
C_2^z	ζ_1	$-\zeta_2$	$-\zeta_3$	ζ_4	$C_2^z\mathcal{T}$	ζ_1	$-\zeta_2$	ζ_3	$-\zeta_4$
σ^{xy}	$-\zeta_1$	ζ_2	ζ_3	$-\zeta_4$	$\sigma^{xy}\mathcal{T}$	$-\zeta_1$	ζ_2	$-\zeta_3$	ζ_4
$\sigma^{\overline{xy}}$	$-\zeta_1$	$-\zeta_2$	$-\zeta_3$	$-\zeta_4$	$\sigma^{\overline{xy}}\mathcal{T}$	$-\zeta_1$	$-\zeta_2$	ζ_3	ζ_4

Action of $C_{3v}^{[111]} \times \mathcal{T}$ on $E_g \oplus E_u$ for the $A^{(3)}$ RE

R	$R\zeta_1$	$R\zeta_2$	$R\zeta_3$	$R\zeta_4$
E	ζ_1	ζ_2	ζ_3	ζ_4
$C_3^{[111]}$	$-\zeta_1-\zeta_2$	ζ_1	$-\zeta_3-\zeta_4$	ζ_3
$(C_3^{[111]})^2$	ζ_2	$-\zeta_1-\zeta_2$	ζ_4	$-\zeta_3-\zeta_4$
σ^{yz}	ζ_2	ζ_1	$-\zeta_4$	$-\zeta_3$
σ^{zx}	ζ_1	$-\zeta_1-\zeta_2$	$-\zeta_3$	$\zeta_3+\zeta_4$
σ^{xy}	$-\zeta_1-\zeta_2$	ζ_2	$\zeta_3+\zeta_4$	$-\zeta_4$
$\mathcal{T}$	ζ_1	ζ_2	$-\zeta_3$	$-\zeta_4$
$C_3^{[111]}\mathcal{T}$	$-\zeta_1-\zeta_2$	ζ_1	$\zeta_3+\zeta_4$	$-\zeta_3$
$(C_3^{[111]})^2\mathcal{T}$	ζ_2	$-\zeta_1-\zeta_2$	$-\zeta_4$	$\zeta_3+\zeta_4$
$\sigma^{yz}\mathcal{T}$	ζ_2	ζ_1	ζ_4	ζ_3
$\sigma^{zx}\mathcal{T}$	ζ_1	$-\zeta_1-\zeta_2$	ζ_3	$-\zeta_3-\zeta_4$
$\sigma^{xy}\mathcal{T}$	$-\zeta_1-\zeta_2$	ζ_2	$-\zeta_3-\zeta_4$	ζ_4

Action of $C_3^{[111]} \wedge \mathcal{T}_s^{\parallel}$ on $E \oplus E$ for the $B^{(3)}$ RE

R	$R\zeta_1$	$R\zeta_2$	$R\zeta_3$	$R\zeta_4$
E	ζ_1	ζ_2	ζ_3	ζ_4
$C_3^{[111]}$	$-\zeta_1-\zeta_2$	ζ_1	$-\zeta_3-\zeta_4$	ζ_3
$(C_3^{[111]})^2$	ζ_2	$-\zeta_1-\zeta_2$	ζ_4	$-\zeta_3-\zeta_4$
$\sigma^{yz}\mathcal{T}$	ζ_2	ζ_1	ζ_4	ζ_3
$\sigma^{zx}\mathcal{T}$	ζ_1	$-\zeta_1-\zeta_2$	ζ_3	$-\zeta_3-\zeta_4$
$\sigma^{xy}\mathcal{T}$	$-\zeta_1-\zeta_2$	ζ_2	$-\zeta_3-\zeta_4$	ζ_4

$\mathbb{S}^2$ has an invariant circle $\mathbb{S}^1$ with stabilizer $\mathcal{T}_2$, which is defined by $X_2 = 0$ (or equivalently $s_1 = s_2 = \sigma = 0$). The Morse requirements of two stationary points, a minimum and a maximum, for both the sphere $\mathbb{S}^2$ and its invariant subspace $\mathbb{S}^1$ can be satisfied if the two points lie on $\mathbb{S}^1$. To find these points we first restrict H_{eff} to the C_s sphere using Table 28 and reexpress it as a function of dynamical variables (X_1, X_2, X_3). If $H_{\text{eff}}(X)$ is a Morse function, we will always find at least two stationary points of $H_{\text{eff}}(X)$ on the $\mathcal{T}_2$-invariant circle $\mathbb{S}^1$. Such points are particular solutions to the Euler–Poisson equations

$$\dot{X} = \begin{pmatrix} 0 & X_3 & -X_2 \\ -X_3 & 0 & X_1 \\ X_2 & -X_1 & 0 \end{pmatrix}^T \nabla_X H_{\text{eff}}(X) = 0, \tag{10.1}$$

where we should set $X_2 = 0$.

11. Examples.

11.1. Vibrational structure of the F_2-mode polyads. Possible configurations and different types of stability of the RE of the F_2-mode subsystem were studied in section 5.3.2. In section 5.2.3 we emphasized the difference between simplest and nonsimplest Hamiltonians on $\mathbb{C}P^2$ and described the system of RE in each case. Below we study this system in more detail on a model example, which is discussed in more detail in [98].

The Hamiltonian of a molecule, which has the F_2 mode, can be written as $\omega H^{\nu_3}_{\text{vib}} + H'$, where to order ϵ^2

$$\begin{aligned} H^{\nu_3}_{\text{vib}} =& \tfrac{1}{2}(q_1^2 + p_1^2) + \tfrac{1}{2}(q_2^2 + p_2^2) + \tfrac{1}{2}(q_3^2 + p_3^2) + \epsilon K_3 q_1 q_2 q_3 + \epsilon^2 K_t \tfrac{1}{2}(q_1^4 + q_2^4 + q_3^4) \\ &+ \epsilon^2 K_s \tfrac{1}{2}(q_1^2 + q_2^2 + q_3^2)^2 + \epsilon^2 K_l \tfrac{1}{2}\left[\mathbf{p} \times \mathbf{q}\right]^2, \end{aligned} \tag{11.1a}$$

and H' represents other degrees of freedom and interaction of these degrees with the F_2-mode subsystem (cf. section 5.3.2). In order to study this subsystem, we should consider H' explicitly, normalize the Hamiltonian $\omega H^{\nu_3}_{\text{vib}} + H'$, and *then* restrict the obtained normal form on $\mathbb{C}P^2$ by setting to zero all dynamical variables of other subsystems. This approach was used in [13] for the case of the A_4 molecule, where we set to zero integrals j, N_e, and N_a, angular momenta (j_1, j_2, j_3), and E-mode vibrational variables (v_1, v_2, v_3); see Table 21. Furthermore, the simple atom–atom bond model of A_4 used in [13] gives

Constant	ω	K_3	K_l	K_s	K_t
Value	$\sqrt{2}$	$3/2^{5/4}$	$2^{-5/2}\lambda$	$-5/2^{9/2}$	$7/2^{-9/2}$

(11.1b)

Here the parameter λ is introduced so that the value of K_l obtained in [13] corresponds to $\lambda = 1$. In the present study we focus on the F_2-mode subsystem without taking interactions with other subsystems into account. To this end we use a simplified model, where H' is neglected *before* normalization. This model turns out to be sufficient for studying the transition from the simplest to the nonsimplest Hamiltonian on $\mathbb{C}P^2$.

The normal form of (11.1a) $H^{\nu_3}_{\text{eff}} = n + \epsilon^2 \mathcal{H}^{\nu_3}_2 + \cdots$ can be expressed using invariants in Table 21. In the second order $\mathcal{H}^{\nu_3}_2$ we obtain

Term		Coefficient
ϵ^2	n^2	$\frac{1}{2}(K_3^2/24 + K_l + K_s + 3K_t/4)$
ϵ^2	$(s_1^2 + s_2^2 + s_3^2)$	$\frac{1}{2}(-K_3^2/4 - K_l + K_s/2)$
ϵ^2	$(2nn_3 - 3n_3^2 - x_3^2)$	$\frac{1}{2}(K_3^2/24 + K_l - K_s/2 - 3K_t/4)$

Taking the $T_d \times \mathcal{T}$ symmetry into account (Table 25), we can verify that $\mathcal{H}_2^{\nu_3}$ has indeed only three independent terms:

Term		Coefficient
ϵ^2	$V^{A_1}_{ffff}$	$(5K_s - 4K_l - K_3^2 + 3K_t)/4$
ϵ^2	V^{E}_{ffff}	$(K_s + K_l + K_3^2/4 + 3K_t/2)/\sqrt{2}$
ϵ^2	$V^{F_2}_{ffff}$	$(K_s + K_l - K_3^2/6)\sqrt{3}/2$

In fact, the Hamiltonian $\mathcal{H}_2^{\nu_3}$ has been long suggested by Hecht [95] as a model Hamiltonian for describing the internal structure of the F_2-mode polyads. Hecht expressed his model $\mathcal{H}_2^{\nu_3}$ in terms of

$$n^2 = V^{A_1}_{ffff} + \sqrt{2}V^{E}_{ffff} + \sqrt{3}V^{F_2}_{ffff}, \tag{11.2a}$$

$$t^2 = t_1^2 + t_2^2 + t_3^2 = \left[\mathbf{p} \times \mathbf{q}\right]^2 = n^2 - 3V^{A_1}_{ffff}, \tag{11.2b}$$

$$m = n_1^2 + n_2^2 + n_3^2 = V^{A_1}_{ffff} + \sqrt{2}V^{E}_{ffff}, \tag{11.2c}$$

where the "vibrational angular momentum" t^2 is often denoted as l^2 [95, 96]. Considering relations (6.13), we note an alternative to m or t,

$$s^2 = s_1^2 + s_2^2 + s_3^2 = 2n^2 - 2m - t^2. \tag{11.2d}$$

Hecht's representation

$$\mathcal{H}_2^{\nu_3} = c_0 n^2 + c_l t^2 + c_m m, \tag{11.3}$$

or, alternatively,

$$\mathcal{H}_2^{\nu_3} = c_0' n^2 + c_l' t^2 + c_s s^2 \tag{11.3′}$$

is particularly convenient for the order ϵ^2 classification of qualitatively different normal forms $H_{\text{eff}}^{\nu_3}$ on $\mathbb{C}P_n^2$. We remark that the term n^2 is just an additive ("scalar") energy constant (for the reduced system on $\mathbb{C}P_n^2$, i.e., within one n polyad). Neglecting this term, the energies of RE of the F_2-mode system with Hamiltonian (11.3) or (11.3′) are given below.

Type of RE		$\mathcal{H}_2 n^{-2} - c_0'$	$\mathcal{H}_2 n^{-2} - c_0$
$C_{2v} \times \mathcal{T}$	A	c_s	$\frac{1}{2}c_m$
$C_{3v} \times \mathcal{T}$	A	$\frac{4}{3}c_s$	$\frac{1}{3}c_m$
$C_3 \wedge \mathcal{T}_s$	B	$c_l' + \frac{1}{3}c_s$	$c_l + \frac{1}{3}c_m$
$D_{2d} \times \mathcal{T}$	A	0	c_m
$S_4 \wedge \mathcal{T}_2$	B	c_l'	$c_l + \frac{1}{2}c_m$
$C_s \wedge \mathcal{T}_2$		$(c_l')^2(c_l' - \frac{1}{4}c_s)^{-1}$	

It follows that reciprocal energies of RE of such system and, therefore, the structure of the vibrational polyads of the F_2 mode, are described (to the lowest order) by *one* parameter, the

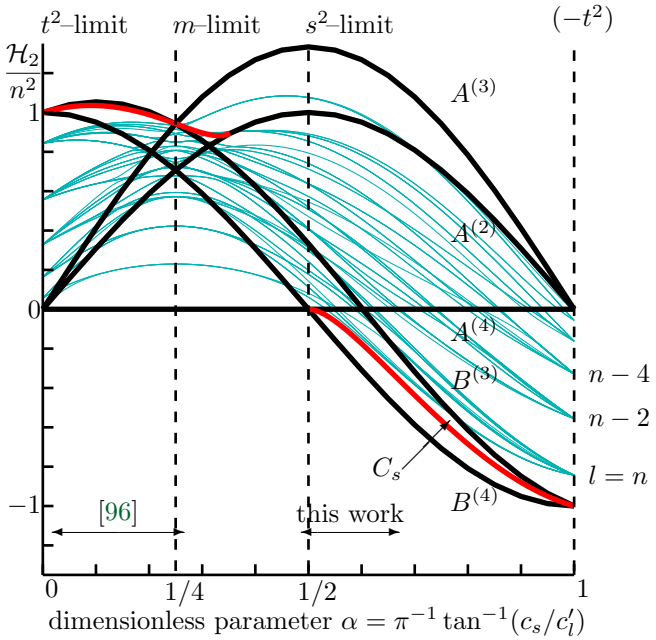

Figure 17. *Reciprocal energies (in units of n^2 and without scalar part $c_0' n^2$) of RE (bold lines) and the structure of the $n = 10$ quantum polyad (thin blue lines) of the F_2-mode system in the second order model (Hecht's Hamiltonian (11.3′)).*

ratio of c_l and c_m or c_l' and c_s. To study all possibilities we set c_l' and c_s in (11.3′) to $\cos(\alpha\pi)$ and $\sin(\alpha\pi)$, respectively. Resulting RE energies $\mathcal{H}_2 n^{-2} - c_0'$ are shown in Figure 17.

We call the three principal limiting cases of the F_2-mode system with $\alpha = 0$, $\frac{1}{4}$, and 1 the t^2, m, and $(-t^2)$ limits, respectively (see Figure 17). All these limits have continuous symmetries and the system is integrable. The s^2 limit shown in Figure 17 is indicated primarily for convenience. It has no simple integrals and, probably, is not integrable.

The symmetry group of the t^2 limit contains the spatial group SO(3). The energy in this limit is a function of the vibrational angular momentum $t^2 = l^2$, which is zero for the A-type RE and maximum $l = n$ for the B-type RE. The corresponding quantum polyad is split into multiplets with $l = n, n-2, \ldots$. The $(-t^2)$ limit is the same as the t^2 limit, albeit for the opposite sign of energies.

The spatial symmetry of the m limit is cubic, so this limit better represents the symmetry of the system. However, this limit has continuous dynamical symmetry $T^3 = S^1 \times S^1 \times S^1$. The energy can be represented as a function of three integrals in involution (n_1, n_2, n_3), i.e., actions of individual oscillators, such that $n_1 + n_2 + n_3 = n$. The quantum states can be labeled with the three corresponding quantum numbers. The number of degenerate states is normally given by the number of permutations of the set of the three integers $[N_1, N_2, N_3]$. In the $n = 10$ example in Figure 17, it is either 3 or 6 (maximum).

Transition between the t^2 and m limits has been studied by Patterson [96], who remarked that F_2-mode polyads of certain molecules, such as SiF_4, SF_6, and UF_6, belong to the interval of $\alpha = [0, \frac{1}{4}]$. On the other hand, our prediction for P_4 suggests that the ν_3 polyads of this molecule fall into the $\alpha \geq \frac{1}{2}$ category. A complimentary approach to classifying ν_3-mode systems is by specifying the intervals of α-values, where the second order normalized

Hamiltonian (11.3′) represents particular classes of $(T_d \times \mathcal{T})$-invariant Morse functions on $\mathbb{C}P^2$ introduced in section 5.2.3. We can see in Figure 17 that there are at least three such regions. Furthermore, we notice that the $\mathcal{H}_2^{\nu_3}$ Hamiltonian is of the simplest Morse type only on the interval $\alpha = (\pi^{-1} \tan^{-1} 2, \frac{1}{2})$, where the additional nonfixed RE of symmetry $C_s \wedge \mathcal{T}_2$ does not exist.

In this paper we would like to uncover the precise role of the vibrational angular momentum term $(\mathbf{p} \times \mathbf{q})^2$ in the transition between the simplest and nonsimplest RE structures. To this end we detail our example in section 5.3.2. Note that even though $(\mathbf{p} \times \mathbf{q})^2$ enters in both the initial Hamiltonian (11.1a) and the normalized (i.e., n-polyad) Hamiltonian (11.3′), the actual vibrational angular momentum of the system is measured by the parameter K_l of (11.1a) and not by the effective parameter c_l or c_l'. Therefore, we should take the vibrational Hamiltonian (11.1a), replace K_l with λK_l, use constants (11.1b) obtained in [13], and make λ vary between, for example, 0 and 2. Normalizing and using the (s^2, t^2, n) representation (11.3′) with parameters (11.1b) gives

$$\frac{c_s}{c_l'} = \frac{5K_3^2 + 18K_t}{18K_t + 12K_s - K_3^2 - 24\lambda K_l} = \frac{51}{5 - 16\lambda}.$$

It follows that we study the F_2-mode system near the s^2 limit in the range $\alpha \approx [0.469, 0.655]$; see Figure 17.

The stability analysis of RE for $\lambda = 0$, i.e., *without* the vibrational angular momentum term $(\mathbf{p} \times \mathbf{q})^2$ in (11.1a), shows that the corresponding normal form $H_{\text{eff}}^{\nu_3}$ is a Morse function on $\mathbb{C}P^2$ of the simplest kind. In the A_4 molecule model of [13] (with $\lambda = 1$ and $\alpha \approx 0.567$), $H_{\text{eff}}^{\nu_3}$ is of the nonsimplest kind. The transition from the simplest to the nonsimplest case is clearly related to the $(\mathbf{p} \times \mathbf{q})^2$ term. The RE energy computed using the normal form of the Hamiltonian (11.1) as a function of the parameter λ is shown in Figure 18, where we also indicate the Morse signatures and stability types of the RE. As can be seen in this figure, the B-type RE, which are shaped as loops in the configuration space (see Figure 16) and thus induce the maximum vibrational angular momentum, respond largely to the change of λ, while the energy of the A-type RE remains unchanged. As a consequence, the RE structure as a whole has to change qualitatively. This change involves two bifurcations.

The first bifurcation happens at $\lambda = 5/16$ ($\alpha = 0$). The $B^{(4)}$ relative equilibrium, which was unstable with Morse index 1 (Poincaré index +2) for $\lambda < 5/16$, becomes stable with index 0 (+4) for $\lambda > 5/16$. At the moment of bifurcation the energies of the $B^{(4)}$ and $A^{(4)}$ RE are equal, then as λ increases, the energy of $B^{(4)}$ becomes greater. At the same time, the $A^{(4)}$ relative equilibrium, which was stable with Morse index 0 (+4), becomes doubly unstable with Morse index 2 (0). In order for the Morse conditions to be satisfied globally, a *new* relative equilibrium bifurcates from $A^{(4)}$. This is the $C_s \wedge \mathcal{T}_2$ symmetric RE described in section 5.2.3. The new relative equilibrium is unstable with Morse index 2 (0). Part of the described bifurcation can be regarded as a so-called "pitchfork bifurcation," or a bifurcation with broken symmetry Z_2. Indeed, the system restricted to the C_s sphere (see section 5.2.3) undergoes such bifurcation. Taken to the whole four-dimensional space, this phenomenon is more complex because it involves the $B^{(4)}$ relative equilibrium.

The second bifurcation happens at $\lambda = 11/8$ ($\alpha \approx 0.1$). The moment of bifurcation is easy to notice because the second normal form energies of the $B^{(3)}$ and $A^{(4)}$ RE (i.e., values of the

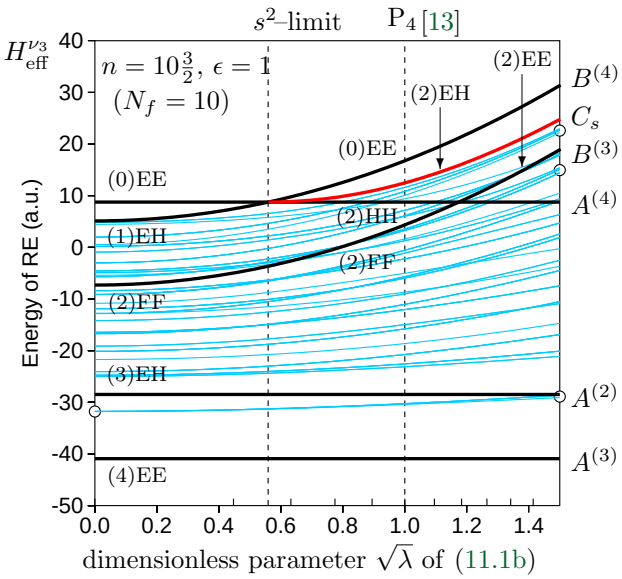

Figure 18. *Quantum (grey lines) and classical RE (bold lines) correlation diagram for the F_2-mode system described by the one-parameter family of Hamiltonians (11.1) with fixed $\epsilon = 1$ and classical action $n = 10\frac{3}{2}$. Quantum polyads are computed for $N_f = 10$. Morse index and Hamiltonian stability are indicated for each RE; EE, EH, HH, and FF stand for elliptic–elliptic (stable), elliptic–hyperbolic (unstable), hyperbolic–hyperbolic (doubly unstable), and focus–focus (complex unstable), respectively. Circles mark level clusters discussed in the text. To compare to Figure 17, inverse the energy axis.*

Hamiltonian (11.3′) shown in Figures 18 and 17) become equal. The $B^{(3)}$ relative equilibrium undergoes a Hamiltonian Hopf bifurcation [97, 98], and from a focus–focus (complex unstable) relative equilibrium at $\lambda < 11/8$ it becomes elliptic (linearly stable) at $\lambda > 11/8$. The Morse index does not change. Unlike the previous case, the Morse requirements remain satisfied globally and there is no need for changing the number and/or stability of other RE.

Information on the RE of the system with Hamiltonian (11.1) can be used to characterize the spectrum of the corresponding quantum system as proposed in section 5.4.3. We consider the RE energies as functions of the action n and compare them to the quantum energy levels (see Figure 19). Levels with the same quantum number N_f form a *polyad* whose structure can be related to the reciprocal RE energies for corresponding classical action $n = N_f + \frac{3}{2}$. Like RE, polyads are described using the normalized Hamiltonian $H^{\nu_3}_{\rm eff}$, where we can distinguish between "scalar" and "splitting" terms. The former depend only on n and describe an average increase in energy; the latter describe the internal structure of polyads. In the simplest approximation given by the second order normal form (11.3′), or the Hecht Hamiltonian, the internal structure of polyads is described by one-parameter α; see Figure 18.

Provided that the model potential of the P_4 molecule [13] is qualitatively correct, the ν_3 polyads of P_4 should correspond to the value of $\alpha \approx 0.6$ near the so-called s^2 limit. The most characteristic feature of the ν_3 polyads with such α is the presence of level clusters at the $A^{(3)}$ end (maximum in Figure 17 and minimum in Figures 18 and 19). The limiting $A^{(3)}$ cluster has four levels and in the case of $N_f = 10$ decomposes into symmetry components $A + F$ (Figure 18). At higher $N_f = 15$ (Figure 19) we can even see the second cluster of eight

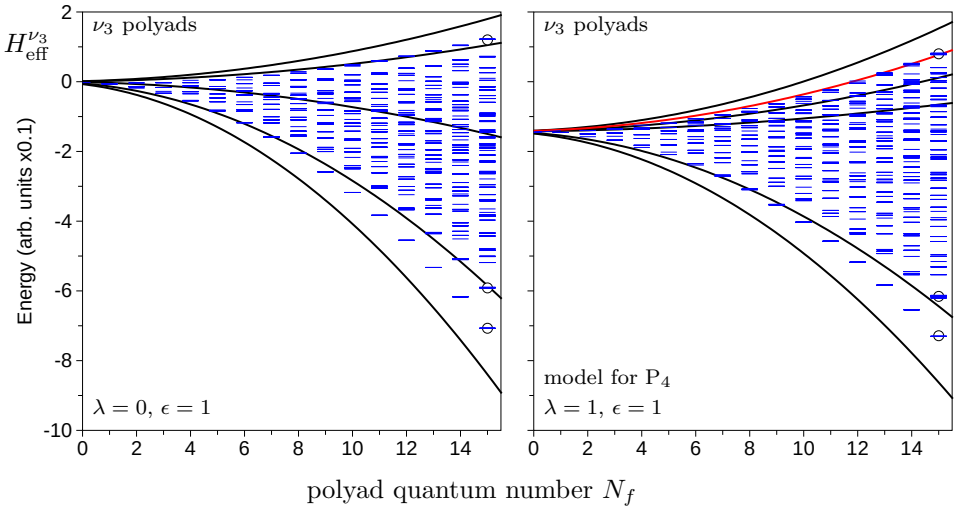

Figure 19. *Spectrum of quantum levels and energies of the RE of the F_2-mode system with Hamiltonian (11.1) with $\epsilon = 1$ and $\lambda = 0$ (left), $\lambda = 1$ (right). Circles mark $N_f = 15$ level clusters discussed in the text, and classical RE energy is plotted for $n = N_f + \frac{3}{2}$.*

levels with components $F + F + E$. As can be seen in Figures 18 and 19, the $A^{(3)}$ clusters remain insensitive to large variations of the structure parameter α or λ. The situation is more unclear at the opposite energy end of the ν_3 polyads. If, as predicted, $\alpha > \frac{1}{2}$, then the $B^{(4)}$ clusters of six levels should appear as shown in Figure 18 (top right) and 19 (topmost level of the $N_f = 10, \ldots, 15$ polyads). They decompose as $A + F + E$ for $N_f = 10$ and $F + F$ for $N_f = 15$. If, however, α for P_4 turns out to be sufficiently smaller than $\frac{1}{2}$, then we should expect $A^{(4)}$ clusters of three levels (such as the lowest energy levels of the $N_f = 10$ polyad for $\alpha = 0.4$ in Figure 17). Furthermore, if the $B^{(3)}$ relative equilibrium becomes sufficiently stable, a corresponding eight-fold cluster might also show up.

Several aspects should be taken into account in order to continue our analysis of the ν_3 polyad structure presented in this paper. A simple analysis based on energy separation fails as different systems of localized states overlap, and complimentary information on expectation values of characteristic dynamical invariants should be used. Degeneracy of quantum states caused by symmetry can either enhance or obscure the presence of level clusters. The position of the limiting localized state and the corresponding RE depends on the stability of the RE and the relation between n and N_f.

11.2. Rotational structure of the F_2-mode polyads. Consider an effective Hamiltonian $H_{\rm eff}$ commonly used to describe rotational structure of low excited F_2-mode vibrations. In the spectroscopic notation of Table 25, this Hamiltonian can be written as

$$H_{\rm eff} = \omega_f n_f + Bj^2 - Dj^4 - h_{ff}^{2(0,A_1)} \frac{4}{3} n_f j^2 \tag{11.4a}$$

$$+ h_{ff}^{1(1,F_1)} H_{ff}^{1(1,F_1)} + \sum_{\Gamma=E,F_2} h_{ff}^{2(2,\Gamma)} H_{ff}^{2(2,\Gamma)} \tag{11.4b}$$

$$+\sum_{K=1,3} h_{ff}^{3(K,F_1)} H_{ff}^{3(K,F_1)} - \frac{\sqrt{30}}{8} D_t H^{4(4,A_1)}, \tag{11.4c}$$

where ω_f is harmonic frequency of the F_2 mode, B is the rotational constant of the molecule (for a tetrahedral molecule A_4 with four atoms of mass m whose equilibrium positions lie at a distance R from the center of mass, the constant B equals $1/(2mR^2)$), and h_{ff}, D, and D_t are parameters of higher order terms in the reduced Hamiltonian. We can omit the terms (11.4a), which have constant value in the reduced system. The energies of fixed RE can be found straightforwardly as values of the H_{eff} in (11.4) at the points listed in Table 27.

To find the two remaining RE, we restrict H_{eff} in (11.4) to the C_s-invariant sphere using the definition of this sphere in Table 28 and express the result as a function of dynamical variables X of the C_s restricted system,

$$H_{\text{eff}}^{C_s} = b(J)X_1 - a(J)X_3 + c(J, N_f), \tag{11.5}$$

where

$$\begin{aligned}
a &= \sqrt{2}\, h_{ff}^{2(2,E)} J^2 - \frac{2}{\sqrt{3}}\, h_{ff}^{2(2,F_2)} J^2, \\
b &= -\frac{2\sqrt{2}}{\sqrt{3}}\, h_{ff}^{1(1,F_1)} J + \left[\frac{8\sqrt{2}}{\sqrt{3}}\, h_{ff}^{3(1,F_1)} + \frac{4}{\sqrt{5}}\, h_{ff}^{3(3,F_1)}\right] \frac{J^3}{\sqrt{3}}, \\
c &= D_t J^4 + \frac{\sqrt{2}}{6}\, h_{ff}^{2(2,E)} N_f J^2 + \frac{1}{\sqrt{3}}\, h_{ff}^{2(2,F_2)} N_f J^2.
\end{aligned}$$

Note that $H_{\text{eff}}^{C_s}$ is linear in X and that it is invariant with regard to $T_d \times \mathcal{T}$ and to its subgroup $\mathcal{T}_2$ and therefore cannot depend linearly on X_2. Equations of motion (10.1) for this Hamiltonian are very simple:

$$\dot{X} = (-aX_2, bX_3 + aX_1, -bX_2).$$

Setting $X_2 = 0$ in these equations gives the condition for an equilibrium point of $H_{\text{eff}}^{C_s}$ on the $\mathcal{T}_2$-invariant circle,

$$bX_3 + aX_1 = 0,$$

which should be satisfied together with the defining equation of the circle

$$X_1^2 + X_3^2 = \frac{1}{4} N_f^2.$$

Since $a(J)$ and $b(J)$ depend differently on J; the two solutions

$$(X_1, X_2, X_3) = \pm \frac{N_f}{2\sqrt{b^2 + a^2}} (b, 0, -a)$$

move along the circle when J changes: when J is small and $b \gg a$ they are close to the point where $X_3 = 0$; at large J they approach $X_1 = 0$. The energies of these RE are

$$\pm \frac{N_f}{2} \sqrt{b(J)^2 + a(J)^2} + c(J, N_f). \tag{11.6}$$

Table 35

Energy of rotation–vibration RE in the case of low excited F_2-mode vibrations of a tetrahedral molecule A_4.

Point[50]	Energy of RE (values of H_{eff})
$A^{(2)}$	$-\frac{\sqrt{2}}{3}h_{ff}^{2(2,E)}N_fJ^2-\frac{2}{\sqrt{3}}h_{ff}^{2(2,F_2)}N_fJ^2+D_tJ^4$
$A^{(3)}$	$-\frac{8\sqrt{3}}{9}h_{ff}^{2(2,F_2)}N_fJ^2+\frac{8}{3}D_tJ^4$
$A^{(4)}$	$-\frac{4\sqrt{2}}{3}h_{ff}^{2(2,E)}N_fJ^2-4D_tJ^4$
$B,C^{(3)}$	$\mp\frac{\sqrt{2}}{\sqrt{3}}h_{ff}^{1(1,F_1)}N_fJ+\frac{4\sqrt{3}}{9}h_{ff}^{2(2,F_2)}N_fJ^2$ $\pm\frac{4\sqrt{2}}{3}\left(h_{ff}^{3(1,F_1)}+\frac{2\sqrt{2}}{\sqrt{15}}h_{ff}^{3(3,F_1)}\right)N_fJ^3+\frac{8}{3}D_tJ^4$
$B,C^{(4)}$	$\mp\frac{\sqrt{2}}{\sqrt{3}}h_{ff}^{1(1,F_1)}N_fJ+\frac{2\sqrt{2}}{3}h_{ff}^{2(2,E)}N_fJ^2$ $\pm\frac{4\sqrt{2}}{3}\left(h_{ff}^{3(1,F_1)}-\frac{\sqrt{2}}{\sqrt{15}}h_{ff}^{3(3,F_1)}\right)N_fJ^3-4D_tJ^4$

The simplest way to compare the energies of RE in Table 35 and (11.6) to molecular energy levels is to plot all of them in a form of an energy-momentum diagram for fixed vibrational integral N_f. In the lowest excited vibrational quantum state of the ν_3 mode, also called the fundamental or harmonic state, the quantum number $\hat{N}_f$, equals 1 which corresponds to the classical value $N_f=1+\frac{3}{2}$.

We illustrate our results using the Hamiltonian H_{eff} (without the scalar part (11.4a)), which describes the ν_3 vibration of the CH_4 molecule. Parameters of this Hamiltonian can be taken from [92].

$h_{ff}^{1(1,F_1)}$	-0.706007	D_t	4.42516×10^{-6}
$h_{ff}^{2(2,E)}$	1.5760×10^{-2}	$h_{ff}^{2(2,F_2)}$	-0.7220×10^{-2}
$h_{ff}^{3(1,F_1)}$	-0.635×10^{-4}	$h_{ff}^{3(3,F_1)}$	-0.187×10^{-4}

The quantum energy level spectrum of the $\nu_3=1$ state is shown schematically by the shaded area. This spectrum exhibits three characteristic branches formed due to the first order Coriolis interaction [81]. As shown in section 7.2.5 and Table 25, the term describing this interaction in the reduced system is the scalar product (t,j), which has spherical symmetry, i.e., to the first order; the energy depends on the angle between the 3-vectors t and j. Assuming $H_1\propto(t,j)$, as in the case of CH_4, the energy is maximal, minimal, or zero when t and j are parallel (RE of type B), antiparallel (RE of type C), or orthogonal (RE of type A), respectively. Since the quantity (t,j) is (approximately) conserved, we can introduce another angular momentum $r=j-t$ and represent the first order energy as function of r^2, t^2, and j^2 called "rotational," "vibrational," and total angular momenta, respectively. In the quantum

[50]Fixed points of the $T_d\times\mathcal{T}$ group action on $\mathbb{C}P^2\times\mathbb{C}P^1\times\mathbb{S}^2$ defined in Table 27; signs $+$ and $-$ in the notation $\pm$ (equivalently, $-$ and $+$ in $\mp$) correspond to points B and C, respectively.

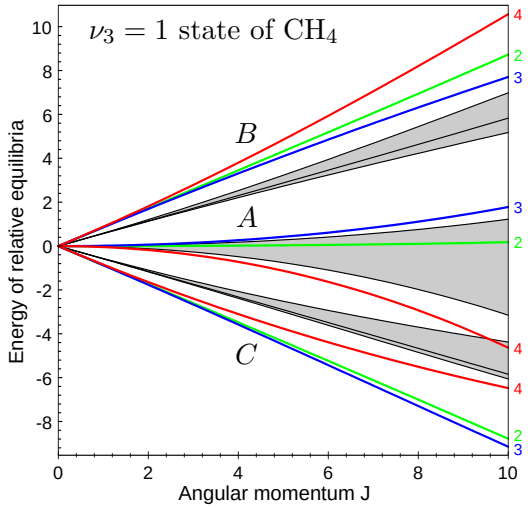

Figure 20. *Energies of rotation–vibration RE for the ν_3 mode of the CH_4 molecule. Colored lines show classical energies (see Table 35 and equation (11.6)) with N_f set to $\frac{5}{2}$; indices $(2,3,4)$ on the right give the symmetry of the corresponding RE. Thin black lines show the same energies with $N_f = 1$; shaded area represents quantum multiplets.*

state with $\hat{N}_f = 1$, the quantum number $\hat{t}$ equals 1 and the quantum number $\hat{r}$ takes the values of $\hat{j}-1$, $\hat{j}$, and $\hat{j}+1$. These values label the three Coriolis branches of the $\nu_3 = 1$ state.

Bold lines in Figure 20 represent energies of the nine RE (two noncritical orbits are given in (11.6) and seven critical orbits in Table 35) with N_f set to its classical value $1+\frac{3}{2}$. The same energies—but with $N_f = 1$—are shown by thin lines, which border *exactly* the three rotational branches of quantum levels. This suggests a straightforward semiclassical interpretation. The RE energy with $N_f = \frac{5}{2}$ gives classical limit (classical extremum) energy for rotation–vibration levels; with $N_f = 1$ we approximate vibrational quantum energy of the state localized near the corresponding RE and obtain classical limit energy for the rotational structure only. In the case of the Hamiltonian (11.4) whose vibrational part is quadratic, this approximation matches exactly the extrema of the so-called "rotational energy surfaces" [32, 36, 35], which are obtained when all rotational operators in H_{eff} are replaced by their quantum analogues. Further examples can be found in [58, 13, 12].

12. Discussion of the results. This paper, together with [13], reports on the first substantial attempt to extend the analysis of molecular energy levels based on RE (also known as nonlinear normal modes and, in some cases, local modes, principal periodic orbits, stationary axes of rotation, etc.) from simple, often model systems to complex rotation–vibration Hamiltonians of real molecules. Our predecessors (see section 1) studied classical vibrational systems with two or three degrees of freedom [14, 15, 16, 77, 70], notably a great number of triatomic molecules [19, 22, 23, 24, 25, 26, 27, 99, 100, 101, 102, 103, 104, 105, 106], and rotational systems [31, 32, 33, 34, 37, 38, 55, 28, 29, 12]. Generalization of these studies to combined systems led to "hybrid" quantum classical systems [36, 35, 41, 42, 43, 56, 107, 108, 109]. We take the next step by studying the whole of the combined system classically and using the results for

the interpretation and prediction of the corresponding quantum system. We consider the example of the rotating tetahedral molecule A_4 with six internal vibrational degrees of freedom, a system which is, arguably, at the limit of molecular systems whose rotation–vibration energy levels have already been studied in detail.

Our principal molecular result is the relation of rotation–vibration RE and the structure of the rotation–vibration energy level spectrum. Thus, we show how extremal quantum states in the rotation–vibration multiplet are associated with particular periodic rotation–vibration motion of the molecule. We took advantage of the simplicity of the classical RE description in order to analyze the structure of highly excited energy levels in different limits. In particular, we compared the structure of rotationally excited polyads to that in the case of high purely vibrational excitation. We found that when the interaction of the rotational and vibrational subsystems is significant, RE become qualitatively different from what can be expected for (or deduced from) the separable system. We predicted qualitative modifications of the system of RE and then followed it with a concrete example. This is our main mathematical result.

We also took advantage of the rich topological structure and high symmetry of our example system in order to predict and explain many important basic qualitative features of this complex system. Subsequently, we confirmed our predictions quantitatively. In particular we analyzed existence and stability of rotation–vibration RE. We extend this study to different parametric limits of molecular potential and corresponding limiting cases of the normalized system (polyads). Our more specialized mathematical results concern group-theoretical aspects of combining two subsystems, in particular the analysis of the group action on the combined phase space on the basis of the action on individual subspaces. The last, but not least, is the dynamically invariant formulation of the theory in section 9, which is the weapon of choice for further analysis of the hidden regular structures of seemingly irregular highly excited molecular states.

REFERENCES

[1] E. B. Wilson, J. C. Decius, and P. C. Cross, *Molecular Vibrations*, McGraw–Hill, New York, 1955.

[2] G. Amat, H. H. Nielsen, and G. Tarrago, *Rotation-Vibrations of Polyatomic Molecules*, Marcel Dekker, New York, 1971.

[3] J. K. G. Watson, *Higher-degree centrifugal distortion of tetrahedral molecules*, J. Mol. Spectrosc., 55 (1975), pp. 498–499.

[4] M. R. Aliev and J. K. G. Watson, *Higher-order effects in the vibration-rotation spectra of semirigid molecules*, in Molecular Spectroscopy: Modern Research, Vol. 3, K. N. Rao, ed., Academic Press, New York, 1985, pp. 1–67.

[5] Vl. I. Arnol'd, *Mathematical Methods of Classical Mechanics*, 2nd ed., Grad. Texts in Math. 60, Springer-Verlag, Berlin, 1989.

[6] Vl. I. Arnol'd, *Geometrical Methods in the Theory of Ordinary Differential Equations*, 2nd ed., Fund. Principles Math. Sci. 250, Springer-Verlag, New York, 1988.

[7] Vl. I. Arnol'd, V. V. Kozlov, and A. I. Neishtadt, *Mathematical Aspects of Classical and Celestial Mechanics: Dynamical Systems* III, Encyclopaedia Math. Sci. 3, Springer-Verlag, Berlin, 1993. Reprinted 1997

[8] J. M. Souriau, *Structure des Systèmes Dynamiques*, Dunod, Paris, 1970.

[9] J. E. Marsden and T. S. Ratiu, *Introduction to Mechanics and Symmetry*, Springer-Verlag, New York, 1994.

[10] R. Abraham and J. E. Marsden, *Foundations of Mechanics*, 2nd ed., Addison–Wesley, Reading, MA, 1978.
[11] R. H. Cushman and L. M. Bates, *Global Aspects of Classical Integrable Systems*, Birkhäuser, Basel, 1997.
[12] Ch. van Hecke, D. A. Sadovskiĭ, and B. I. Zhilinskiĭ, *Qualitative analysis of molecular rotation starting from inter-nuclear potential*, European Phys. J. D At. Mol. Opt. Phys., 7 (1999), pp. 199–209.
[13] Ch. van Hecke, D. A. Sadovskiĭ, B. I. Zhilinskiĭ, and V. Boudon, *Rotational-vibrational relative equilibria and the structure of quantum energy spectrum of the tetrahedral molecule P_4*, Eur. Phys. J. D At. Mol. Opt. Phys., 17 (2001), pp. 13–35.
[14] J. Montaldi, R. M. Roberts, and I. Stewart, *Periodic solutions near equilibria of symmetric Hamiltonian systems*, Philos. Trans. Roy. Soc. London Ser. A, 325 (1988), pp. 237–293.
[15] J. Montaldi, M. Roberts, and I. Stewart, *Existence of nonlinear normal modes of symmetric Hamiltonian systems*, Nonlinearity, 3 (1990), pp. 695–730.
[16] J. Montaldi, M. Roberts, and I. Stewart, *Stability of nonlinear normal modes of symmetric Hamiltonian systems*, Nonlinearity, 3 (1990), pp. 730–772.
[17] B. I. Zhilinskiĭ, *Qualitative analysis of vibrational polyads: N mode case*, Chem. Phys., 137 (1989), pp. 1–13.
[18] D. A. Sadovskiĭ and B. I. Zhilinskiĭ, *Group theoretical and topological analysis of localized vibration-rotation states*, Phys. Rev. A, 47 (1993), pp. 2653–2671.
[19] N. Fulton, J. Tennyson, D. A. Sadovskiĭ, and B. I. Zhilinskiĭ, *Nonlinear normal modes and local bending vibrations of H_3^+ and D_3^+*, J. Chem. Phys., 99 (1993), pp. 906–918.
[20] R. H. Cushman and D. Rod, *Reduction of the semisimple* 1:1 *resonance*, Phys. D, 6 (1982), pp. 105–112.
[21] R. H. Cushman, *Geometry of the bifurcations of the Henon–Heiles family*, Proc. Roy. Soc. London Ser. A, 382 (1982), pp. 361–371.
[22] L. Xiao and M. E. Kellman, *Unified semiclassical dynamics for molecular resonance spectra*, J. Chem. Phys., 90 (1989), pp. 6086–6098.
[23] Z.-M. Lu and M. E. Kellman, *Phase space structure of triatomic molecules*, J. Chem. Phys., 107 (1997), pp. 1–15.
[24] L. E. Fried and G. S. Ezra, *Semi-classical quantization using classical perturbation theory: Algebraic quantization of multidimensional spectra*, J. Chem. Phys., 86 (1987), pp. 6270–6282.
[25] Ch. Jaffé, *Comment on "Semiclassical phase space evolution of Fermi resonance spectra,"* J. Chem. Phys., 89 (1988), pp. 3395–3396.
[26] M. E. Kellman, *Approximate constants of motion for vibrational spectra of many-oscillator systems with multiple anharmonic resonances*, J. Chem. Phys., 93 (1990), pp. 6630–6635.
[27] M. E. Kellman and G. Chen, *Approximate constants of motion and energy transfer pathways in highly excited acetylene*, J. Chem. Phys., 95 (1991), pp. 8671–8672.
[28] J. Montaldi, *Persistence and stability of relative equilibria*, Nonlinearity, 10 (1997), pp. 449–466.
[29] J. Montaldi and R. M. Roberts, *Relative equilibria of molecules*, J. Nonlinear Sci., 9 (1999), pp. 53–88.
[30] I. N. Kozin, D. A. Sadovskiĭ, and B. I. Zhilinskiĭ, *Assigning Vibrational Polyads Using Relative Equilibria. Application to Ozone*, in preparation.
[31] A. Dorney and J. K. G. Watson, *Forbidden rotational spectra of polyatomic molecules. Stark effect and $\Delta J = 0$ transitions of T_d molecules*, J. Mol. Spectrosc., 42 (1972), pp. 135–148.
[32] W. G. Harter and C. W. Patterson, *Orbital level splitting in octahedral symmetry and SF_6 rotational spectra*, J. Chem. Phys., 66 (1977), pp. 4872–4885.
[33] C. W. Patterson and W. G. Harter, *Orbital level splitting in octahedral symmetry and SF_6 rotational spectra* II. *Quantitative features of high J levels*, J. Chem., Phys., 66 (1977), pp. 4886–4892.
[34] W. G. Harter and C. W. Patterson, *Rotational energy surfaces and high-J eigenvalue structure of polyatomic molecules*, J. Chem. Phys., 80 (1984), pp. 4241–4261.
[35] W. G. Harter, *Computer graphical and semiclassical approaches to molecular rotations and vibrations*, Comp. Phys. Rep., 8 (1988), pp. 319–394.

[36] W. G. Harter, *Molecular symmetry and dynamics*, in Atomic, Molecular, and Optical Physics Handbook, G. W. F. Drake, ed., AIP Press, New York, 1996, pp. 378–393.
[37] B. I. Zhilinskiĭ and I. M. Pavlichenkov, *Critical phenomena in rotational spectra*, Soviet Phys. JETP, 65 (1987), pp. 221–229.
[38] I. M. Pavlichenkov and B. I. Zhilinskiĭ, *Critical phenomena in rotational spectra*, Ann. Phys., 184 (1988), pp. 1–32.
[39] B. I. Zhilinskiĭ, *Topological and symmetry features of intramolecular dynamics through high-resolution molecular spectroscopy*, Spectrochim. Acta A, 52 (1996), pp. 881–900.
[40] B. I. Zhilinskiĭ, *Teoriya slozhnykh molekulyarnykh spektrov*, Moscow University Press, Moscow, 1989.
[41] D. A. Sadovskiĭ and B. I. Zhilinskiĭ, *Qualitative analysis of vibration-rotation Hamiltonians for spherical top molecules*, Molec. Phys., 65 (1988), pp. 109–128.
[42] Vl. M. Krivtsun, D. A. Sadovskiĭ, and B. I. Zhilinskiĭ, *Critical phenomena and diabolic points in rovibrational energy spectra of spherical top molecules*, J. Molecular Spectr., 139 (1990), pp. 126–46.
[43] D. A. Sadovskiĭ, B. I. Zhilinskiĭ, J.-P. Champion, and G. Pierre, *Manifestations of bifurcations and diabolic points in molecular energy spectra*, J. Chem. Phys., 92 (1990), pp. 1523–1537.
[44] P. Chossat and R. Lauterbach, *Methods in Equivariant Bifurcations and Dynamical Systems*, World Scientific, Singapore, 2000.
[45] M. Golubitsky and D. G. Schaeffer, *Singularities and Groups in Bifurcation Theory, Vol.* 1, Springer-Verlag, Berlin, 1985.
[46] M. Golubitsky, I. Stewart, and D. G. Schaeffer, *Singularities and Groups in Bifurcation Theory, Vol.* 2, Springer-Verlag, Berlin, 1988.
[47] V. Boudon, E. B. Mkadmi, H. Bürger, and G. Pierre, *High-resolution FTIR spectroscopy and analysis of the ν_3 fundamental band of P_4*, Chem. Phys. Lett., 305 (1999), pp. 21–27.
[48] L. Michel and B. I. Zhilinskiĭ, *Symmetry, invariants, topology. Basic tools*, Phys. Rep., 341 (2001), pp. 11–86.
[49] L. Michel and B. I. Zhilinskiĭ, *Rydberg states of atoms and molecules. Basic group-theoretical and topological analysis*, Phys. Rep., 341 (2001), pp. 173–264.
[50] B. I. Zhilinskiĭ, *Symmetry, invariants, and topology in molecular models*, Phys. Rep., 341 (2001), pp. 85–172.
[51] R. Littlejohn and M. Reinsch, *Gauge fields in the separation of rotations and internal motions in the n-body problem*, Rev. Modern Phys., 69 (1997), pp. 213–275.
[52] A. Tachibana and T. Iwai, *Complete molecular Hamiltonian based on the Born–Oppenheimer adiabatic approximation*, Phys. Rev. A, 33 (1986), pp. 2262–2269.
[53] A. Guichardet, *On rotation and vibration motions of molecules*, Ann. Inst. H. Poincaré Phys. Théor, 40 (1984), pp. 329–342.
[54] D. A. Sadovskiĭ and B. I. Zhilinskiĭ, *Counting levels within vibrational polyads. Generating function approach*, J. Chem. Phys., 103 (1995), pp. 10520–10536.
[55] I. N. Kozin and I. M. Pavlichenkov, J. Chem. Phys., 104 (1996), pp. 4105–4113.
[56] G. Pierre, D. A. Sadovskiĭ, and B. I. Zhilinskiĭ, *Organization of quantum bifurcations: Crossover of rovibrational bands in spherical top molecules*, Europhys. Lett., 10 (1989), pp. 409–414.
[57] O. I. Davarashvili, B. I. Zhilinskiĭ, V. M. Krivtsun, D. A. Sadovskiĭ, and E. P. Snegirev, *Experimental study of the sequence of bifurcations which causes the crossover of the rotational multiplet*, Soviet JETP Lett., 51 (1990), pp. 17–19.
[58] G. Dhont, D. A. Sadovskiĭ, B. I. Zhilinskiĭ, and V. Boudon, *Analysis of the "unusual" vibrational components of triply degenerate vibrational mode $\boldsymbol{\nu_6}$ of $Mo(CO)_6$ based on the classical interpretation of the effective rotation-vibration Hamiltonian*, J. Molec. Spectr., 201 (2000), pp. 95–108.
[59] V. E. Pavlov-Verevkin, D. A. Sadovskiĭ, and B. I. Zhilinskiĭ, *On the dynamical meaning of diabolic points*, Europhys. Lett., 6 (1988), pp. 573–578.
[60] D. A. Sadovskiĭ and B. I. Zhilinskiĭ, *Monodromy, diabolic points, and angular momentum coupling*, Phys. Lett. A, 256 (1999), pp. 235–244.
[61] R. H. Cushman and J. J. Duistermaat, *The quantum mechanical spherical pendulum*, Bull. Amer. Math. Soc., 19 (1988), pp. 475–479.
[62] San Vũ Ngọc, *Quantum monodromy in integrable systems*, Comm. Math. Phys., 203 (1999), pp. 465–479.

[63] D. A. Sadovskiĭ and R. H. Cushman, *Monodromy in perturbed Kepler systems: Hydrogen atom in crossed fields*, Europhys. Lett., 47 (1999), pp. 1–7.
[64] D. A. Sadovskiĭ and R. H. Cushman, *Monodromy in the hydrogen atom in crossed fields*, Phys. D, 142 (2000), pp. 166–196.
[65] M. S. Child, T. Weston, and J. Tennyson, *Quantum monodromy in the spectrum of H_2O and other systems*, Molecular Phys., 96 (1999), p. 371.
[66] L. D. Landau and E. M. Lifshitz, *Quantum Mechanics*, Pergamon Press, Oxford, UK, 1965.
[67] M. Hamermesh, *Group Theory and Its Application to Physical Problems*, Addison–Wesley, Reading, MA, 1964.
[68] L. C. Biedenharn and J. D. Louck, *Angular Momentum in Quantum Physics. Theory and Applications*, Addison–Wesley, Reading, MA, 1981.
[69] J. Schwinger, *On angular momentum*, in Quantum Theory of Angular Momentum, L. C. Biedenharn and H. van Dam, eds., Academic Press, New York, 1975, pp. 229–279.
[70] D. A. Sadovskiĭ and B. I. Zhilinskiĭ, *Qualitative study of a model three level Hamiltonian with $SU(3)$ dynamical symmetry*, Phys. Rev. A, 48 (1993), pp. 1035–1044.
[71] W. Gröbner, *Die Lie-Reihen und ihre Anwendungen*, Mathematische Monographien 3, VEB Deutscher Verlag der Wissenschaften, Berlin, 1960.
[72] W. Gröbner, *Contributions to the Method of Lie Series*, Bibliographisches Institut, Mannheim, 1967.
[73] A. Deprit, *Canonical transformations depending on a small parameter*, Celestial Mech., 1 (1969), pp. 12–30.
[74] J. Henrard, *On a perturbation theory using Lie transforms*, Celestial Mech., 3 (1970), p. 107–120.
[75] L. Michel, *Points critiques des fonctions invariantes sur une G-varieté*, C. R. Acad. Sci. Paris Sér. A-B, 272 (1971), pp. 433–436.
[76] L. Michel, *Symmetry defects and broken symmetry*, Rev. Modern Phys., 52 (1980), pp. 617–650.
[77] R. C. Churchill, M. Kummer, and D. L. Rod, *On averaging, reduction and symmetry in Hamiltonian systems*, J. Differential Equations, 49 (1983), pp. 359–414.
[78] D. A. Sadovskiĭ, *Normal forms, geometry, and dynamics of atomic and molecular systems with symmetry*, in Symmetry and Perturbation Theory, D. Bambusi, M. Cadoni, and G. Gaeta, eds., World Scientific, Singapore, 2001, pp. 191–205.
[79] W. G. Harter and C. W. Patterson, *Asymptotic eigensolutions of fourth and sixth rank octahedral tensor operators*, J. Math. Phys., 20 (1979), pp. 1453–1459.
[80] B. I. Zhilinskiĭ and S. Brodersen, *Symmetry of the vibrational components in the T_d molecules*, J. Mol. Spectrosc., 163 (1994), pp. 326–338.
[81] G. Herzberg, *Spectra and Structure of Polyatomic Molecules*, R. E. Kreiger, Malabar, FL, 1989.
[82] F. Faure and B. I. Zhilinskiĭ, *Topological Chern indices in molecular spectra*, Phys. Rev. Lett., 85 (2000), pp. 960–963.
[83] H. Weyl, *Classical Groups. Their Invariants and Representations*, Princeton University Press, Princeton, NJ, 1939.
[84] V. E. Pavlov-Verevkin and B. I. Zhilinskiĭ, *Effective Hamiltonians for vibrational polyads: Integrity basis approach*, Chem. Phys., 126 (1988), pp. 243–253.
[85] J. Moret-Bailly, *Introduction au calcul de l'energie de vibration-rotation des molécules à symétrie sphèrique*, Cahiers de Phys., 13 (1959), pp. 476–494.
[86] J. Moret-Bailly, *Sur l'interpretation des spectres des molécules à symètrie tetraedrique*, Cahiers de Phys., 15 (1961), pp. 237–314.
[87] J. Moret-Bailly, L. Gautier, and J. Montagutelli, *Clebsch-Gordan coefficients adapted to cubic symmetry*, J. Mol. Spectrosc., 15 (1965), pp. 355–377.
[88] F. Michelot, J. Moret-Bailly, and K. Fox, *Rotational energy for spherical tops* I. *Vibronic ground state*, J. Chem. Phys., 60 (1974), pp. 2606–2609.
[89] J.-P. Champion, G. Pierre, F. Michelot, and J. Moret-Bailly, *Composantes cubiques normales des tenseurs sphèriques*, Canad. J. Phys., 55 (1977), pp. 512–520.
[90] J.-P. Champion, *Development complet de l'hamiltonien de vibration-rotation adapté à l'étude des interactions dans les molécules toupies sphèriques*, Canad. J. Phys., 55 (1977), pp. 1802–1828.

[91] J.-P. Champion, M. Loëte, and G. Pierre, *Spherical top spectra*, in Spectroscopy of the Earth's Atmosphere and Interstellar Medium, K. Narahari Rao and A. Weber, eds., Academic Press, Boston, 1992, pp. 339–422.

[92] J.-P. Champion and G. Pierre, *Vibration–rotation energies of harmonic and combination levels in tetrahedral $XY4$ molecules*, J. Mol. Spectrosc., 79 (1980), p. 255–280.

[93] B. I. Zhilinski í, V. I. Perevalov, and Vl. G. Tŷuterev, *Method of Irreducible Tensor Operators in the Theory of Molecular Spectra*, Nauka, Moscow, 1987. (In Russian.)

[94] J. Patera, R. T. Sharp, and P. Winternitz, *Polynomial irreducible tensors for point groups*, J. Math. Phys., 19 (1978), pp. 2362–2376.

[95] K. T. Hecht, *Vibration-rotation energies of tetrahedral XY_4 molecules* I. *Theory of spherical top molecules*, J. Mol. Spectrosc., 5 (1960), pp. 355–389.

[96] Ch. W. Patterson, *Quantum and semiclassical description of a triply degenerate anharmonic oscillator*, J. Chem. Phys., 83 (1985), pp. 4618–4632.

[97] K. Efstathiou, R. H. Cushman, and D. A. Sadovskií, *Linear Hamiltonian Hopf bifurcation for point-group-invariant perturbations of the* 1:1:1 *resonance*, R. Soc. London Ser. A Math. Phys. Eng. Sci., 459 (2003), pp. 2997–3019.

[98] K. Efstathiou and D. A. Sadovskií, *Perturbations of the* 1:1:1 *resonance with tetrahedral symmetry: A three degree of freedom analogue of the two degree of freedom Hénon–Heiles Hamiltonian*, Nonlinearity, 17 (2004), pp. 415–446.

[99] C. Jaffé and W. P. Reinhardt, *Time-independent methods in classical mechanics: Calculation of invariant tori and semiclassical energy levels via classical Van Vleck transformations*, J. Chem. Phys., 71 (1979), pp. 1862–1869.

[100] C. Jaffé and W. P. Reinhardt, *Uniform semiclassical quantization of regular and chaotic classical dynamics on the Henon–Heiles surface*, J. Chem. Phys., 77 (1982), pp. 5191–5203.

[101] A. B. McCoy and E. L. Sibert, *Calculation of infrared intensities of highly excited vibrational states of HCN using Van Vleck perturbation theory*, J. Chem. Phys., 95 (1991), pp. 3488–3493.

[102] A. B. McCoy and E. L. Sibert, *Perturbative calculations of vibrational* $(J = 0)$ *energy levels of linear molecules in normal coordinate representations*, J. Chem. Phys., 95 (1991), pp. 3476–3487.

[103] A. B. McCoy and E. L. Sibert, *An algebraic approach to calculating rotation-vibration spectra of polyatomic molecules*, Molecular Phys., 77 (1992), pp. 697–708.

[104] A. B. McCoy and E. L. Sibert, *Determining potential energy surfaces from spectra: An iterative approach*, J. Chem. Phys., 97 (1992), pp. 2938–2947.

[105] E. L. Sibert and A. B. McCoy, *Quantum, semiclassical and classical dynamics of the bending modes of acetylene*, J. Chem. Phys., 105 (1996), pp. 469–478.

[106] M. Joyeux, *Gustavson's procedure and the dynamics of highly excited vibrational states*, J. Chem. Phys., 109 (1998), pp. 2111–2122.

[107] D. Sugny and M. Joyeux, *On the application of canonical perturbation theory to floppy molecules*, J. Chem. Phys., 112 (2000), pp. 31–39.

[108] D. Sugny, M. Joyeux, and E. L. Sibert, *Investigation of the vibrational dynamics of the HCN/CNH isomers through high order perturbation theory*, J. Chem. Phys., 113 (2000), pp. 7165–7177.

[109] D. Sugny and M. Joyeux, *New canonical perturbation procedure for studying nonadiabatic dynamics*, Chem. Phys. Lett., 337 (2001), pp. 319–326.

[110] R. P. Stanley, *Invariants of finite groups and their applications to combinatorics*, Bull. Amer. Math. Soc., 1 (1979), pp. 475–511.

[111] B. Sturmfels, *Algorithms in Invariant Theory*, Springer-Verlag, Berlin, 1993.